INFORMATION TO USERS

This manuscript has been reproduced from the microfilm master. UMI films the text directly from the original or copy submitted. Thus, some thesis and dissertation copies are in typewriter face, while others may be from any type of computer printer.

The quality of this reproduction is dependent upon the quality of the copy submitted. Broken or indistinct print, colored or poor quality illustrations and photographs, print bleedthrough, substandard margins, and improper alignment can adversely affect reproduction.

In the unlikely event that the author did not send UMI a complete manuscript and there are missing pages, these will be noted. Also, if unauthorized copyright material had to be removed, a note will indicate the deletion.

Oversize materials (e.g., maps, drawings, charts) are reproduced by sectioning the original, beginning at the upper left-hand corner and continuing from left to right in equal sections with small overlaps. Each original is also photographed in one exposure and is included in reduced form at the back of the book.

Photographs included in the original manuscript have been reproduced xerographically in this copy. Higher quality 6" x 9" black and white photographic prints are available for any photographs or illustrations appearing in this copy for an additional charge. Contact UMI directly to order.

UMI

A Bell & Howell Information Company
300 North Zeeb Road, Ann Arbor MI 48106-1346 USA
313/761-4700 800/521-0600

Université d'Ottawa · University of Ottawa

A Study of the human X-Linked Inhibitory Apoptosis Protein Xiap and its Murine Homologue Miap-3

by:

© **Reza Farahani**

Submitted to
the Department of Biochemistry, Microbiology and Immunology
Faculty of Medicine, University of Ottawa
as a partial requirement for
the degree of doctor of philosophy
Summer 1997

Abstract

Apoptosis or programmed cell death is a gene directed mechanism with unique biochemical and physiological features including nuclear and cytoplasmic condensation, protease activation, DNA degradation and formation of apoptotic bodies. Apoptosis plays an important role in development, and homeostasis as well as defense against viral infections. Dysregulation of apoptosis has been implicated in various types of cancer, Acquired Immunodeficiency Syndrome (AIDS), immune system diseases, and neurodegenerative disorders such as Spinal Muscular Atrophy (SMA), Alzheimer's, and Parkinson's diseases and amyotrophic lateral sclerosis (ALS).

IAPs (inhibitor of apoptosis proteins) are a new family of proteins capable of interacting with the components of the cell death machinery thus, inhibiting apoptosis. IAPs contain two or three 70 amino acid domains in their N-terminus called BIR (baculovirus IAP repeat) domains and a C-terminus C_3HC_4 type RING zinc finger. Four human genes

called *naip*, *xiap* (X-linked IAP), *hiap*-1 and *hiap*-2 (human IAP- 1 and 2) have been cloned in our laboratory and others in the past several years. Although all of these genes exhibit some degree of apoptosis suppression capability, it is not clear which region of the protein (i.e. BIR domains or RING zinc finger) is responsible for the anti-apoptotic function. To investigate the role of IAPs in the suppression of apoptosis, *miap*-3, the mouse homologue of *xiap* was cloned by cDNA and genomic library screening and characterized. *miap*-3 has a coding sequence of 1491 bp translating into a protein with 496 amino acids and predicted size of 55 kDa. The mouse gene has 89% and 94% homology with human *xiap* at DNA and amino acid levels respectively and has been assigned to mouse chromosome X in the A3-A5 region by FISH. Northern blot analysis showed that *miap*-3 expresses as an over 8 kb message in all tissues examined indicating large 3' and/or 5' UTRs.

To elucidate the site of anti-apoptotic capability in the IAPs, the capacity of various *miap*-3 and *xiap* constructs to protect cells against apoptotic insult was assessed. Expression of full-length *xiap* or *miap*-3 cDNAs in CHO cells conferred only modest protection above the level observed for controls (i.e. CHO cells expressing plasmids with no insert which demonstrate 15-20% cell survival level). Expression of the RING zinc finger provides no protection to CHO cells. In contrast, expression of a construct encoding only the BIR domains (and not the RING zinc finger) resulted in four fold enhancement of survival after 72 hours of serum deprivation. The anti-apoptotic capability of IAPs thus appears to be conferred by BIR domains. It also appears that the RING zinc finger may act as a negative regulator of the IAPs' anti-apoptotic function.

Given that BIR domains appear to confer the anti-apoptotic capability of IAPs, it was of interest to investigate the cellular distribution of IAPs and any possible change in their distribution pattern under normal and apoptotic conditions. Immunofluorescent microscopy performed on CHO cells expressing *xiap* revealed that under normal conditions, Xiap concentrates in the cytoplasm. During apoptosis, however, Xiap appears in the nucleus as well. Change of localization pattern during apoptosis was further investigated by immunofluorescent studies of COS cells expressing various portions of IAPs. These studies revealed that full-length Xiap and Miap-3 as well as RING zinc-finger proteins concentrate in the cytoplasm. In contrast, BIR domains appeared to localize both in the cytoplasm and nucleus, suggesting that BIR domains may be cleaved and trans-localized to the nucleus during apoptosis. It is, therefore, intriguing to speculate that the anti-apoptotic effect of IAPs during apoptosis may depend on the cleavage and/or translocation of BIR domains to the nucleus.

In the present dissertation, details of cloning and characterization of *miap*-3, functional analysis of *xiap* and *miap*-3, as well as the significance of the acquired results in the further delineation of IAPs and SMA-associated NAIP involvement in various apoptosis signaling pathways are discussed. These and other complementary experiments may provide diagnostic tools and also be helpful in engineering therapeutic strategies e.g. gene therapy against SMA, as well as other neurodegenerative disorders.

Acknowledgments

This is past mid-night of August 31, 1997 that I am writing this. Therefore, I may not remember all the people whose assistance was important in the accomplishment of this project. Above of all for sure stands Dr. Alex MacKenzie, my supervisor who provided me with financial support and useful advice and guidelines when necessary and also Dr. Bob Korneluk who was perhaps one of the rare persons who once in a while told me a few nice words praising me for my "hard and good work". I would like to thank members of my research advisory committee Drs. Donald Hickey, MarioChevrette, and Doug Gray.

I would like to thank all of the over 50 graduate students, summer students, technicians, office employees, post doctoral fellows and junior and senior scientists who were working at some point during 1993 and 1997 in the Molecular Genetics Laboratory at Children's Hospital of Eastern Ontario (CHEO). I would like to especially thank Mr. Charles Lefebvre whose technical assistance was important here and there. I would also like to thank technicians who carried most of the tedious work of sequencing especially Ms. X. Kang. I would like to thank Dr. Mohammad Hussein Ghahremani for assisting me with the statistical analysis and Mr. Stephen Baird for his computer assistance. Special thanks is in order to Mr. Carl-Henri Gomez, my dear close friend for all his emotional supports and technical advice.

There is one special person that I would like to mention here, my dearest wife Ms. Jila Valadkhani. I really hesitate to thank her for a few words are not capable of conveying what she means to me and what she has done for me over the past 19 years and especially during the past seven years of my graduate studies. There were times that I was about to quit but her love and support encouraged me to continue. I just would like to say I love you and you mean everything to me. Thanks are also due to my children Shima, Saeid and Hamid who were supportive and sometimes had to suffer because of a father who was also a student and could not always deliver or be there.

To all those who have rose since the beginning and
stood in their own blood.

va be har kas ke az aghaz ta konoon barkhast
va dar khoon khode istad.

Table of contents

Chapter II

Cloning and characterization of *miap*-3

Chapter III

Functional characterization of *xiap* and *miap*-3

List of Tables

List of Figures

List of Abbreviations

a.a.	amino acid
AcMNPV	*Autographa californica* multiply embedded nuclear polyhedrosis virus
AIDS	Acquired Immunodeficiency Syndrome
α-MEM	Minimum Essential Media
ALS	amyotrophic lateral sclerosis
AML-1	acute myeloid leukemia 1
ATCC	American Type Culture Collection
ATG	translation initiation codon
BH	Bcl-2 homology domain
BHRF1	BamHI fragment H rightward open reading frame 1
BIR	baculovirus IAP repeat
Brdu	bromodeoxyuridine
°C	degree Celsius
C. elegans	*Caenerohabditis elegans*
cDNA	complementary DNA
CHO	Chinese hamster ovary
CMV	cytomegalovirus
CNS	central nervous system

CpGV	*Cydia pomonella* granulosis virus
crmA	cytokine response modifier A
COS	African green monkey kidney cells
Cy3	Cyanine fluorophore 3 (carbons)
Δ1	BIR 1 deleted
Δ2	BIR 1+2 deleted
Δ3	BIR 1+2+3 deleted
ΔBIR	BIR domains deleted
ΔRZF	RING zinc finger deleted
DAPI	diamidinophenylindole
Diap-1/2	*Drosophila* IAP-1/2
DNA	deoxribonucleic acid
EBV	Epstein-Barr virus
ECL	enhanced chemiluminescence
FISH	fluorescence *in situ* hybridization
FL	full length
FITC	fluorescein isothiocyanate
GCG	Genetic Computer Group
gld	global (general) lymphoproliferative disease
GPC	genomic phage clone
GST	glutathione S-transferase

hr	hour
HA	hemaglutinin
Hiap-1/2	Human IAP-1/2
HIV	human immunodeficiency virus
HRP	horseradish peroxidase
IAP	Inhibitor of Apoptosis Protein
ICE	interleukin-1β converting enzyme
Ig	immunoglobulin
IGF	insulin-like growth factor
IPTG	isopropyl thiogalactopyranoside
l	liter
IL	interleukin
kb	kilo base
kDa	kilo Dalton
LMP-1	latent membrane protein-1
lpr	lymphoproliferative disease
M	mole
Mag	magnification
Miap-3	Murine IAP-3
min	minute
ml	milliliter
mM	millimolar

mRNA	messenger ribonucleic acid
MTG	human Myc tag
µg	microgram
NA	not applicable
NAIP	Neuronal Apoptosis Inhibitory Protein
ND	not determined
NFκB	nuclear factor κB
NLS	nuclear localization signal
OpMNPV	*Opgyia psuedotsugata* nuclear polyhedrosis virus
PARP	poly (ADP-ribose) polymerase
PBS	phosphate buffered saline
PBST	PBS Tween
PCR	polymerase chain reaction
RNA	ribonucleic acid
RT-PCR	reverse-transcriptase polymerase chain reaction
RZF	RING zinc finger
SDS	sodium dodecyl sulfate
SDS-PAGE	SDS polyacrylamide gel electrophoresis
SMA	Spinal Muscular Atrophy
SSC	sodium chloride / sodium citrate
TAG/TAA	translation termination codon
TNF	tumor necrosis factor

TNFR-1/2	TNF receptor 1/2
TRAF	TNF receptor associated family
UTR	untranslated region
vAcAnh	*Autographa californica* multiply embedded nuclear polyhedrosis virus annihilator
Xiap	X-linked IAP
XLP	X-linked lymphoproliferative

Chapter I

An overview of the current knowledge of apoptosis

Introduction

More than two decades ago, Kerr and his co-workers published their observations on a unique form of cell death they called "apoptosis", Greek for leaves falling from trees (Kerr et al., 1972). Apoptosis or programmed cell death is a gene directed mechanism with unique biochemical and physiological features including nuclear and cytoplasmic condensation, protease activation, DNA degradation and formation of apoptotic bodies. Our understanding of the field has since advanced greatly, especially during the present decade. Landmark works have unveiled many details of apoptosis and its implications in numerous clinically significant human disorders (Thompson, 1995; Hale et al., 1996;

Fisher, 1994; Gruss and Dower, 1995). Nevertheless, there are many key questions concerning apoptosis that remain unanswered. The present work is part of the on-going effort aimed at answering some of the outstanding questions concerning this important physiological process. In the opening chapter of this dissertation, I will present an overview of our current knowledge of apoptosis.

Genetics of Apoptosis

Apoptosis is an active process that requires products of many specific genes. Developmental studies in mutants of the nematode *Caenorhabditis elegans* has resulted in the identification of more than a dozen genes implicated in apoptosis (Ellis et al., 1991). During *C. elegans* development, 131 of the nematode's 1090 cells are eliminated through apoptosis (Sulston and Horvitz, 1977; Sulston, 1983; Ellis and Horvitz, 1986). These genes function in a single hierarchical pathway controlling the three stages of apoptosis in *C. elegans* i.e. commitment, execution, and engulfing of the dead cell corpse (Fig. 1.1) (Ellis et al., 1991; Steller, 1995).

One of these genes, ced-9 (cell death abnormal) functions to protect cells against apoptosis (Hengartner et al., 1992). Loss of function in *ced*-9 has been shown to be embryonically lethal due to massive cell death, while a gain of function mutation results in preservation of cells that are normally eliminated through apoptosis (Hengartner et al., 1992). The gene product of *ced*-9 appears to function upstream of the products of *ced*-3 and *ced*-4, two other nematode genes involved in apoptosis. *ced*-3 encodes a cysteine protease while *ced*-4 encodes a protein that does not demonstrate functional or sequence

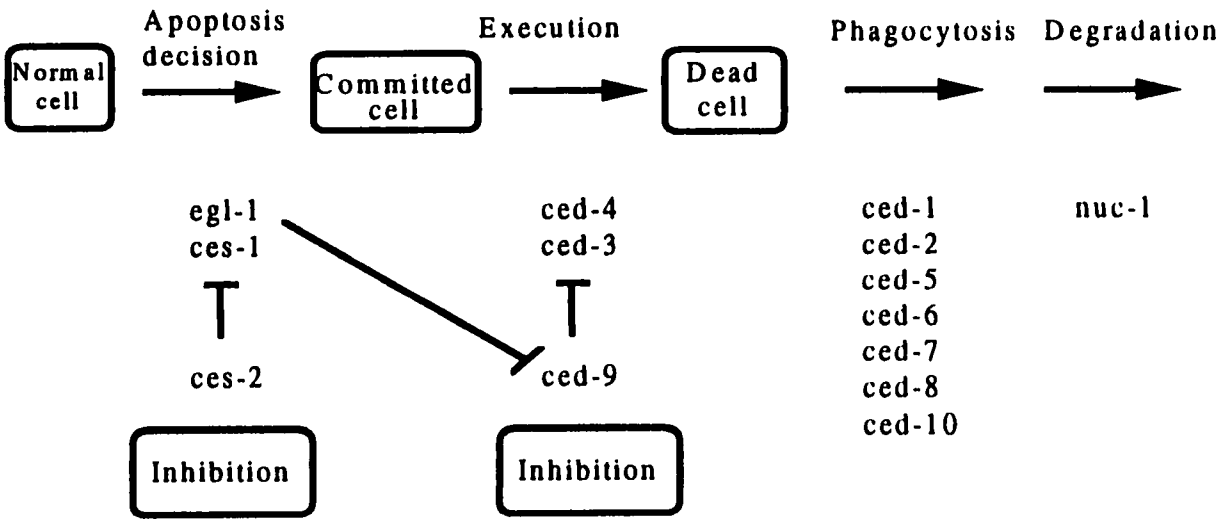
Normal cell
Apoptosis decision
Committed cell
Execution
Dead cell
Phagocytosis
Degradation
egl-1
ces-1
ces-2
Inhibition
ced-4
ced-3
ced-9
Inhibition
ced-1
ced-2
ced-5
ced-6
ced-7
ced-8
ced-10
nuc-1

Figure 1.1. Genes implicated in various stages of apoptosis in the nematode *C. elegans*.

At least 14 genes have been identified to date in *C. elegans* that function in a linear apoptosis pathway. These genes include promoters and inhibitors of cell death, as well as gene product which are involved in disposing of the dead cell corpse (modified from Driscoll and Calfie, 1992 and Steller, 1995).

similarity to any known proteins. Loss of function mutations in *ced*-3 and/or *ced*-4 result in blocking cell death (Ellis et al., 1986; Yuan and Horvitz, 1992; Yuan et al., 1993). Additional *C. elegans* genes, ced-1, 2, 5, 6, 7, 8, and 10 that have been implicated in apoptosis are involved in the removal of dead cells (reviewed by Driscoll and Chalfie, 1992).

Stages of Apoptosis

Homologues of ced-3 and ced-9 have been identified in other animals. Products of some of these genes demonstrate amino acid homology and functional similarity (Yuan et al., 1993; Vaux et al., 1994; Miura et al., 1993) indicating that at least some components of the apoptotic machinery have been conserved throughout evolution. Human Bcl-2, for instance, which shows 22% amino acid homology with *C. elegans* Ced-9, is capable of functionally replacing it (Hengartner and Horvitz, 1994). Nevertheless, the apoptotic machinery and its components appear more complex in higher animals than in simpler organisms. There are, for example, more than a dozen proteases identified in higher animals that resemble *C. elegans* Ced-3 (reviewed by Vaux and Stasser, 1996). Identification of several mammalian proteins with homology to Ced-9 is another example of this expansion. It thus appears that for a number of *C. elegans* proteins implicated in apoptosis, a family of such proteins can be found in metazoa. These protein families have provided multiple apoptotic signaling pathways, each of which may potentially involve interaction of a ligand with its specific receptor. Multiple convergence points of these parallel pathways through common proteins have generated a complex network of apoptotic signal transduction. Components of this apparatus are still poorly understood.

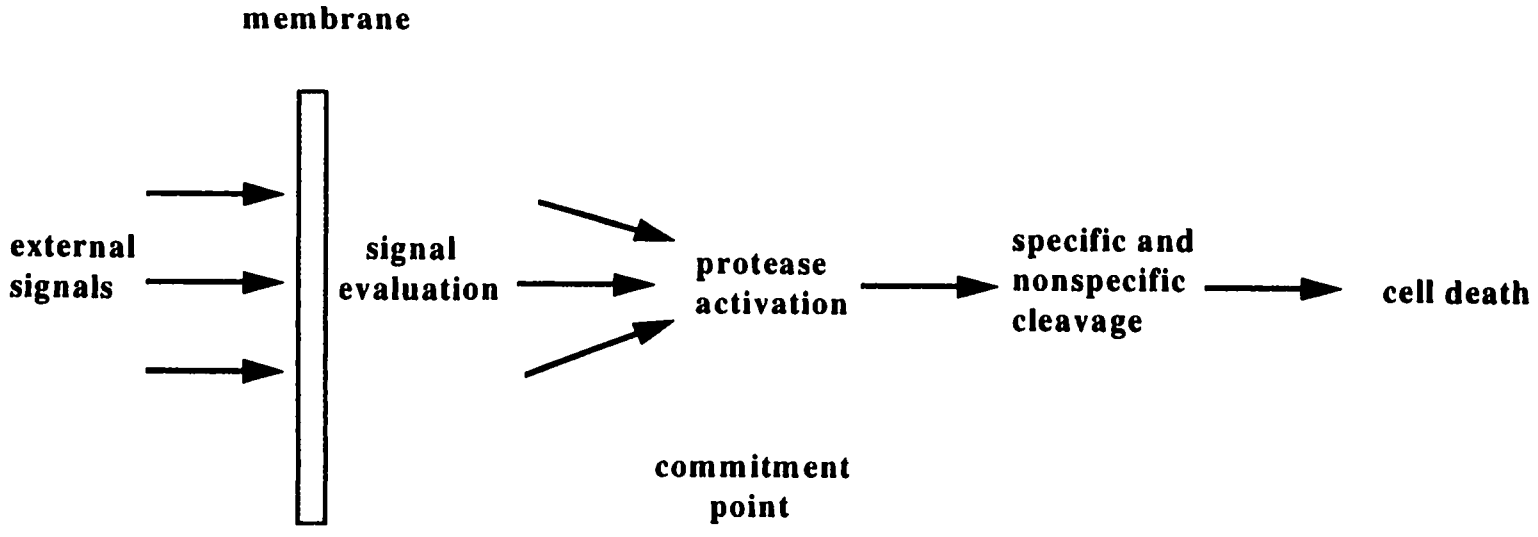
membrane
external signals
signal evaluation
protease activation
specific and nonspecific cleavage
cell death
commitment point

b

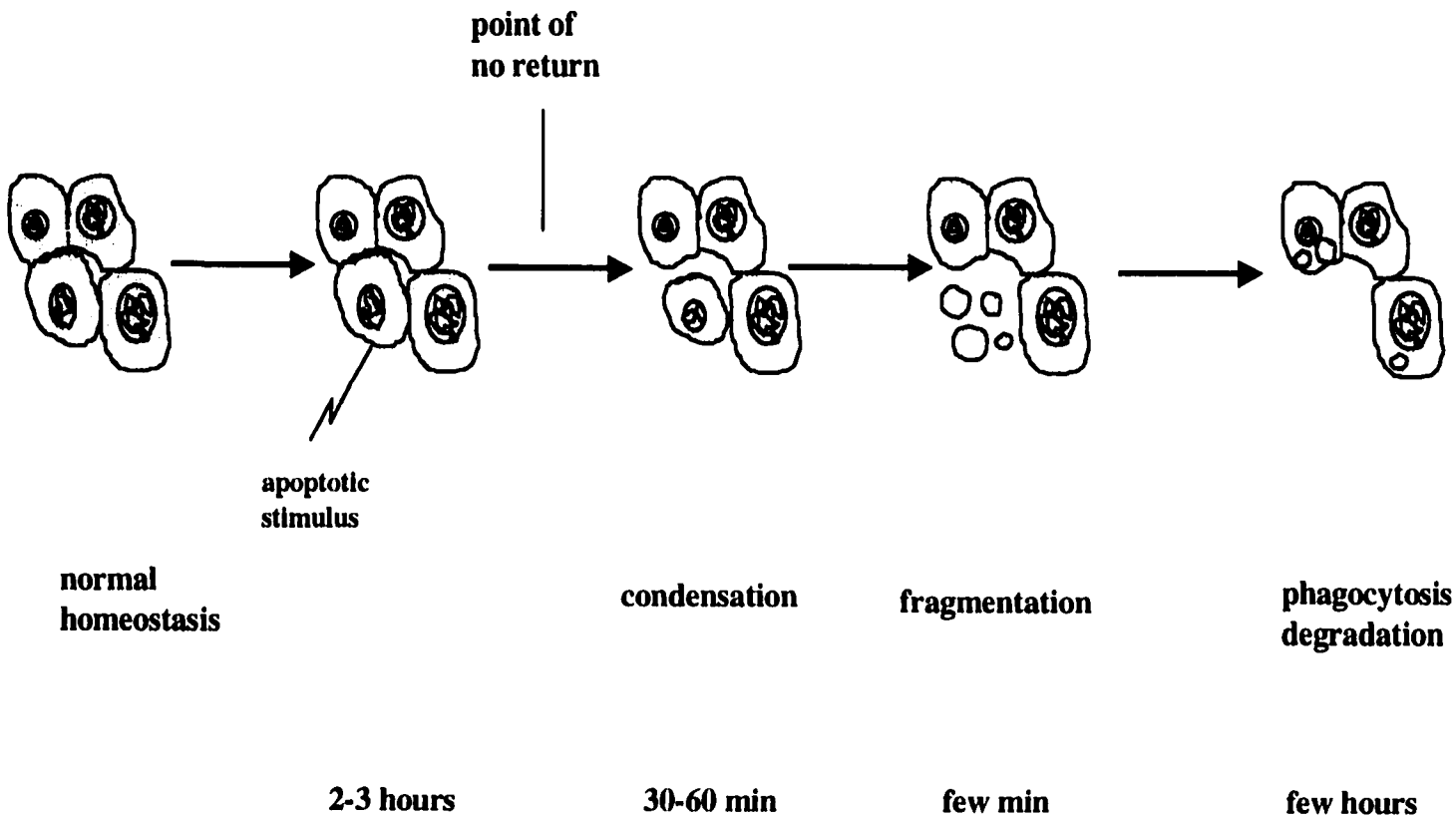
point of
no return
apoptotic
stimulus
normal
homeostasis
condensation
fragmentation
phagocytosis
degradation
2-3 hours
30-60 min
few min
few hours

a

Figure 1.2. Apoptosis stages.

a. Apoptosis involves three stages (modified from Driscoll and Calfie, 1992). These stages, shown schematically in this figure are: condensation, fragmentation and removal of the dead cell remaining. Completion of apoptosis can take from several min., in some rapidly developing tissues, to several weeks, in neurons.

b. Death signal received by the cell will ultimately cause apoptosis by protease activation. Protease activation appears to be the commitment point, or points of no return. Cells that pass this point endure cellular damage due to proteolytic activity that can not be repaired and therefore die.

Nevertheless, it is clear that the initiation and enactment of apoptosis includes four basic stages in all animals: (1) receiving an apoptosis signal, (2) a cellular assessment of the signal and commitment to apoptosis, (3) execution of cell death causing condensation and fragmentation of nuclear and cytoplasmic contents of the cell, and (4) removal of the dead cell by phagocytosis which may take from several minutes to several days to complete (Fig. 1.2a and 1.2b). In *C. elegans*, the analogous stages are commitment, execution and post-mortem. In the following sections of this chapter, I will describe some of the proteins involved in the various stages of apoptosis.

Signaling in apoptosis

Cell surface receptors that belong to the tumor necrosis factor (TNF) super family (reviewed in Smith et al., 1994; Gruss and Dower, 1995) have been the most extensively studied proteins involved in apoptotic signaling. TNF is a pleotropic cytokine, the biological activities of which are mediated by two distinct receptors; TNFR-1 (Loetscher et al., 1990), and TNFR-2 (Smith et al., 1990). The 50 kDa TNFR-1 and 75 kDa TNFR-2 are both type I proteins. Binding of TNF to TNFR-1 or TNFR-2 causes their oligomerization which results in generation of a signal. Most of the TNF biological activities, including its involvement in cell death, antiviral activity and activation of the nuclear factor kB (NFkB), have been associated with TNFR-1 (Espevik et al. 1990, Tartaglia et al., 1991; Wong et al., 1992; Pfeffer et al., 1993; Ting et al., 1996).

Binding of TNF to TNFR-1 appears to be facilitated by TNFR-2 through ligand passing

(Tartaglia et al., 1993). The similarity between TNFR-1 and TNFR-2 is limited to their external cellular region, suggesting that the two receptors are capable of interacting with different downstream components. While induction of TNFR-1 is associated with apoptosis, TNFR-2 is known to be involved in proliferation and differentiation, suggesting an overlap between cellular components that regulate life, death and differentiation. The fact that TNF can bind both TNFR-1 and TNFR-2 (Grell et al., 1995) suggests that external information is balanced with the internal information, resulting in a specific cellular response. While TNFR-2 and the highly homologous CD40 form the proliferative flank of the TNF super-family signaling pathway, TNFR-1 and Fas form the apoptotic flank (Fig. 1.3). The latter share homology over an 80 amino acid conserved sequence called the death domain. The death domain implicated in apoptosis signal transduction (Itoh and Nagata, 1993) has been identified in a few other proteins involved in apoptosis (Golstein et al., 1995).

Fas is a 55 kDa type I membrane receptor and a member of the TNF super-family implicated in cell death regulation in the immune system (Itoh et al., 1993; Oehm et al., 1992). A high percentage of T cells produced in the immune system die by apoptosis during the processes of negative and positive selection (maturation process of T cells). Fas has been shown to be involved in this process, suggesting an important role for Fas in immune system homeostasis (Brunner et al., 1996; Ju et al., 1995; also reviewed by Gruss and Dower, 1995). Induction of Fas by its ligand (FasL), or even FasL analogs, will cause

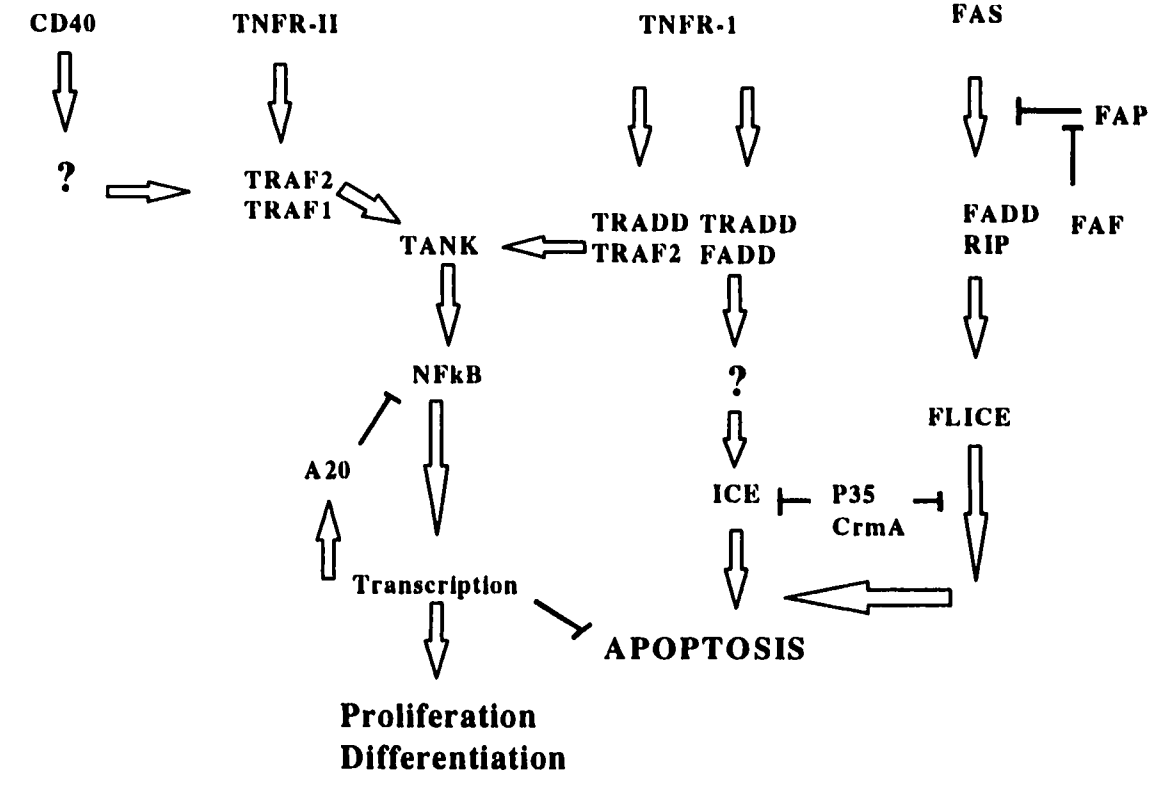
Proliferative Flank
Apoptotic Flank
CD40
TNFR-II
TNFR-1
FAS
FAP
?
TRAF2
TRAF1
TRADD
TRAF2
TANK
TRADD
FADD
FADD
RIP
FAF
NFkB
?
FLICE
A20
ICE
P35
CrmA
Transcription
APOPTOSIS
Proliferation
Differentiation

Figure 1.3. Proliferative and apoptosis signaling pathways.

Proliferative and apoptosis signaling pathways are both part of the larger signaling pathway that controls life and death of the cell. These two pathways appear to share common components. These components determine the fate of cell by directing signals to proper responding targets, causing proliferation/differentiation orapoptosis (see text for references).

rapid apoptosis of T cells. Mutations in Fas and/or its ligand result in immune system disorders that resemble systemic lupus erythematosus (Cohen and Eisenberg, 1991).

Study of *gld* (global lymphoproliferative disease) and *lpr* (lymphoproliferative) mice has revealed that the underlying cause of these phenotypes are mutations in the FasL and Fas respectively (Takahashi et al., 1994; Watanabe-Fukunagata et al., 1992; reviewed by Nagata and Golstein, 1995). In *gld* mice, the FasL is unable to bind its receptor due to a mutation in its C-terminus. In *lpr* mice, mutations occur in the death domain. Both mutations preclude generation of the death signal (Watanabe-Fukunagata et al., 1992).

Extensive use of the two hybrid system has defined some components of the apoptosis signaling pathway downstream of TNFR-1 and Fas, by identifying a number of death domain containing proteins that are capable of interacting with these receptors. These proteins include RIP (Stranger et al., 1995), FADD/MORT (Chinnaiyan et al., 1995; Boldin et al., 1995), and TRADD (Hsu et al., 1995). RIP, a 74 kDa protein and FADD, a 23.3 kDa protein both interact with the death domain of Fas (Fig. 1.3). A point mutation in human Fas similar to that observed in *lpr* mice abolishes the ability of these proteins to interact. Association of Fas, FADD and RIP activates FLICE (Muzio et al., 1996), a downstream protease resulting in cell death. FADD association with Fas appears to require phosphorylation of FADD which is mediated by FAF, a Fas associated Kinase. FAF function can be antagonized by FAP-1, a tyrosine phosphatase that can associate with the C-terminus of Fas and thereby block association of FADD and Fas (Sato et al., 1995). FADD can also bind TNFR-1. This association appears to be mediated by

TRADD, yet another death domain containing protein which functions as an adapter molecule (Hsu et al., 1996). Association of FADD, TRADD and TNFR-1 activates a downstream cascade of caspases resulting in apoptosis (Fig. 1.3).

Induction of both Fas and TNFR-1 can cause apoptosis through protease activation. Apoptotic signal generated by TNFR-1 or Fas can be inhibited by protease inhibitors (Milligan et al., 1995) suggesting that the death signal generated by the two receptors converge downstream of the point of caspase activation. The common protein that functions at this merging point has yet to be identified. Inhibition of TNFR-1 induced protease activation does not, however, block TNFR-1 activation of NFkB (Hsu et al., 1996). This suggests that the two activities of TNFR-1 diverge upstream of the protease activation point (Fig. 1.3). Over expression of TRADD results in both functions of TNFR-1 i.e. protease activation and NFkB activation. Therefore, TRADD may function as an adapter molecule directing TNFR-1 generated signals to the appropriate downstream components (Fig. 1.3).

TRADD also binds TRAF2, a member of the TRAF family of signal transducers characterized by an N-terminus RING zinc finger, a leucine zipper and the so called "TRAF domain", a C-terminus coiled coiled domain (Rothe et al., 1994). Association of TRADD and TRAF2 results in the activation of NFkB (Hsu et al., 1996). TRAF proteins also interact with the other TNF family receptors implicated in cellular proliferation i.e.

TNFR-2 and CD40 (Rothe et al., 1995a). Interaction of CD40 and TNFR-2 with TRAF proteins results in the activation of NFkB. Activation of NFkB through TRAF-receptors association requires TANK (Cheng and Baltimore, 1996) a protein which is negatively regulated by its own C-terminus domain. Activation of NFkB through TRAF2 and TANK association can be antagonized by the TNF inducible A20 protein (Song et al., 1996). A20 overexpression can make cells sensitive to apoptosis (Opipari et al., 1992; Sarma et al., 1995). A20 can interact with NFkB through its C-terminus zinc finger on one hand and on the other hand it can interact with TRAF2 through its N-terminus sequences providing a negative feed back regulating TNF induced NFkB activation (Fig. 1.3). NFkB is a general transcription factor capable of upregulating transcription of many genes that bear cognate sites in their promoter region (Thanos and Maniatis, 1995). Binding of NFkB to its cognate sites is facilitated by various high mobility group (HMG) proteins and other co-factors (Reviewed by Thanos and Maniatis, 1995) which may confer binding specificity to NFkB in response to a specific stimulus.

Enactment of cell death

Several lines of evidence have implicated cysteine proteases as final mediators of cell death (reviewed in Hale et al., 1996; Vaux and Stasser, 1996): 1. induction of apoptosis by purified granzyme B/fragmentin-2, a cysteine protease (Shi et al., 1992); 2. blockage of normally occurring apoptosis in *C. elegans* mutants lacking the cysteine protease *ced*-3; 3. significant homology of Ced-3 with interleukin-1β converting enzyme (ICE) 4. induction of apoptosis by an over-expression of ICE (Yuan et al., 1993; Miura et al.,

1993); 5. inhibition of apoptosis by protease inhibitors (Sarin et al., 1993); and 6. cleavage of proteins such as β-actin (Kayalar et al., 1996) and lamin B1 (Neamati et al., 1995) during apoptosis.

Cysteine proteases are normally present in the cytoplasm as inactive heterodimer proenzymes (e.g. in the case of ICE (caspase-1), each consisting of two subunits of p10 and p20). Activation of proenzyme requires specific cleavage at their aspartic acid residue. A variety of apoptotic signals cause this cleavage thus converting the inactive heterodimers into active heterotetramers (Wilson et al., 1994). The mechanism of protease activation by a given apoptotic signal is not, however, clear. In the nematode *C. elegans*, mutations in *ced*-4 prevent cell death suggesting that Ced-4 functions upstream of the ICE-like Ced-3. It has been recently shown that the ced-4 product plays a role in the stimulation of Ced-3 (Seshagiri and Miller, 1997). Characterization of the exact role that Ced-4 plays in activation of Ced-3 may provide insight into caspase activation. Completion of the picture may have to await characterization of the recently identified Ced-4 homologues (Zou et al., 1997). One possible mechanism of protease activation may be dimerization of the proenzyme monomers due to stimulation and subsequent ligation of the receptor monomers resulting in their auto-catalysis and formation of an active heterotetrameric caspase. Such an induction/activation mechanism is fairly well characterized in the activation of membrane receptors such as insulin receptors or insulin-like growth factors receptors (IGF-I and IGF-II) which results in the auto- and/or cross-phosphorylation activities which relay the signal to second messengers (De Meyts et al.,

1995a and b; Takata and Kobayashi, 1994). Other possibilities include autocleavage of proenzyme due to an increase in the steady state of the intrinsic level of death signal (reviewed by Vaux and Stasser, 1996). This may cause transcriptional upregulation of protease subunits by transcription factors such as P53 and thus increase the level of cellular proteases resulting in their auto-cleavage (Faucheu et al., 1995; Tewari et al., 1995b). This is in keeping with the over expression of cysteine proteases causing cell death in various cultured cells. Whether these proteases function in linear pathways leading to the activation of one or more downstream proteases that execute cell death or in a parallel fashion is presently unclear.

ICE appears to be the first protoenzyme that becomes activated during apoptosis (Yuan et al., 1993; Interleukin-1β converting enzyme/ICE has be reviewed by Thornberry, 1994) and therefore, plays an important role in apoptosis. ICE knockout mice are defective in IL-1β production but interestingly, however, demonstrated a normal development (Kuida et al., 1995 and Li et al., 1995). This was an early indication of existence of other ICE-like proteases functioning during development. ICE knockout mice, however, develop immune system disorders later in life suggesting the importance of ICE in homeostatic cell death (Hale et al., 1996; Vaux and Strasser, 1996). In the past three years, over a dozen cysteine proteases implicated in apoptosis have been identified in various animals (reviewed in Vaux and Strasser, 1996). These proteases (now called caspases, Alnemri et al., 1996) include NEDD2/Ich-1 (Kumar et al., 1994; Wang et al., 1994), CPP32/YAMA/apopain (Fernandes-Alnemri et al., 1994; Tewari et al., 1995b; Nicholson

et al., 1995) ICErelII/TX/ICH-2 (Munday et al., 1995; Faucheu et al., 1995; Kamens et al., 1995), ICErelIII (Munday et al., 1995), MCH2 (Fernandes-Alnemri et al., 1995a), Mach/FLICE (Boldin et al., 1995; Muzio et al., 1996), and Mch-1/ICE-LAP3/MCH-3 (Lippke et al., 1996; Duan et al., 1996; Fernandes-Alnemri et al., 1995b). Caspases share a conserved pentamer QACRG motif. Mutations in the residues of this conserved domain result in the loss of function. Proteases can also be blocked by naturally occurring protease inhibitors such as viral protein CrmA or synthetic inhibitors such as YVAD tetramer that sequesters this conserved pentamer. A substitution of R to Q has been identified in the members of a recently identified sub-class of aspartate-specific cysteine proteases (Fernandes-Alnemri et al., 1996) suggesting variability in the conserved pentamer.

ICE, activated by apoptotic signals, in turn, cleaves and activates several downstream proteases including YAMA (Fig. 1.4). YAMA has been shown to specifically target the 116 kDa nuclear protein PARP (poly ADP-ribose polymerase), producing a signature 85 kDa cleavage product (Kaufmann et al, 1993; Lazebnik et al., 1994; Tewari et al., 1995b). It has recently been shown that PARP can also be cleaved by Mch4 (Fernandes-Alnemri et al., 1996). Mch4 is capable of *in vitro* cleavage of another close relative Mch3. Auto-cleavage and mutual cleavage of proteases during apoptosis generate a network of active proteases causing cell death by destroying proteins that are important for cell survival. Only a number of substrates for these proteases have been identified. PARP, for instance, is specifically cleaved by CPP32 (Tewari et al., 1995b). Yet other proteases may act in a more non-specific manner.

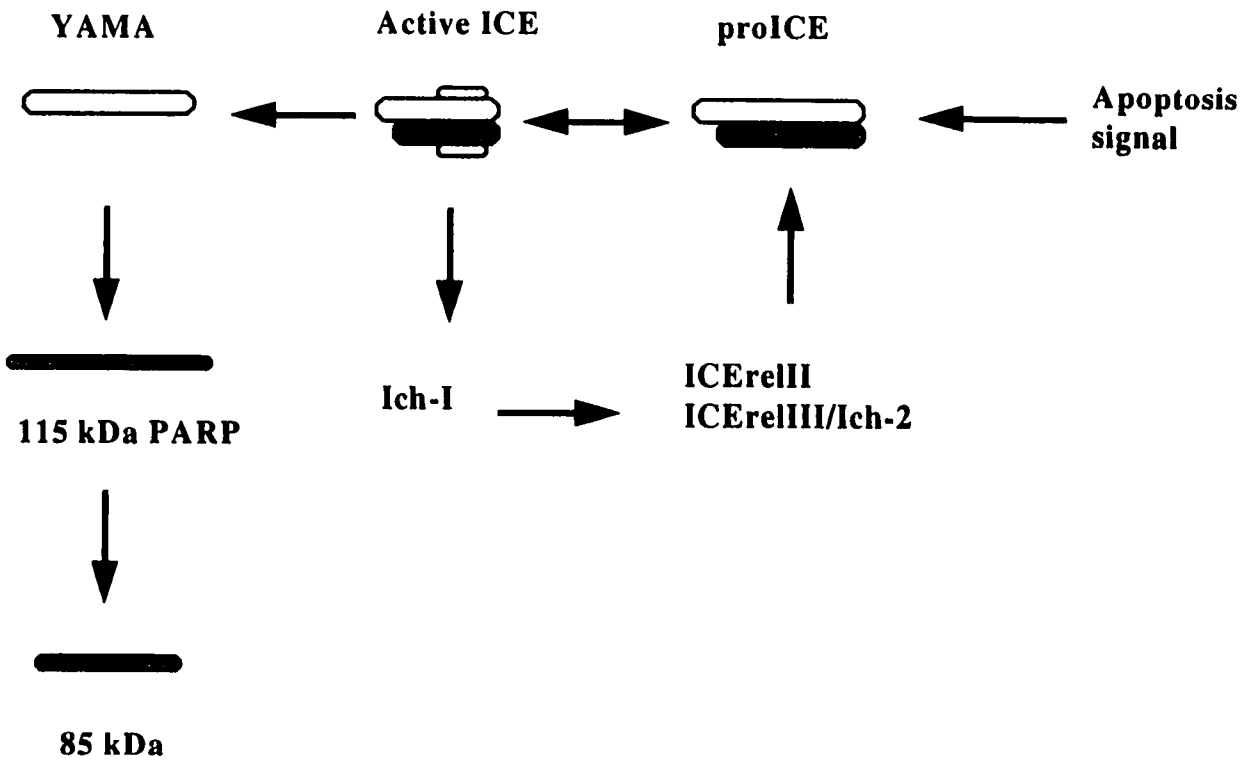
YAMA
Active ICE
proICE
Apoptosis signal
115 kDa PARP
Ich-I
ICErelII
ICErelIII/Ich-2
85 kDa

Figure 1.4. Cascade of protease activation during apoptosis.

Apoptosis signal activates proteases that function as cell death effectors. The first protease that is activated appears to be ICE which can in turn activate several downstream proenzymes. This figure depicts activation of protease cascade during apoptosis. One important outcome of proteotytic activity during apoptosis is cleavage of 116 kDa PARP. This generates an 85 kDa cleavage product which is used as an apoptosis marker (see text for references).

None of the proteases substrates identified to date have an indispensable function, the absence of which may cause total cellular collapse. The cellular death may, nevertheless, be due to the accumulation of cleavage of various substrates. There may be one exception to this and that is PARP which is involved in DNA repair and its cleavage is viewed as a marker for apoptotic cells. Knockouts and transgenics of PARP however develop normally (Wang et al., 1995; Simbulan-Rosenthal et al., 1996) suggesting that PARP function could be replaced by other proteins. Moreover, further characterization of proteases specificity may result in the identification of target proteins that are indispensable for cell survival, the cleavage of which results in inevitable death.

Apoptosis regulation

Cellular decision between life and death is subject to the effect of internal elements capable of promoting and/or inhibiting cell death thereby regulating this important process. Many mammalian apoptosis regulators belong to the expanding protein family of Bcl-2 (reviewed in Hale et al., 1996). Bcl-2 is a 26 kDa protein encoded by *bcl*-2 that was originally cloned from a break point on chromosome 14, in individuals suffering from B cell lymphoma (Tsujimoto and Croce, 1986). The most common genetic abnormality observed in these patients is a translocation t(14:18) which places *bcl*-2 under the control of a constitutively expressed immunoglobulin promoter enhancer. Overexpression of Bcl-2, which was initially thought to be an oncoprotein, does not cause cell cycle progression or proliferation. Rather it makes cells resistant to apoptosis (Seto et al., 1988) and thus results in an abnormal accumulation of cells (e.g. B cells in the case of B cell lymphomas). The anti-apoptotic capability of Bcl-2 was delineated by rescuing Ced-9 null *C. elegans*

mutants (Vaux et al., 1992; Hengartner and Horvitz, 1994). Ced-9 is the sole nematode protein capable of negatively regulating apoptosis. The existence of a mammalian protein family corresponding to *C. elegans* protein involved in apoptosis is not restricted to caspases. This redundancy is also true for the expanding Bcl-2 family, members of which show structural and functional homology to Ced-9. Mammalian homologues of Ced-9, however, include proteins that are capable of regulating apoptosis both positively and negatively (Boise et al., 1993; Yin et al., 1994).

Ced-9 loss of function mutation in *C. elegans* has lethal effect (Yuan, 1995) but Bcl-2 knockout mice initially develop normally (Veis et al., 1993; Kamada et al., 1995). Both Bcl-2 knockout and transgenic mice, however, develop various tissue and immune system disorders caused by dysregulation of cell death in their later stages of life (McDonnell et al., 1989; Sentman et al., 1991; Kamada et al., 1995; Sorenson et al. 1995). Nevertheless, the initial normal development of these mice indicate the existence of other proteins capable of functionally replacing Bcl-2. Several proteins with homology to Bcl-2 have been identified including: Bax (Oltvai et al., 1993), Bcl-x (Boise et al., 1993), Bak (Chittenden et al., 1995; Farrow et al., 1995; Kiefer et al., 1995) and Bad (Yang et al., 1995). These proteins share common sequences called Bcl-2 homology (BH) regions. Four BH domains have been identified in various members of Bcl-2 proteins designated BH1, BH2, BH3, and BH4. Every Bcl-2 protein bears one or more BH domains which are involved in protein:protein interactions (Yin et al., 1994; Sato et al., 1994). This indicates that BH domains confer interaction specificity to Bcl-2 family members. BH1 and BH2, for example, are used in heterodimerization of Bcl-2 with Bax (Yin et al., 1994) while Bax

homodimerization is mediated by BH3 (Zha et al., 1996). Mutations in Bcl-2 homology domains disrupt the ability of these proteins to form homo- and/or hetero-dimers (Yin et al., 1994). BH1 and BH2 are found in almost all of the Bcl-2 family members. BH4 is, however, found only in the Bcl-2 family members that are capable of inhibiting apoptosis.

Extensive interaction among members of the Bcl-2 protein family has been documented employing the yeast two hybrid system (Sato et al., 1994). Formation of homo- and hetero-dimers by these proteins appear to regulate apoptosis (Oltvai and Korsmeyer, 1994) (Fig. 1.5). One of the proteins that Bcl-2 forms heterodimers with is Bax (Oltvai et al., 1993). Bax (Bcl-2 associated protein X) is a 21 kDa protein capable of forming homodimers particularly at high intracellular concentration (Oltvai et al., 1993). Formation of Bax homodimers does not, however, cause apoptosis unless an appropriate apoptotic signal is present (Korsmeyer et al., 1993). Mutations within Bcl-2 BH1 and BH2 domains that interrupt its heterodimerization with Bax are associated with a loss of apoptotic suppression (Yin et al., 1994). These mutations, however, do not prevent the formation of Bcl-2 homodimers suggesting that Bcl-2 must interact with Bax to exert its anti-apoptotic function. One model is that Bcl-2 and Bax exist in a balanced steady state in the cytosol. Under normal circumstances, Bax forms homodimers which makes cells sensitive to apoptosis (Fig. 1.5). Increased Bcl-2 level can competitively prevent formation of Bax homodimers and thus make cells resistant to apoptosis. It appears that Bax homodimerization (promoting cell death) and Bax/Bcl-2 heterodimerization

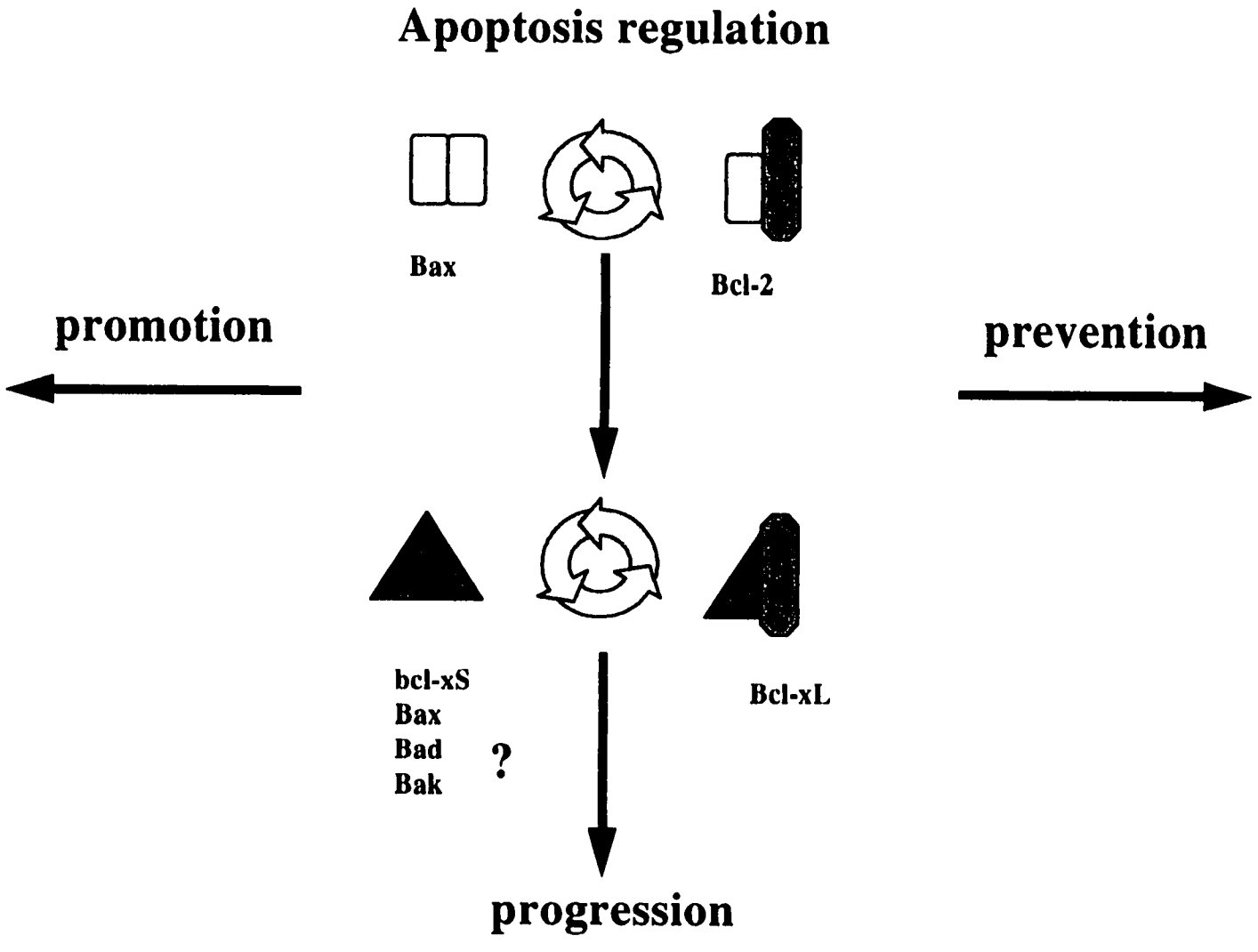
Apoptosis regulation
Bax
Bcl-2
promotion
prevention
bcl-xS
Bax
Bad
Bak
?
Bcl-xL
progression

Figure 1.5. Regulation of apoptosis.

Interaction of various Bcl-2 family members appear to constitute a multiple level switching mechanism which regulates progression of apoptosis. Dimerization of Bax, for instance, promotes apoptosis while dimerization of Bax and Bcl-2 inhibit apoptosis. In this figure, interactions of several Bcl-2 related proteins have been shown to involve in progression or prevention of apoptosis and their possible sequence of function have been depicted (see text for references).

(inhibiting apoptosis) function as a switch capable of turning apoptosis machinery on and off (Fig. 1.5). In keeping with this model, it has been demonstrated that cells with high level of Bax and low level of Bcl-2 are more susceptible to apoptosis (Krajewski et al., 1995) (Fig. 1.5).

Bax can be functionally replaced by two other members of the Bcl-2 family, Bad (Bcl-2 associated death protein) and Bak (Bcl-2 associated kinase). Bcl-2 can interact with Bad and Bak through their BH1 and BH2 domains forming heterodimers that block apoptosis (Yang et al., 1995).

Overproduction of both Bad or Bak, similar to Bax, promotes formation of their homodimers leading to sensitivity to apoptosis. Heterodimerization of Bcl-2 with Bak inhibits Bak homodimerization and thus blocks apoptosis (White, 1996). Moreover, Bax can heterodimerize with Bak. This interaction in a manner similar to Bax:Bax interaction can rival the anti-apoptotic ability of Bcl-2 (Chittenden et al., 1995; Farrow et al., 1995).

Bcl-x (Bcl-2 related X protein), another member of the Bcl-2 protein family (Boise et al., 1993) is comprised of two isoforms, Bcl-xL (large) and Bcl-xS (small) generated through alternative splicing. Bcl-xL has 43% sequence homology with Bcl-2 and inhibits apoptosis. Bcl-xS is missing a 63 a.a. region including BH1 and BH2 and promotes apoptosis (Boise et al., 1993). Bcl-xL and Bcl-xS can form hetero- and homodimers in a manner very similar to Bax and Bcl-2, inhibiting or promoting apoptosis respectively. Bcl-xL can heterodimerize with Bax or Bad and inhibit apoptosis (Yang et al., 1995; Chittenden et al.,

1995; Farrow et al., 1995). Interaction of Bak and Bax with Bcl-xL does not, however, prevent its ability to suppress apoptosis. This suggest that Hetero- and homodimers of Bcl-x isoforms (Oltvai et al., 1993) are also involved in regulation of apoptosis (Cheng et al., 1996) (Fig. 1.5). Therefore, it appears that the ratio of Bcl-2 and Bcl-xL to Bax, Bak and Bcl-xS produces multiple level of check points determining apoptosis progression (Fig. 1.5). Generation of two isoforms capable of performing opposite functions from the same mRNA through alternative splicing is a rare event worthy of further investigation.

What is the molecular mechanism of apoptosis suppression by Bcl-2 or Bcl-xL? Recent studies have shown that Bcl-2 localizes to cytoplasmic surface of the nuclear membrane, the outer mitochondrial membrane and the endoplasmic reticulum (Jacobson et al., 1994; Akao et al., 1994; Lithgow et al., 1994). Bcl-xL has also been localized to mitochondria (Fang et al., 1994b). Several mechanisms have been proposed for Bcl-2 function including suppression of proteases activity, prevention of cytochrome C release to the cytoplasm, modulation of reactive oxygen species and free Ca2+ regulation (reviewed by Hale et al, 1996). A role in the translocation of specific proteins to the nucleus are among the mechanisms of actions proposed for Bcl-2 (reviewed in Hale et al., 1996). It has been suggested that Bcl-2 may function as antioxidant or free radical scavenger as well (Hockenbery et al., 1993). These suggestions are in keeping with the localization of Bcl-2 in the mitochondrial membrane where reactive oxygen species are high (Hockenbery et al., 1990). Models of Bcl-2 function based on its localization to mitochondria and its antioxidant function, however, have to be formulated with caution. It has been shown that Bcl-2 or Bcl-xL can suppress apoptosis in cells lacking intact mitochondria or in cells kept

under anaerobic conditions, hence with the production of minimal free radicals (Jacobson and Raff, 1995; Shimizu et al., 1995).

The inhibition of apoptosis by Bcl-2 through regulation of Ca2+ concentration also falls short of completely explaining the mode of action of Bcl-2. Apoptosis can occur and be blocked by Bcl-2 without modulation in the cellular level of free calcium ions (Zhong et al., 1993). Furthermore, no direct interaction between Bcl-2 and any of the proteases implicated in apoptosis have been documented. These studies may suggest that Bcl-2 is not directly involved in suppressing apoptosis, rather it may play a central role in regulating and/or modulating other elements or pathways important in apoptosis. It has recently been shown that Bcl-2 may function as an ion channel (Schendel et al., 1997), which may be subject to modulation by homologue proteins such as Bax and Bcl-xS. Elucidating the true mode of Bcl-2 action requires further examinations. Nevertheless, the ability of bcl-2 to protect a variety of cell lines against apoptosis induced by various triggers (Vaux et al., 1988; Rabizadeh et al., 1993; Mah et al., 1993; Batistou et al., 1993; Nunez et al., 1990; Hockenbery et al., 1993; Allsopp et al., 1993; Garcia et al., 1992) suggests its important function as a central control or check point in the apoptosis.

Viral inhibitors of apoptosis

Viral infection can cause early cell death demonstrating features of apoptosis. This has been deemed as a cellular defense mechanism to maintain viral propagation (Clouston and Kerr, 1985; Clem and Miller, 1993). The infected cell sets off an intrinsic suicide

mechanism to protect the organism against intracellular propagation and further spread of viral infection (White, 1993).

In a counter measure, viruses have developed proteins that can interact with the components of apoptosis signaling pathway(s) and block it (reviewed by Clem and Miller, 1994a; White and Gooding, 1994a). Baculovirus IAPs (inhibitor of apoptosis proteins), for instance, have been shown to bind to the membrane receptor (TNFR) complexes (Rothe et al., 1995a). This interaction may prevent progression of the death signal. Additional viral proteins such as Epstein-Barr virus (EBV) BHRF1 (BamHI fragment H rightward open reading frame 1), African swine fever virus LMW5HL, and EBV LMP-1 (latent membrane protein-1) modulate further downstream regulators of apoptosis (Oudejans et al., 1995; Neilan, et al., 1993). Both BHRF1, a putative transmembrane protein and LMW5HL show sequence similarity to Bcl-2 (Henderson et al., 1993). This indicates that BHRFI and LMW5HL may inhibit apoptosis in a fashion similar to Bcl-2 (Henderson et al., 1993) or function as Bcl-2 modulators. LMP-1 inhibits apoptosis by increasing the level of Bcl-2 (Henderson et al., 1991). Yet other viral apoptosis inhibitor such as Cowpox virus CrmA (cytokine response modifier A) interacts with ICE (Ray et al., 1992; Komiyama et al., 1994) and with lesser affinity, with other ICE-like proteases (Wang et al., 1994; Tewari et al., 1995a, b; Nicholson et al., 1995), to inactivate them. Interaction and subsequent cleavage of CrmA by ICE results in the formation of a permanent complex occupying the ICE active site.

Baculoviruses inhibitors of apoptosis (IAPs)

Baculoviruses are large DNA containing viruses that infect insect cells. Baculoviruses have developed two sets of proteins that are capable of interacting with components of the host apoptosis pathway inhibiting cell death. These proteins are p35 and IAPs (inhibitor of apoptosis proteins). p35, encoded by *Autographa californica* multiply embedded nuclear polyhedrosis virus (AcMNPV) (Friesen and Miller, 1987; Clem et al., 1991) and by *Bombyx mori* nuclear polyhedrosis virus (Clem et al., 1991; Hershberger et al., 1992; Kamita et al., 1993) has 299 amino acids with a molecular weight of 34.8 kDa and no known signal sequence or transmembrane domains (Clem and Miller, 1994b; Hershberger et al., 1994). p35 interaction with ICE as well as its weaker binding to other ICE-like caspases results in the formation of a permanent complex that inhibits its protease activity (Bump et al., 1995) in a manner similar to CrmA. Infection of cells by viruses that lack p35 causes premature apoptotic cell death (Clem et al., 1991; Hershberger et al., 1992; Kamita et al., 1993) in keeping with an anti-apoptotic activity of p35.

Genetic complementation of an AcMNPV mutant known as annihilator (vAcAnh) lacking p35 resulted in the discovery of a second set of baculovirus inhibitors of apoptosis proteins (IAPs) in *cydia pomonella* granulosis virus (CpGV) and *Opgyia pseudotsugata* nuclear polyhedrosis virus (OpMNPV) (Crook et al., 1993). These new proteins, designated Cp-IAP and Op-IAP respectively, are both anti-apoptotic and can rescue cells infected with vAcAnh. Viral IAPs inhibit apoptosis induced by a variety of triggers in different cellular backgrounds suggesting a central site of action in the apoptosis signaling pathway (reviewed by Clem et al, 1996). Interestingly, Ac-IAP, a very similar protein

encoded by AcMNPV shows no anti-apoptotic capability (Braunagel et al., 1992; Crook et al., 1993).

The 31-33 kDa viral IAPs contain two 70 amino acid repeats BIR (baculovirus inhibitor of apoptosis protein repeat) domains in the N-terminus which show no similarity to any known protein motifs (reviewed by Clem et al., 1996). IAPs, also, have a C_3HC_4 type RING zinc-finger motif in their C-terminus (Crook et al., 1993; Clem and Miller, 1994b; Birnbaum et al., 1994). Similar RING zinc fingers have been found in many other proteins that may be involved in protein:protein interaction. In domain swapping experiments, Op-IAP BIR motif fusion to an Ac-IAP RING zinc finger generated a chimeric protein with no anti-apoptotic activity (Clem and Miller, 1994b). This suggested that despite high similarity among RING zinc fingers, they can not freely substitute for one another indicating as yet unidentified critical specific structural differences between various RING zinc finger motifs.

Viral IAPs were demonstrated to protect various cells against a variety of apoptotic signals (Clem and Miller, 1994b; Hawkins et al., 1996; Crook et al., 1993) instigating a search for IAPs in higher life forms, including mammals. This search resulted in the identification of several proteins with significant homology to viral IAPs and their ability to inhibit apoptosis in different cell lines induced by a variety of triggers e.g. TNFα, menadione (a free radical inducer), staurosporine (a general kinase inhibitor) and serum deprivation (Liston et al., 1996). More than a dozen IAPs have been reported to date including four human (Liston et al., 1996; Rothe et al., 1995a; Duckett et al., 1996), and

their four murine homologues (Yaraghi, Z., unpublished; Farahani et al., 1997; Liston et al, 1997a), an avian (Digby et al., 1996), and two *Drosophilia* IAPs (Hay et al., 1995).

Human IAPs

The first human protein with strong homology to baculovirus IAPs to be identified was the spinal muscular atrophy (SMA) associated NAIP (Roy et al., 1995). Surprisingly, *naip*, with 18 exons, a 6.1 kb mRNA and encoding a protein of approximately 154 kDa, has no RING zinc finger and possesses three BIR domains instead of the two found in viral IAPs. NAIP has been shown to be capable of inhibiting apoptosis induced by different triggers in a variety of cell lines (Liston et al., 1996). Consistent with the premature death of motorneurons observed in SMA due to enhanced apoptosis (Oppenheim, 1991), NAIP is strongly expressed in motorneurons of the spinal cord and has been shown to protect neurons against ischemia induced apoptosis (Xu et al., 1997).

The other human IAP genes i.e. *hiap-1*, *hiap-2*, (human IAP-1 and -2) and *xiap* (X-linked IAP) each encodes a protein containing three N-terminal BIR domains and as with the baculoviral IAPs but not NAIP, a C-terminal RING zinc-finger motif (Liston et al., 1996). All mammalian IAPs cloned to date possess apoptotic suppression activity (Liston et al., 1996; Hay et al., 1995; Uren et al., 1996; Duckett et al., 1996; Farahani, R., unpublished). Two of the four human IAPs cloned to date (i.e. *hiap*-1 and *hiap*-2) have been shown to interact with components of the TNF (tumor necrosis factor) apoptotic pathway (Rothe et al., 1995a and b) suggesting one mechanism through which IAP family members may exert their anti-apoptotic function.

Cloning and characterization of *miap*-3

The main objective of this project was to clone and characterize the murine homologue of *xiap* in an effort to develop resources for further examination of the role of IAPs in apoptosis. To that end, a *xiap* cDNA probe was used to screen mouse cDNA libraries that lead to the identification of *miap*-3 (for murine *iap*-3) the homologue of *xiap*. Sequence data demonstrate that *miap*-3 is the true murine homologue of the human *xiap* and similarly is able to protect cells against apoptosis. Further characterization of Xiap and Miap-3 revealed that the anti-apoptotic function of IAPs resides in their BIR domains and that BIR domains are cleaved and translocated to the nucleus during apoptosis.

Chapter II

Cloning and characterization of *miap*-3

Introduction

Physiological cell death or apoptosis is used by multicellular organisms as a mechanism to eliminate harmful cells such as cells infected with virus (Clouston and Kerr, 1985; White, 1993; and Clem and Miller, 1993). In turn, viruses have developed proteins that can inhibit apoptosis so that they obtain sufficient time for propagation (reviewed by Clem and Miller, 1994a; and White and Gooding, 1994). Among the best characterized of such viral proteins are the baculovirus inhibitor of apoptosis proteins (IAPs) (Crook et al., 1993, and Clem and Miller, 1994a). These proteins interact with components of the cell death signaling pathway and thus inhibit apoptosis (for a review see Hale et al., 1996 and references therein).

The first non-viral IAP identified was NAIP, one of the two genes deleted in patients with spinal muscular atrophies (Roy et al., 1995). Database searches for other sequences with homology to viral IAPs revealed two STSs (site tag sequences) with homology to the RING zinc finger found in baculovirus IAPs. Primers were designed and used in PCR (polymerase chain reaction) to amplify a 200 bp fragment from a human liver cDNA library with high similarity to the baculoviral IAP RING zinc finger. This fragment was used as a probe to screen human cDNA libraries. Screening human fetal brain and liver cDNA libraries resulted in the identification of three other human genes encoding IAPs (Liston et al., 1996) designated *xiap* (X-linked IAP), *hiap*-1 and *hiap*-2 (for human *iap*-1 and -2). Identification of *xiap*, *hiap*-1, and *hiap*-2 has increased the number of human IAPs to four including NAIP.

xiap has a coding region of approximately 1494 bp which translates into a protein with 497 amino acids and calculated size of 55 kD. Northern blot analysis revealed that a *xiap* message of approximately 9 kb is present in all the tissues examined (Liston et al., 1996). This indicated that *xiap* possessed large 5' and/or 3' UTRs (untranslated regions). Further analysis of *xiap* genomic structure revealed that, it, indeed, had a greater than 6 kb 5' UTR. *xiap* is composed of 7 exons separated by 6 intervening sequences spanning an approximately 25 kb genomic DNA (Lagace, M., unpublished) on the human Xq25 (Rajcan-Separovic et al., 1996). A similar genomic structure has been observed for *hiap*-1 and *hiap*-2 which were assigned to the region of q23 on the short arm of chromosome 11 in a tandem array spanning 40 kb of genomic DNA (Rajcan-Separovic et al., 1996; and Liston, et al, 1997a). *hiap*-1 and *hiap*-2 5' UTRs, however, do not appear to be so large

as *xiap* 5' UTR. *hiap*-1 and *hiap*-2 express a 6.6 and a 3.9 kb message respectively in all tissues examined (reviewed in Liston et al., 1997b).

xiap, *hiap*-1 and *hiap*-2 each encode three N-terminal BIR domains and a C-terminal RING zinc-finger motif. The BIR domains are encoded by the first N-terminal large exon extended to the 5' UTR. The last exon encodes the RING zinc finger extending to 3' UTR. The two large 5' and 3' exons flank 4 internal exons that encode the linker region between BIR domains and the RING zinc finger. The high degree of similarity in the structure of *xiap*, *hiap*-1, and *hiap*-2 may indicate a single ancient gene as the progenitor of all human *iaps*.

Similar to NAIP, expression of *xiap*, *hiap*-1, and *hiap*-2 protects various cell types against apoptosis induced by different triggers (Liston et al., 1996). In fact *xiap* has proved to be the most potent of all the human IAPs. To facilitate further examination of *xiap* function as a prototype of human IAPs, I have cloned and characterized its murine homologue. The mouse gene called *miap*-3 (for murine *iap*-3) has a coding sequence of 1491 bp translating into 496 amino acids with the calculated size of approximately 55 kDa. *miap*-3 encodes three N-terminal BIR domains and a C-terminal RING zinc-finger motif. *miap*-3 has been assigned to the region of A3-A5 on mouse chromosome X. Miap-3 shows 94% a.a. homology to Xiap and much like *xiap*, its unusually large message of approximately 8 kb is present in all of the tissues examined (Farahani, et al., 1997).

This chapter will describe the details of isolation and preliminary characterization of *miap*-3. Cloning and characterization of *miap*-3 provided valuable information that later proved to be useful in generating research tools such as cell lines, and knockout mice. These tools are currently being used to delineate some of the enigma of IAPs function and their role in apoptosis.

Materials and Methods

Nucleic acid isolation and characterization. Phage and plasmid DNA were prepared as previously described (Sambrook et al., 1989). RNA was isolated with Trizol (GibcoBRL) reagent using manufacturer's guidelines. Briefly, tissues were isolated from adult and newborn Balb C mice sacrificed by CO_2 asphyxiation and total RNA was extracted. Northern blot analysis was performed using standard methods. Approximately 20 μg of total RNA samples were fractionated on an 1.0%/2.2 M agarose/formaldehyde gel in MOPS buffer and transferred to nylon membrane (Amersham) by capillary blotting. Blots were UV cross-linked and/or baked at 85 °C for 2 hours. Total RNA and Poly(A)$^+$ blots (Clontech) were hybridized at 42 °C overnight to a 1.8 kb ^{32}P-labeled (*redi*prime, Amersham) probe containing most of the *miap*-3 coding sequence plus a portion of the 3' UTR. Blots were washed with 2xSSC, 0.1xSDS at room temperature followed by two consecutive washes in 0.5 and 0.2xSSC, 0.1xSDS at 55 °C for a total of 30 min.

Genomic and cDNA library screenings. A murine embryonic cDNA library in λgt11 and two independent murine liver genomic libraries in λFIXII (Clontech) were screened (approximately 10^6 clones from each library) with human *xiap* cDNA probes. Positive

cDNA plaques were purified and amplified by PCR and sub-cloned into pCRII vector (Invitrogen TA cloning kit). Positive genomic DNA clones were prepared by infecting appropriate *E. coli* strains using a high titer phage sample, growing transfected cultures overnight and extracting phage DNA. Genomic and cDNA clones were arranged in separate respective contigs by Southern blotting and restriction mapping analysis.

DNA sequencing. The ends of each cDNA and genomic clone were sequenced (Applied Biosystems ABI 373 automated sequencer) using T3 and T7 or M13 and M13 reverse universal primer sets. Sequence data were analyzed using Wisconsin Genetics Computer Group (GCG) software package and BLAST network service of the National Center for Biotechnology Information. Gaps were covered by sequencing sub-cloned fragments and/or primer walking. For a list of primers used, see Table 2.1. Exon-intron boundaries were determined by sequencing genomic clones using cDNA-specific primers and aligning cDNA and genomic sequences.

Fluorescent *In Situ* Hybridization. Mouse chromosomes were prepared as before (Fang et al., 1994a). Briefly, mouse spleen lymphocytes were isolated and cultured in RPMI 1640, supplemented with 15% fetal calf serum, 3 μg/ml Concanavalin A, 10 μg/ml lipopolysaccharide and $5x15^{-5}$ M mercaptoethanol at 37 °C for 4 hr. Cells were treated with 0.18 μg/ml BrdU for an additional 14 hr and were cultured in α-MEM containing 2.5 μg/ml thymidine for 4 hr at 37 °C. Chromosome slides were prepared by hypotonic treatment and fixation. The *miap*-3 GPC (genomic phage clone) 3a probe was

labeled using a BRL BioNick labeling kit for 1 hr at 15 °C. FISH detection was performed as before (Heng and Tsui, 1993). The slides were baked, RNase A treated, denatured and ethanol dehydrated. Denatured probe was hybridized with the chromosome spread overnight. Signal amplification and detection were performed as previously outlined (Heng et al., 1992 and Heng and Tsui, 1993).

Expression of mouse full-length coding cDNA. Full-length *miap*-3 coding cDNA was constructed by ligating two overlapping clones using an AvaI site common to the two clones (Fig 2.1). The full-length coding region was PCR amplified using a primer set in which one primer contained a BamHI site and the second contained an EcoRI site (Table 2.1). PCR products were double digested with BamHI and EcoRI and then sub-cloned into the BamHI/EcoRI linearized expression vectors pcDNA3 (Invitrogen). A 300-bp human *myc* epitope tag encoding six repeat of the sequence MEQKLISEEDL allowing detection of Myc-IAP fusion proteins by monoclonal anti-Myc antibody, was

2736	CCCCGGGCTG CAGGAATTC*	R
2935	TGGAGACCAA TGCTAACAGC	Exon 6 F
2936	GCTCAGAAAG ATAATACGGA GG	Exon 5 F
2966	GTGTTTGGGC TTCACATAAT G	Exon 1 R
2968	GTGTTTTAGG ATTCTGCCC	Exon 6 F
2997	CTCATCCAAT AGGTATTTGC AC	Exon 3 R
3046	ACGTAGGTAA ATGTACACGC C	Exon 6 F
3047	GTGTTGAGTC TTCTTTTGAT GG	Exon 1 R
3055	CACTTAGCAT GCTGGTCCC	Exon 2 R
3056	GGCGATAAAG TGAAGTGCTT C	Exon 2 F
3057	AAAGATTCCT CAAGTGGATG G	Exon 3 R
3059	AATACCTATT GGATGAGAAG GG	Exon 3 R

primer number	primer sequence	primer orientation
2261	TGCTTCAGCA CATTGTTTAC A	Exon 6 R
2262	CAGCTAAGGC GCCTGCAAGA G	Exon 6 F
2264	ATGTCCACAA GGAACAAAAA CG	Exon 6 R
2375	TCCCGAGGAA CCCTGCCATG	Exon 1 F
2415	GGAGCAGCTT GCAAGAGCTG G	Exon 1 F
2416	AGTGTCCCAT GTGCTACACA G	Exon 6 F
2421	TGTCTTTCTG AGCATTCACT AG	Exon 5 R
2440	CCTATCAGAA CTCACACCAG A	Exon 1 F
2442	CACTGGCTAA ATGATACAGC TGA	Exon 6 R
2490	TTATCGCCTT CACCTAAAGC	Exon 2 R
2491	CACTTGAGGA ATCTTCGGGA AG	Exon 3 F
2543	GTACTTGCAG ACACCAATAA GG	Exon 1 F
2544	CCTTATTTGG TGTCTGCAAG TAC	Exon 1 R
2565	CCACAAGGAA CAAAAACGAT A	Exon 6 R
2566	AAAATGGCCA GTACAAATCT G	Exon 1 F
2574	CCAGAGAAGA TGACTTTTAA CAG	Exon 1 F
2575	TGTGGTGCCC CACTAAGAC	Exon 6 R
2576	ACCCATCCAC TTGAGGAATC	Exon 3 F
2577	TTTTTCAGCA GTTCTTCCC	Exon 4 R
2735	CGGTATCGAT AAGCTATGGA G *	F

Table 2.1. *miap*-3 primers list:

List of PCR primers that were used in sequencing *miap*-3 cDNA and/or sequencing *miap*-3 exon-intron boundaries. The exons, to which every primer binds and the orientation of each primer have been indicated; forward (F) and reversed (R). Primers marked with asterisks have been used in PCR amplification of a human Myc epitope tag (see Fig. 2.1) which was used to tag *miap*-3 constructs, identified by α-Myc antibody. Primers numbers indicate the number assigned to each primer in Molecular Genetics Laboratory sequencing facility and data base.

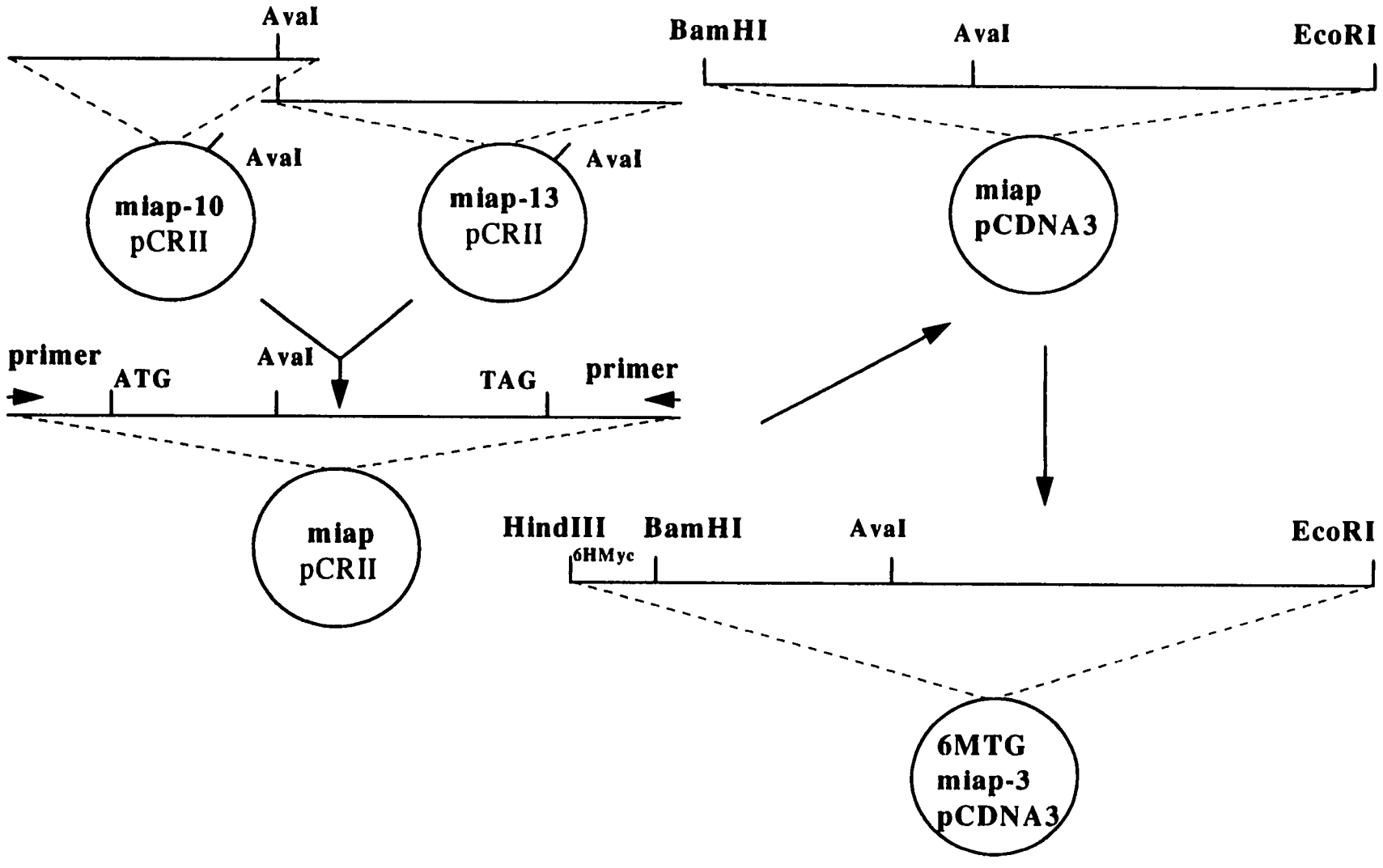
AvaI
AvaI
AvaI
miap-10
pCRII
miap-13
pCRII
primer
ATG
AvaI
TAG
primer
miap
pCRII
BamHI
AvaI
EcoRI
miap
pCDNA3
HindIII
6HMyc
BamHI
AvaI
EcoRI
6MTG
miap-3
pCDNA3

Figure 2.1. Construction and subcloning of *miap*-3 in the expression vector pCDNA3 downstream of a six human Myc epitope repeat tag.

The two overlapping cDNA clones i.e. miap-10 and miap-13 (Fig. 2.2) were subcloned in pCRII vector. Both clones were digested with the restriction enzyme AvaI. Digestion mixes were fractionated on 1% agarose gel. Insert fragment of miap-13 was subcloned in the vector fragment of miap-10 to construct a pCRII clone containing *miap*-3 coding sequence.

Primers 2574 and 2577 which had BamHI and EcoRI site respectively were used in a PCR to amplify *miap*-3 coding region from ATG (translation start codon) to TAG (translation stop codon). The PCR product was double digested with BamHI and EcoRI and subcloned in pCDNA3. The pCDNA3 containing *miap*-3 was double digested with HindIII and BamHI and a PCR product containing a six human Myc tag repeat was sub-cloned into it. The Myc epitope tag was amplified by PCR using primers 2735 and 2736 bearing HindIII or BamHI restriction sites respectively (for a list of primers see Table 2.1).

also PCR amplified from a Bluescript clone using primers bearing a HindIII or a BamHI site. The PCR product was digested with HindIII and BamHI and sub-cloned upstream of the cDNA in the *miap*-3 pcDNA3 construct in HindIII-BamHI site.

***In vitro* translation.** Two μg of the cesium chloride purified pCDNA3 containing *miap*-3 cDNA was added to 50 μL of a rabbit reticulocyte lysate (Promega TNT Kit) for *in vitro* translation. The cocktail was incubated at 30 °C for over an hour as suggested by the manufacturer. A portion of the *in vitro* translated product was fractionated on an 8% SDS-PAGE and autoradiographed. A band of the expected size was detected demonstrating that the CMV construct could be transcribed and translated.

Miap-3 cellular localization. A CMV driven *miap*-3 construct was transfected into COS (African Green Monkey Kidney) cells by Lipofectace (GibcoBRL). Cells were maintained in regular α-MEM medium for 24 hours post transfection. Protein detection was carried out by the standard immunohistochemical methods. Briefly, cells were grown to 70-90% confluence on slides, fixed by cold methanol for 10-20 min followed by incubation of the slides in α-Myc monoclonal antibody for 1 hr at room temperature. Slides were then washed extensively and incubated with secondary (total rabbit Ig conjugated to FITC) antibody conjugated to FITC (Amersham). Slides were examined under a Zeiss fluorescent microscope and photographed.

Results

Cloning and Sequencing of the Mouse X-Linked IAP cDNA.

Fourteen clones from the mouse embryonic cDNA library which hybridized to a 1.6 kb human X-linked IAP cDNA were arranged in a 3 kb contig by Southern blotting and restriction mapping analysis (Fig. 2.2). Analysis of approximately 2700 bp sequence from the isolated clones revealed a coding region of 1491 bp encoding 496 amino acids that correspond to a 55 kDa protein (Fig. 2.3). The murine gene, *miap*-3 (for murine *iap*-3), shows 87% and 94% homology to the corresponding human gene *xiap* at DNA and amino acid levels respectively (Fig. 2.4 and 2.5). The 5' and 3' UTRs of *miap*-3 and *xiap* show greater divergence with less than 60% identity. Miap-3 has three BIR domains in the N-terminus and a C_3HC_4 type RING zinc finger in the C-terminus that are linked by an intervening coding sequence of approximately 285 bp (Fig. 2.3). Analysis of Miap-3 amino acid sequence reveals one potential N-glycosylation site at asparagine 251 (Fig. 2.3). Consensus sequences that would enable the protein to function as a transmembrane unit or to be transported to nucleus (Gorlich, 1997). are not found in the amino acid sequence of Miap-3. *miap*-3 sequence has been deposited in the GenBank with the accession number of **U88990**.

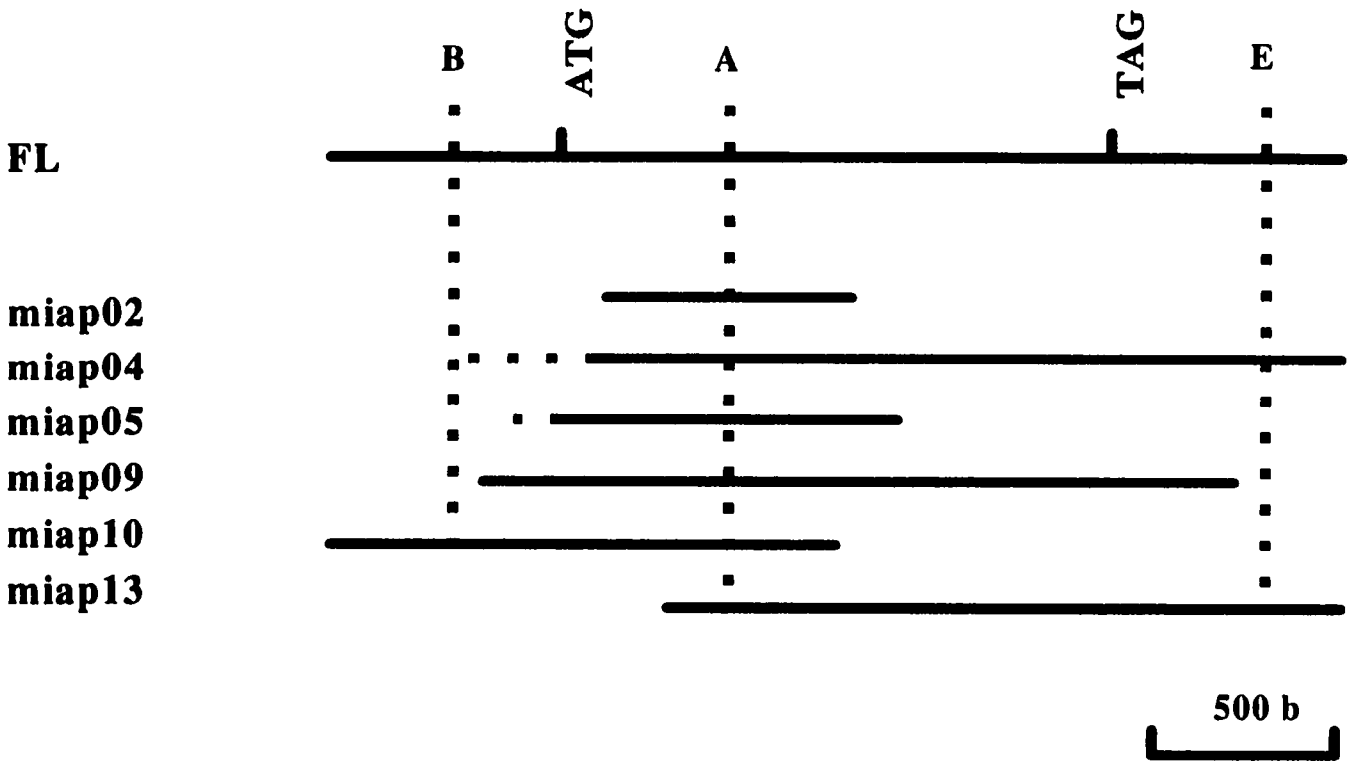
B
ATG
A
TAG
E
FL
miap02
miap04
miap05
miap09
miap10
miap13
500 b

Figure 2.2. *miap*-3 cDNA clones.

Screening a mouse cDNA library resulted in the isolation of 14 *miap*-3 positive clones. These clones were arranged in a contig by restriction mapping and sequencing analysis. Depicted is a contig constructed using six *miap*-3 cDNA clones. Horizontal dots indicate chimeric fragments. FL, full length; E,EcoRI; B, BamHI; A, AvaI; ATG translation initiationcodon; and TAG, translation stop codon.

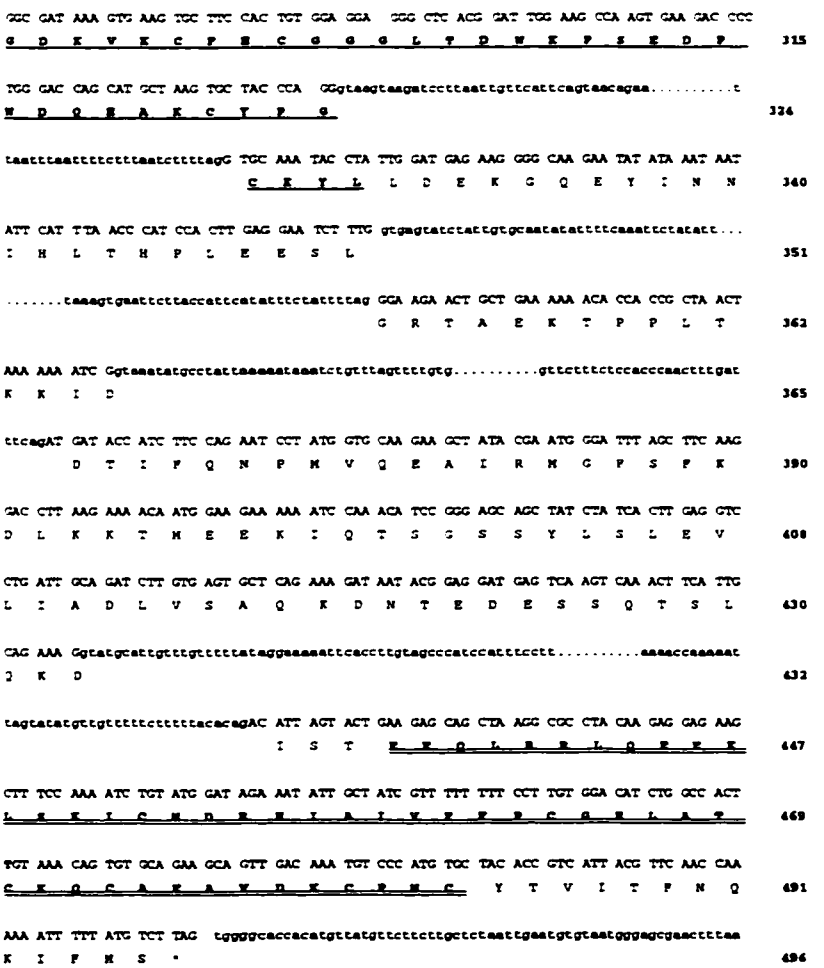

```
ttctagaaaaggtggcaagtcctattttccagagaag ATG ACT TTT AAC AGT TTT GAA GGA ACT AGA ACT TTT
                                      M   T   F   N   S   F   E   G   T   R   T   F     12

TTA CTT GCA GAC ACC AAT AAG GAT GAA GAA TTT GTA GAA GAG TTT AA  T AGA TTA AAA ACA TTT GCT
V   L   A   D   T   N   K   D   E   E   F   V   E   E   F   E   R   L   K   T   F   A    34

AAC TTC CCA AGT AGT AGT CCT GTT TCA GCA TCA ACA TTG GCG CGA GCT GGG TTT CTT TAT ACC GGT
N   F   P   S   S   S   P   V   S   A   S   T   L   A   R   A   G   F   L   Y   T   G    56

GAA GGA GAC ACC GTG CAA TGT TTC AGT TGT CAT GCG GCA ATA GAT AGA TGG CAG TAT GGA GAC TCA
E   G   D   T   V   Q   C   F   S   C   H   A   A   I   D   R   W   Q   Y   G   D   S    78

GCT GTT GGA AGA CAC AGG AGA  ATA TCC CCA AAT TGC AGA TTT ATC AAT GGT TTT TAT TTT GAA AAT
A   V   G   R   H   R   R   I   S   P   N   C   R   F   I   N   G   F   Y   F   E   N   100

GGT GCT GCA CAG TCT ACA AAT CCT GGT ATC CAA AAT GGC CAG TAC AAA TCT GAA AAC TGT GTG GGA
G   A   A   Q   S   T   N   P   G   I   Q   N   G   Q   Y   K   S   E   N   C   V   G   122

AAT AGA AAT CCT TTT GCC CCT GAC AGG CCA CCT GAG ACT CAT GCT GAT TAT CTC TTG AGA ACT GGA
N   R   N   P   F   A   P   D   R   P   P   E   T   H   A   D   Y   L   L   R   T   G   144

CAG GTT GTA GAT ATT TCA GAC ACC ATA TAC CCG AGG AAC CCT GCC ATG TGT AGT GAA GAA GCC AGA
Q   V   V   D   I   S   D   T   I   Y   P   R   N   P   A   M   C   S   E   E   A   R   166

TTG AAG TCA TTT CAG AAC TGG CCG GAC TAT GCT CAT TTA ACC CCC AGA GAG TTA GCT AGT GCT GGC
L   K   S   F   Q   N   W   P   D   Y   A   H   L   T   P   R   E   L   A   S   A   G   188

CTC TAC TAC ACA GGG GCT GAT GAT CAA GTG CAA TGC TTT TGT TGT GGG GGA AAA CTG AAA AAT TGG
L   Y   Y   T   G   A   D   D   Q   V   Q   C   F   C   C   G   G   K   L   K   N   W   210

GAA CCC TGT GAT CGT GCC TGG TCA GAA CAC AGG AGA CAC TTT CCC AAT TGC TTT TTT GTT TTG GGC
E   P   C   D   R   A   W   S   E   H   R   R   H   F   P   N   C   F   F   V   L   G   232

CGG AAC GTT AAT GTT CGA AGT GAA TCT GGT GTG AGT TCT GAT AGG AAT TTC CCA AAT TCA ACA AAC
R   N   V   N   V   R   S   E   S   G   V   S   S   D   R   N   F   P   *N   S   T   N   254

TCT CCA AGA AAT CCA GCC ATG GCA GAA TAT GAA GCA CGG ATC GTT ACT TTT GGA ACA TGG ATA TAC
S   P   R   N   P   A   M   A   E   Y   E   A   R   I   V   T   F   G   T   W   I   Y   276

TCA GTT AAC AAG GAG CAG CTT GCA AGA GCT GGA TTT TAT GCT TTA Ggtaaacttcaccagcacaattactttc
S   V   N   K   E   Q   L   A   R   A   G   F   Y   A   L   G                           291

caaatgtcacagagctcctgctcttttagtctt.........gcacagaaaggcacagttttccttgcatgttttgttagGT GAA
                                                                                      E   293
```

Figure 2.3. Nucleotide and amino acid sequence of *miap*-3.

miap-3 coding sequence and the corresponding amino acid sequence, below, have been shown in capital letters. Small letters indicate intervening sequences. Amino acid sequences corresponding to BIR domains and RING zinc finger have been shown in bold letters and (thin) underlined or double (thick) underlined respectively. Asparagine 251 has been marked with an asterisk.

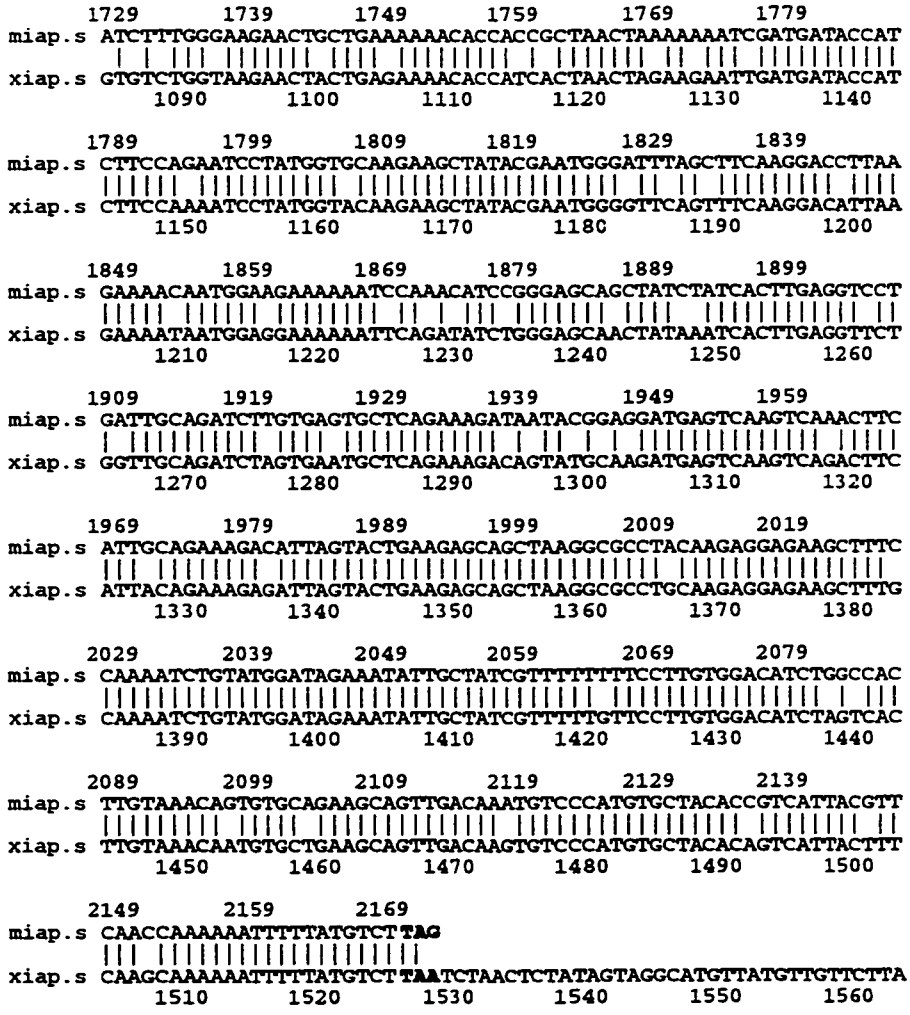
1729 1739 1749 1759 1769 1779
miap.s ATCTTTGGGAAGAACTGCTGAAAAAACACCACCGCTAACTAAAAAAATCGATGATACCAT
xiap.s GTGTCTGGTAAGAACTACTGAGAAAACACCATCACTAACTAGAAGAATTGATGATACCAT
1090 1100 1110 1120 1130 1140
1789 1799 1809 1819 1829 1839
miap.s CTTCCAGAATCCTATGGTGCAAGAAGCTATACGAATGGGATTTAGCTTCAAGGACCTTAA
xiap.s CTTCCAAAATCCTATGGTACAAGAAGCTATACGAATGGGGTTCAGTTTCAAGGACATTAA
1150 1160 1170 1180 1190 1200
1849 1859 1869 1879 1889 1899
miap.s GAAAACAATGGAAGAAAAAATCCAAACATCCGGGAGCAGCTATCTATCACTTGAGGTCCT
xiap.s GAAAATAATGGAGGAAAAAATTCAGATATCTGGGAGCAACTATAAATCACTTGAGGTTCT
1210 1220 1230 1240 1250 1260
1909 1919 1929 1939 1949 1959
miap.s GATTGCAGATCTTGTGAGTGCTCAGAAAGATAATACGGAGGATGAGTCAAGTCAAACTTC
xiap.s GGTTGCAGATCTAGTGAATGCTCAGAAAGACAGTATGCAAGATGAGTCAAGTCAGACTTC
1270 1280 1290 1300 1310 1320
1969 1979 1989 1999 2009 2019
miap.s ATTGCAGAAAGACATTAGTACTGAAGAGCAGCTAAGGCGCCTACAAGAGGAGAAGCTTTC
xiap.s ATTACAGAAAGAGATTAGTACTGAAGAGCAGCTAAGGCGCCTGCAAGAGGAGAAGCTTTG
1330 1340 1350 1360 1370 1380
2029 2039 2049 2059 2069 2079
miap.s CAAAATCTGTATGGATAGAAATATTGCTATCGTTTTTTTTCCTTGTGGACATCTGGCCAC
xiap.s CAAAATCTGTATGGATAGAAATATTGCTATCGTTTTTGTTCCTTGTGGACATCTAGTCAC
1390 1400 1410 1420 1430 1440
2089 2099 2109 2119 2129 2139
miap.s TTGTAAACAGTGTGCAGAAGCAGTTGACAAATGTCCCATGTGCTACACCGTCATTACGTT
xiap.s TTGTAAACAATGTGCTGAAGCAGTTGACAAGTGTCCCATGTGCTACACAGTCATTACTTT
1450 1460 1470 1480 1490 1500
2149 2159 2169
miap.s CAACCAAAAAATTTTTATGTCTTAG
xiap.s CAAGCAAAAAATTTTTATGTCTTAATCTAACTCTATAGTAGGCATGTTATGTTGTTCTTA
1510 1520 1530 1540 1550 1560

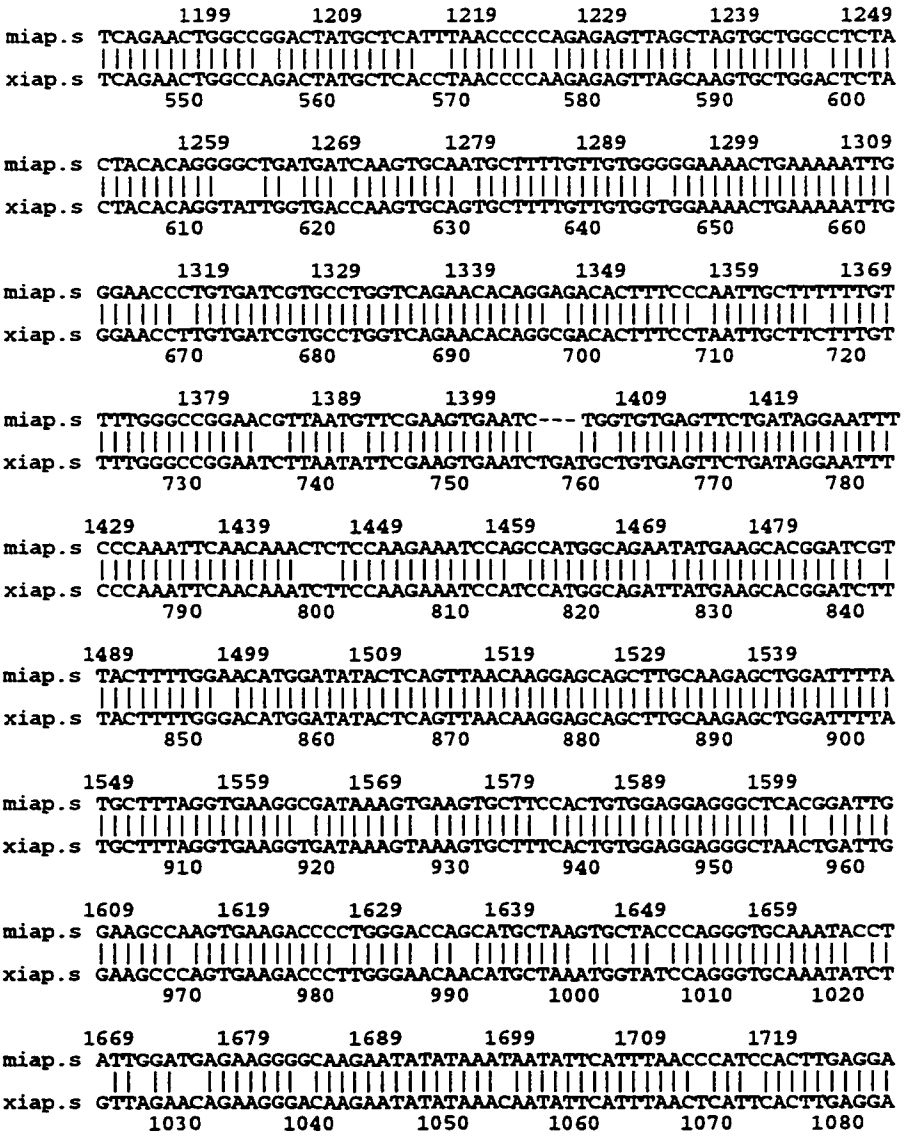
1199 1209 1219 1229 1239 1249
miap.s TCAGAACTGGCCGGACTATGCTCATTTAACCCCCAGAGAGTTAGCTAGTGCTGGCCTCTA
xiap.s TCAGAACTGGCCAGACTATGCTCACCTAACCCCAAGAGAGTTAGCAAGTGCTGGACTCTA
550 560 570 580 590 600
1259 1269 1279 1289 1299 1309
miap.s CTACACAGGGGCTGATGATCAAGTGCAATGCTTTTGTTGTGGGGGAAAACTGAAAAATTG
xiap.s CTACACAGGTATTGGTGACCAAGTGCAGTGCTTTTGTTGTGGTGGAAAACTGAAAAATTG
610 620 630 640 650 660
1319 1329 1339 1349 1359 1369
miap.s GGAACCCTGTGATCGTGCCTGGTCAGAACACAGGAGACACTTTCCCAATTGCTTTTTTGT
xiap.s GGAACCTTGTGATCGTGCCTGGTCAGAACACAGGCGACACTTTCCTAATTGCTTCTTTGT
670 680 690 700 710 720
1379 1389 1399 1409 1419
miap.s TTTGGGCCGGAACGTTAATGTTCGAAGTGAATC---TGGTGTGAGTTCTGATAGGAATTT
xiap.s TTTGGGCCGGAATCTTAATATTCGAAGTGAATCTGATGCTGTGAGTTCTGATAGGAATTT
730 740 750 760 770 780
1429 1439 1449 1459 1469 1479
miap.s CCCAAATTCAACAAACTCTCCAAGAAATCCAGCCATGGCAGAATATGAAGCACGGATCGT
xiap.s CCCAAATTCAACAAATCTTCCAAGAAATCCATCCATGGCAGATTATGAAGCACGGATCTT
790 800 810 820 830 840
1489 1499 1509 1519 1529 1539
miap.s TACTTTTGGAACATGGATATACTCAGTTAACAAGGAGCAGCTTGCAAGAGCTGGATTTTA
xiap.s TACTTTTGGGACATGGATATACTCAGTTAACAAGGAGCAGCTTGCAAGAGCTGGATTTTA
850 860 870 880 890 900
1549 1559 1569 1579 1589 1599
miap.s TGCTTTAGGTGAAGGCGATAAAGTGAAGTGCTTCCACTGTGGAGGAGGGCTCACGGATTG
xiap.s TGCTTTAGGTGAAGGTGATAAAGTAAAGTGCTTTCACTGTGGAGGAGGGCTAACTGATTG
910 920 930 940 950 960
1609 1619 1629 1639 1649 1659
miap.s GAAGCCAAGTGAAGACCCCTGGGACCAGCATGCTAAGTGCTACCCAGGGTGCAAATACCT
xiap.s GAAGCCCAGTGAAGACCCTTGGGAACAACATGCTAAATGGTATCCAGGGTGCAAATATCT
970 980 990 1000 1010 1020
1669 1679 1689 1699 1709 1719
miap.s ATTGGATGAGAAGGGGCAAGAATATATAAATAATATTCATTTAACCCATCCACTTGAGGA
xiap.s GTTAGAACAGAAGGGACAAGAATATATAAACAATATTCATTTAACTCATTCACTTGAGGA
1030 1040 1050 1060 1070 1080

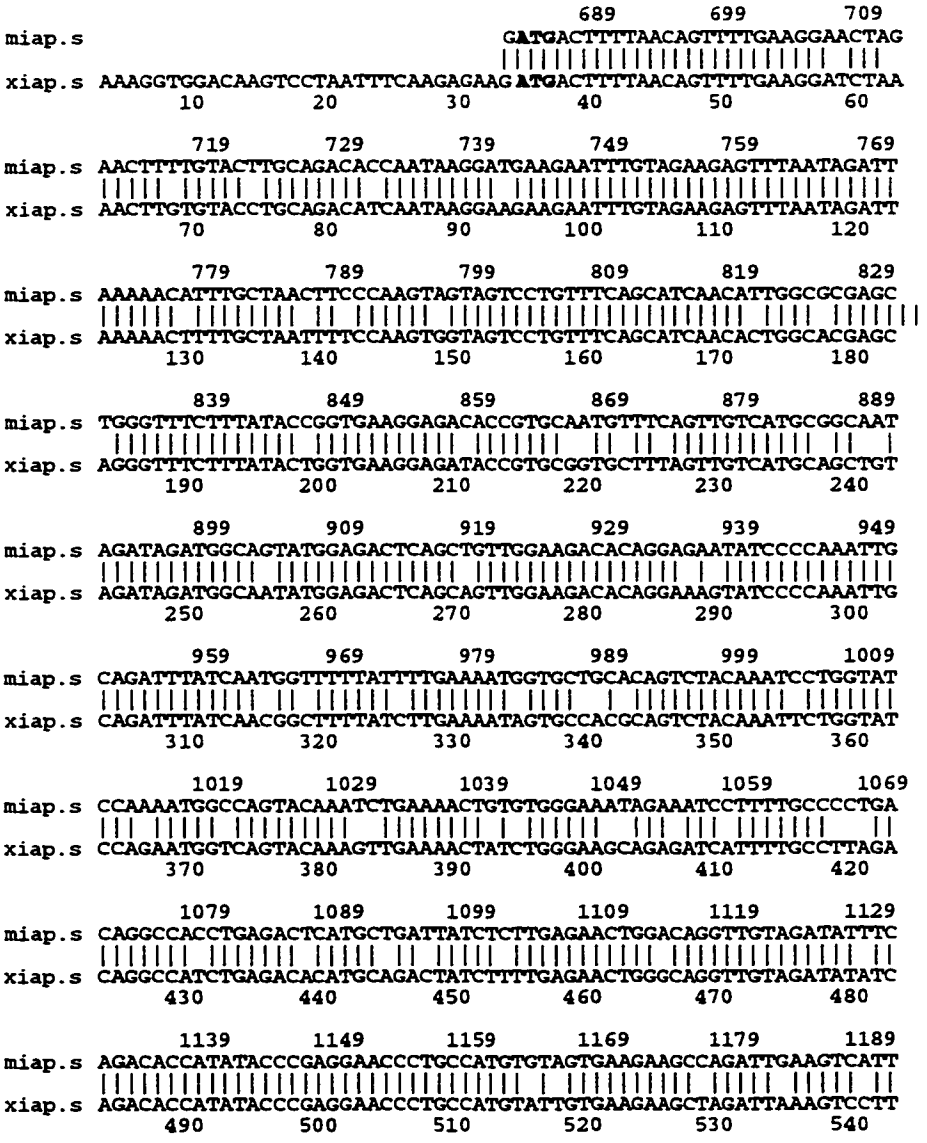
miap.s
xiap.s
AAAGGTGGACAAGTCCTAATTTCAAGAGAAGATGACTTTTAACAGTTTTGAAGGATCTAA
AACTTTTGTACTTGCAGACACCAATAAGGATGAAGAATTTGTAGAAGAGTTTAATAGATT
AACTTGTGTACCTGCAGACATCAATAAGGAAGAAGAATTTGTAGAAGAGTTTAATAGATT
AAAAACATTTGCTAACTTCCCAAGTAGTAGTCCTGTTTCAGCATCAACATTGGCGCGAGC
AAAAACTTTTGCTAATTTTCCAAGTGGTAGTCCTGTTTCAGCATCAACACTGGCACGAGC
TGGGTTTCTTTATACCGGTGAAGGAGACACCGTGCAATGTTTCAGTTGTCATGCGGCAAT
AGGGTTTCTTTATACTGGTGAAGGAGATACCGTGCGGTGCTTTAGTTGTCATGCAGCTGT
AGATAGATGGCAGTATGGAGACTCAGCTGTTGGAAGACACAGGAGAATATCCCCAAATTG
AGATAGATGGCAATATGGAGACTCAGCAGTTGGAAGACACAGGAAAGTATCCCCAAATTG
CAGATTTATCAATGGTTTTTATTTTGAAAATGGTGCTGCACAGTCTACAAATCCTGGTAT
CAGATTTATCAACGGCTTTTATCTTGAAAATAGTGCCACGCAGTCTACAAATTCTGGTAT
CCAAAAATGGCCAGTACAAATCTGAAAACTGTGTGGGAAATAGAAATCCTTTTGCCCCTGA
CCAGAATGGTCAGTACAAAGTTGAAAACTATCTGGGAAGCAGAGATCATTTTGCCTTAGA
CAGGCCACCTGAGACTCATGCTGATTATCTCTTGAGAACTGGACAGGTTGTAGATATTTC
CAGGCCATCTGAGACACATGCAGACTATCTTTTGAGAACTGGGCAGGTTGTAGATATATC
AGACACCATATACCCGAGGAACCCTGCCATGTGTAGTGAAGAAGCCAGATTGAAGTCATT
AGACACCATATACCCGAGGAACCCTGCCATGTATTGTGAAGAAGCTAGATTAAAGTCCTT

Figure 2.4. Sequence homology between *miap*-3 and its human homologue *xiap*: 89.3% identity.

An aligning of *miap*-3 and *xiap* cDNA sequences by FASTA (GCG) reveals that the two genes share 89% identity over their coding sequence. Top line represents *miap*-3 and bottom line represents *xiap* sequence. Numbers refer to the number of each base in our sequences data base and does not reflect the actual position of each base in their respective cDNAs. *miap*-3 ATG begins at position 682 corresponding to *xiap* ATG beginning at position 34 in the respective sequences (both shown in bold). Translation initiation and termination codons (ATG and TAG/TAA) are indicated in bold. | indicates identical bases.

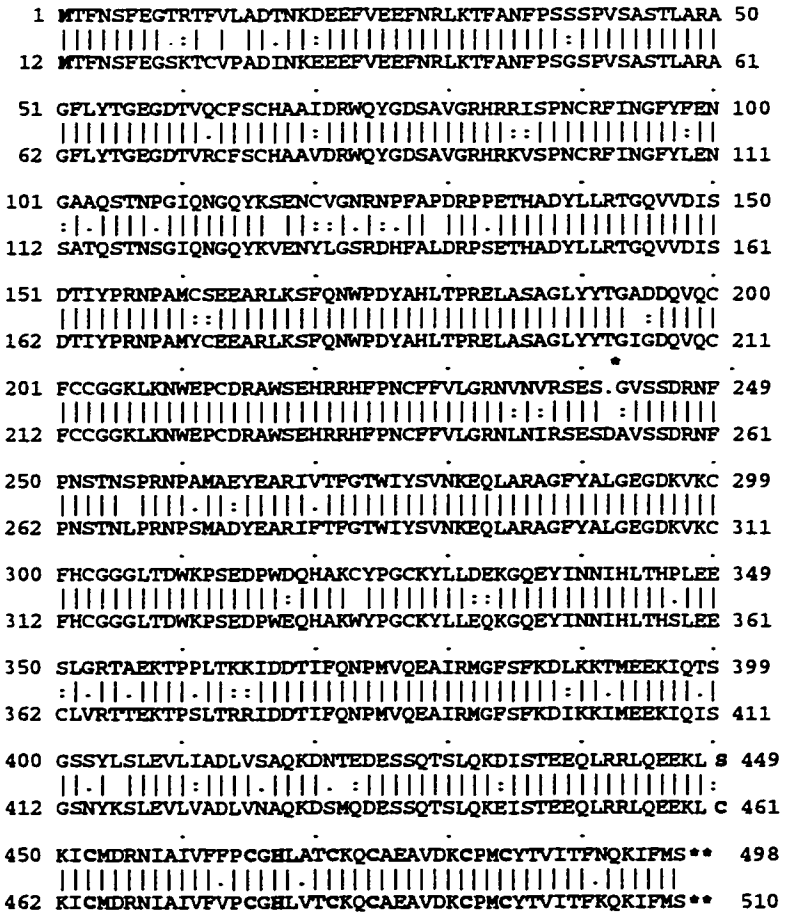

Figure 2.5. Amino acid homology between Xiap and Miap-3. 93.373 Percent Identity; 1 Gap.

An aligning of Miap-3 and Xiap a.a. sequences in FASTA (GCG) reveals that Miap-3 and Xiap share 93.37% identity. Top line represents Miap-3 and bottom line represents Xiap a.a. sequences. Numbers refer to the number of each a.a. in our sequence data base and does not necessarily reflect the actual position of each a.a. Translation initiation methionine residues shown in bold have been indicated in position 1 for Miap-3 and position 12 for Xiap. | indicates identical bases. RING zinc finger conserved cysteine and histidine residues have also been shown in bold letters. Absence of an aspartic acid residue in Miap-3 generates a gap in position 241, marked with an asterisk. Translation termination codons have been shown with double asterisks.

Expression Pattern of *miap*-3

Northern blot analysis using cDNA probes containing parts of coding region extending to either the 5' or the 3' UTR hybridized to membranes containing total RNA extracted from adult and newborn mice tissues as well as poly(A)$^+$ RNA revealed an approximately 8 kb band in all the tissue tested including lung, heart, kidney, liver, testis and uterus (Fig. 2.6).

Cellular Localization of Miap-3

Full-length coding *miap*-3 cDNA was cloned into pcDNA3 expression vector and examined in an *in vitro* system as described under Materials and methods. The *miap*-3 construct was then transiently expressed in COS cells. Immunofluorescent microscopy - used to detect Miap-3 protein as described under Materials and Methods- revealed that Miap-3 protein concentrates in the cytoplasm with no apparent staining detected in the nuclei (Fig. 2.7).

Genomic Organization of the Mouse X-Linked IAP Gene

Six clones from two independent mouse strain 129/Sv genomic libraries in λFIXII were identified with a full-length coding *miap*-3 cDNA probe. A 30 kb contiguous array was then constructed by Southern blotting and restriction enzyme analysis of four mouse *xiap* positive genomic clones (Fig. 2.8). Analysis of this genomic contig showed that murine X-linked *iap* genomic locus spans approximately 25 kb of DNA and is composed of six exons and five introns. Introns were sized by PCR amplification using primer sets

b

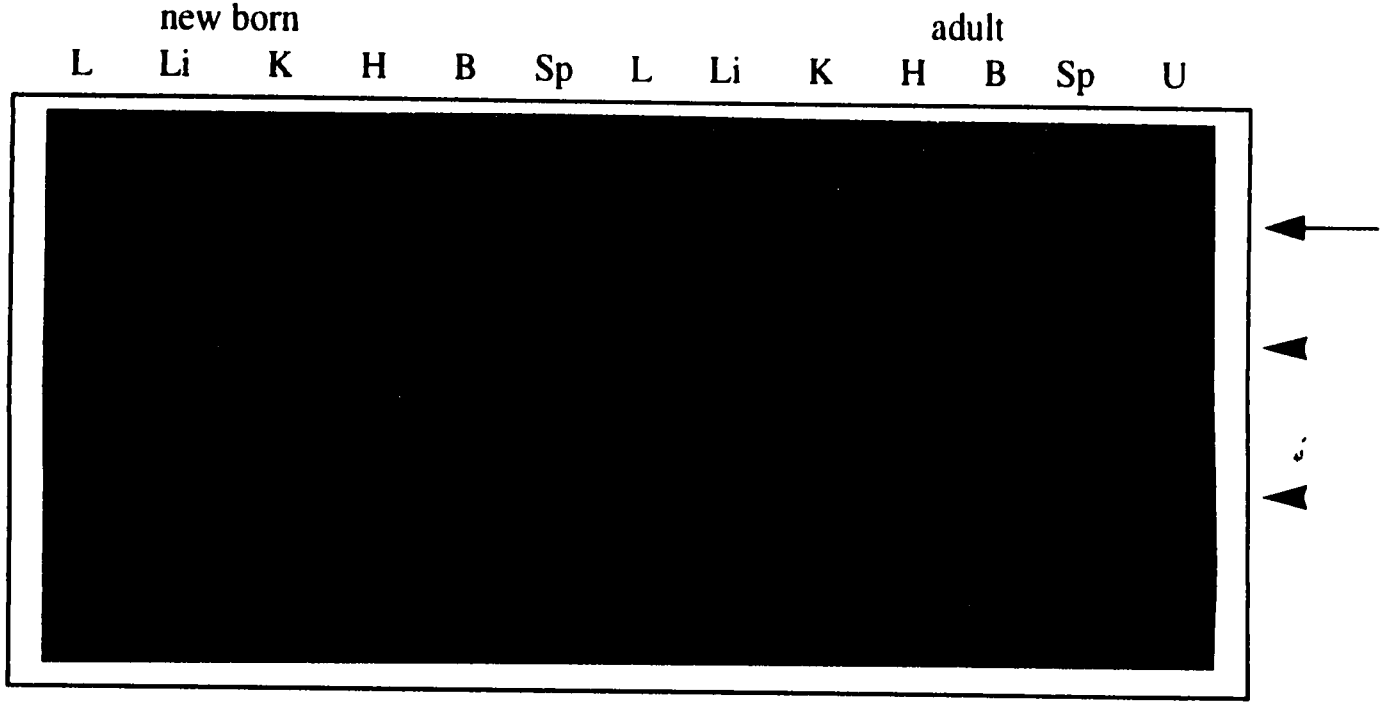

a

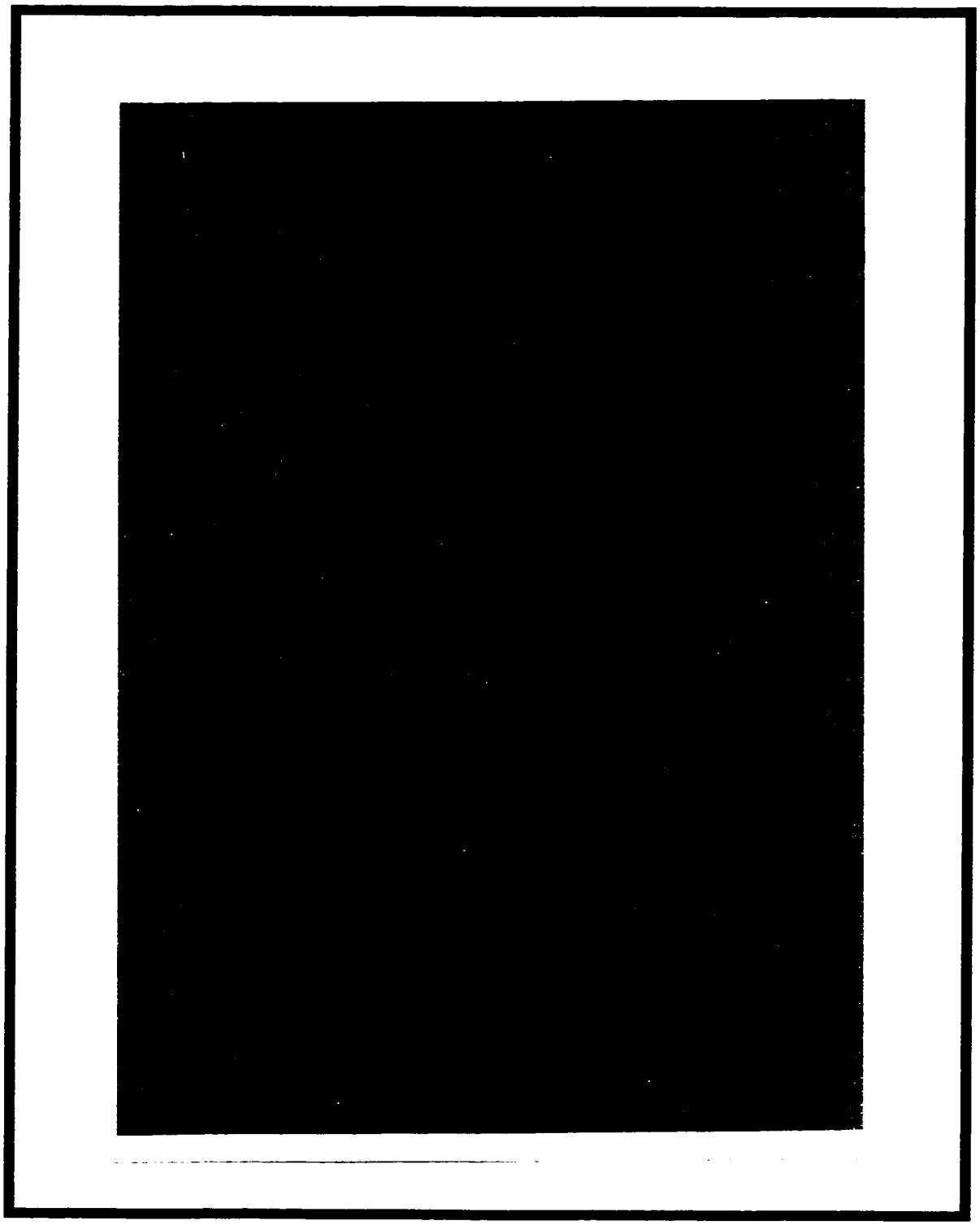

Figure 2.6. Tissue expression profile of *miap*-3 message.

Northern blots containing (**a**) Poly(A)$^+$ or (**b**) total mRNA from different adult mouse tissues including Heart (H), brain (B), spleen (Sp), lung (L), liver (Li), skeletal muscle (S), kidney (K), testis (T) and uterus (U) were hybridized with a 1.8 kb cDNA clone containing most of the *miap*-3 coding region and a portion of 3' UTR. Arrow indicate 7 kb. Arrow heads (**b**) indicate 28S and 18S ribosomal RNA species. The lower bands in (**a**) are actin controls. There is a faint band in testis mRNA (**b** last lane) which may not be easily visible in the reproduced photo. In lanes corresponding to spleen and skeletal muscle no bands were detected. As presence of *miap*-3 message was later confirmed in these tissues by RT-PCR (data not shown), it appears that the inability to detect *miap*-3 message in these two lanes is due to degradation of higher molecular weight RNA samples.

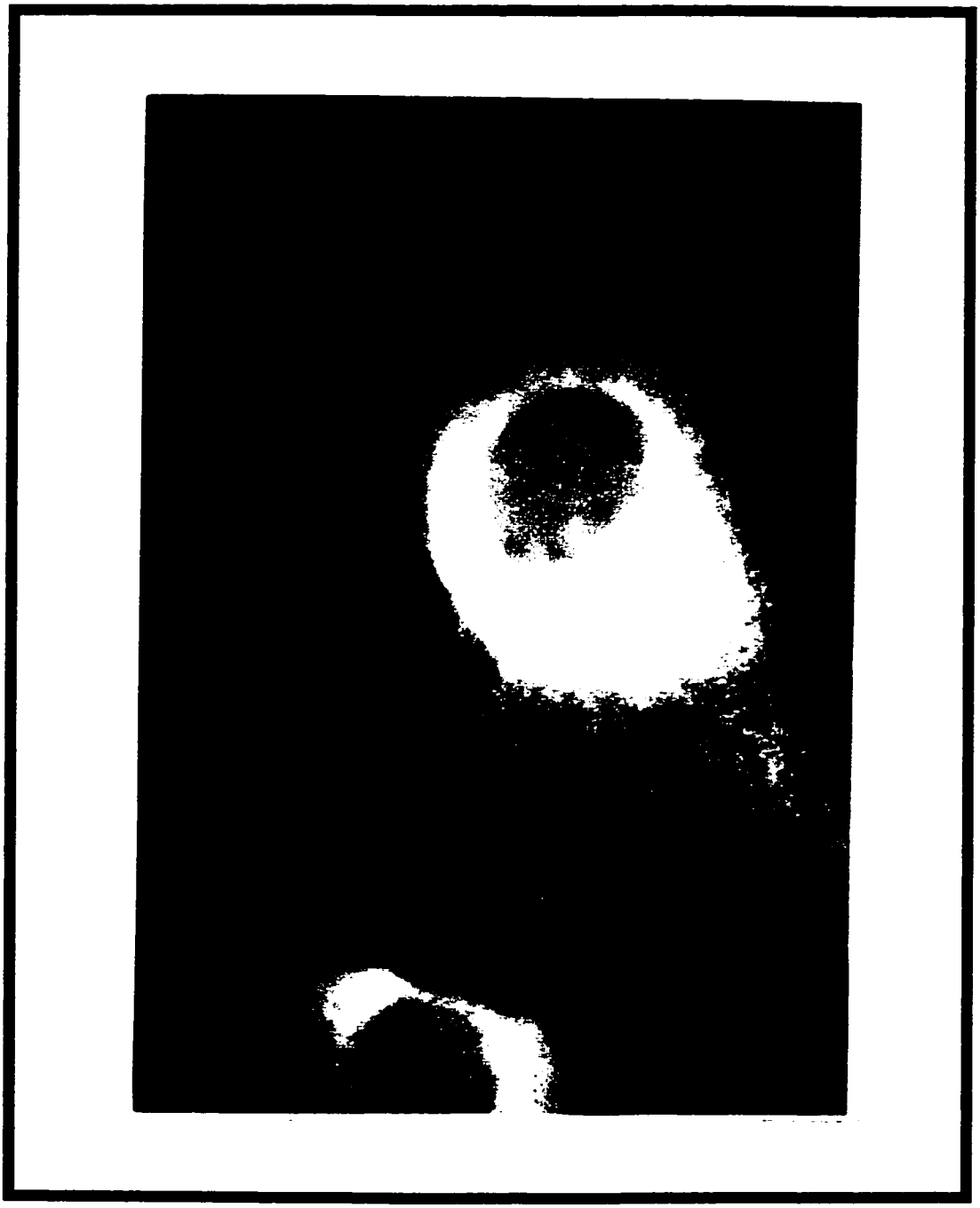

Figure 2.7. Immunofluorescent detection of Miap-3 cellular localization in COS cells.

COS cells were transiently transfected with a CMV promoter driven *miap*-3 cDNA (Fig. 3.2, FL). Cells were stained with primary α-Myc antibody and secondary total Ig antibody conjugated to FITC. Slides were examined and photographed using a Zeiss fluorescent microscope (mag 1000x). Level of signal in negative controls (prepared as described in Materials and Methods without using primary antibody) was below detection by Immunofluorescent photography.

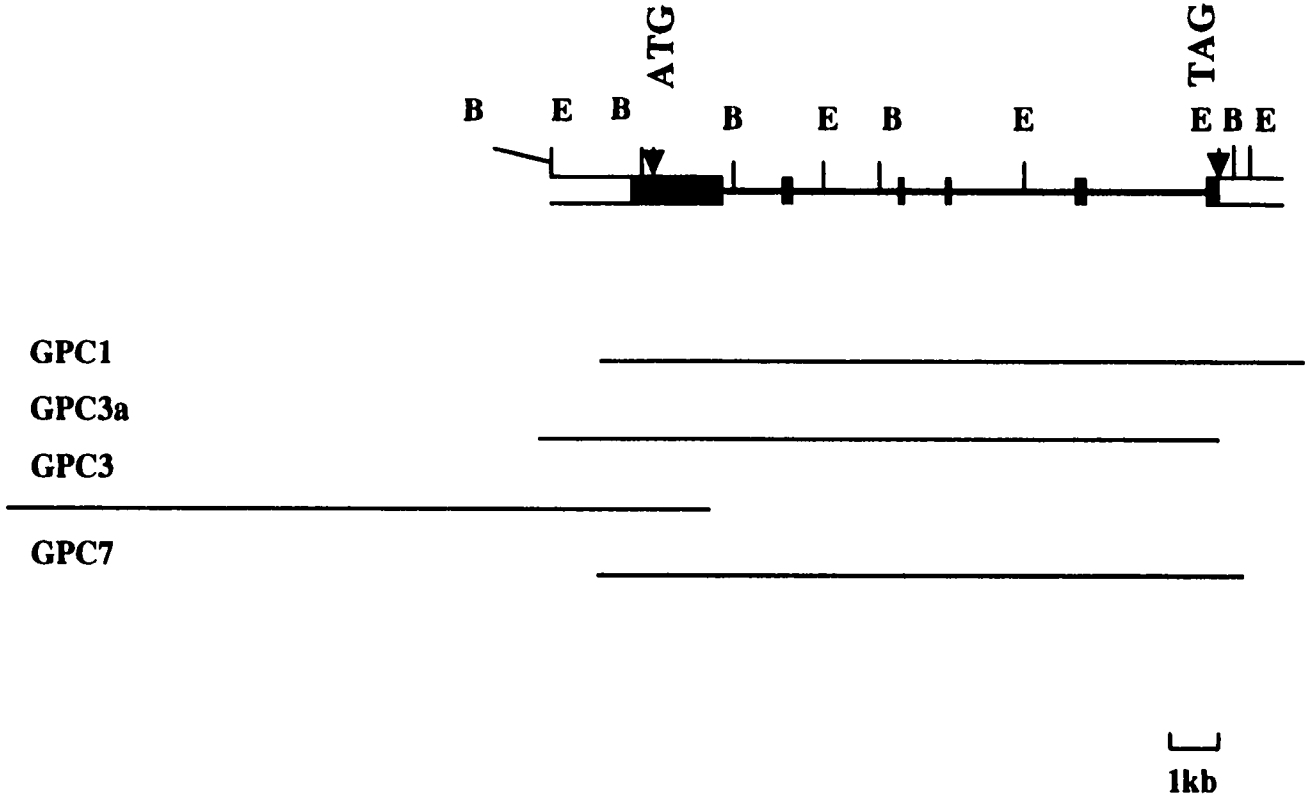
ATG
TAG
B E B B E B E E B E
GPC1
GPC3a
GPC3
GPC7
1kb

Figure 2.8. Genomic structure of *miap*-3.

This figure shows a contig constructed with four *miap*-3 genomic clones (i.e. GPC 1, 3a, 3, and 7). *The* mouse gene consists of six exon and five introns. Solid boxes represent the exons containing coding sequences and open boxes represent those exons containing noncoding regions. Intervening sequences are shown as solid lines. Relevant restriction site as well as translation initiation and termination codons are indicated with arrowheads. λFIXII clones from which the genomic structure was derived are shown below as solid lines. E, EcoRI; B, BamHI; GPC, genomic phage clone; ATG, translation initiation codon; and TAG, translation stop codon.

Exon	Exon size bp/aa	Acceptor site	Exon sequence	Donor site	Intron size kb
1	>1500/291	-	CTTTAG	**gt**aaac	~ 1.5
2	100/33	ttgtt**ag**	GTGAAG...CCCAGG	**gt**aagt	~ 2.2
3	79/27	ttt**ag**	GTGCAA...TCTTTG	**gt**gagt	~ 1.0
4	43/14	ttt**ag**	GGAAGA...AAATCG	**gt**aaat	~ 2.5
5	201/67	ttc**ag**	ATGATA...AGAAAG	**gt**atgc	~ 2.5
6	> 720/64	acac**ag**	ACATTA	-	-

Table 2.2 *miap*-3 exon-intron organization.

maip-3 exon-intron organization, sizes of exons and introns, and boundary sequences have been summarized in this table. Sequence of acceptor and donor sites have been shown in lowercase letters with the consensus sequences (i.e. ag.....gt) in bold. Six letters of each coding exon and six letters of the following exon have been shown in capital letters. Introns sizes are estimates of the PCR products fractionated on agarose gel.

specific to two consecutive exons (Table 2.1). Exon-intron boundaries were determined by sequencing genomic clones using cDNA specific primers (Table 2.2). All exon-intron junctions conform to the 5'-donor and 3'-acceptor consensus (Breathnach et al., 1987).

Chromosomal Localization of *miap*-3

Mapping of the mouse X-linked *iap* gene was determined by fluorescence *in situ* hybridization (FISH) on mouse lymphocyte metaphase spreads using GPC3a, a 15 kb *miap*-3 genomic clone (Fig. 2.9). DAPI banding was used to identify the specific mouse chromosomes (Fig. 2.9b). Detailed *miap*-3 mapping on mouse chromosome X in the region of A3-A5 (Fig. 2.9c) was determined based on the summary of 10 photos. Results of mapping revealed that *miap*-3 is located in the region of A3-A5 on mouse chromosome X.

C

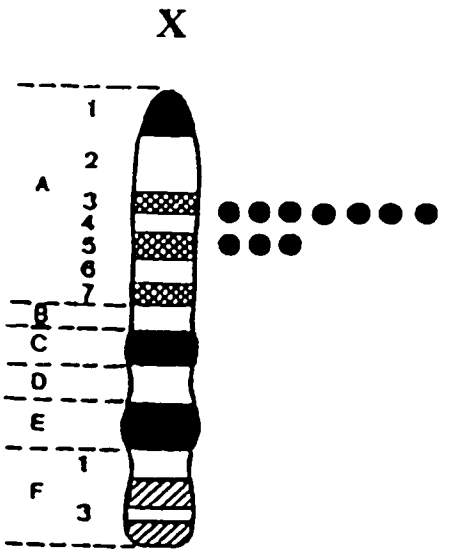

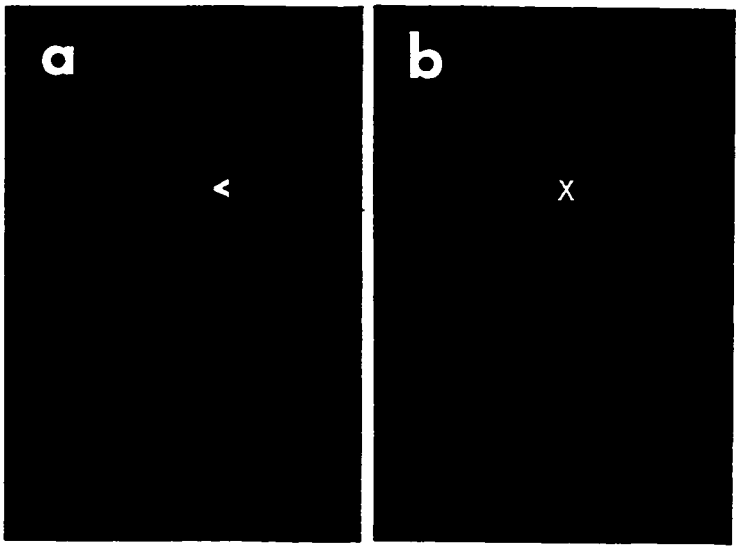
a
<
b
X

Figure 2.9. Chromosomal localization of *miap*-3.

(**a**) GPC3a, a 15 kb mouse genomic phage clone was labeled with biotin and used as a FISH probe on a mouse chromosome spread. The arrowhead indicates FISH signals on the X chromosome. (**b**) The same chromosome spread was stained with DAPI to identify mouse chromosome X. (**c**) Diagram of FISH mapping results. Each dot represents the double FISH signal detected on mouse chromosome X in the region of A3-A5.

Discussion

In this chapter, cloning and characterization of a new mammalian *iap* gene designated *miap*-3 has been described. Similar to the other mammalian *iaps*, *miap*-3 encodes three N-terminal BIR domains (Liston et al., 1996, and Rothe et al., 1995a) instead of the two BIR domains seen in baculoviral IAPs (reviewed in Clem and Miller, 1996; Crook et al., 1993; and Clem and Miller., 1993). As seen in the baculoviral IAPs but in contrast to the case with NAIP (Roy et al., 1995), the three recently cloned human IAPs i.e. Xiap, Hiap-1, and Hiap-2 also contain a C-terminal RING zinc-finger motif (Liston et al., 1996).

Human X-linked *xiap* has a 1.5 kb coding region corresponding to a 55 kDa protein. *xiap* transcripts have been detected in all fetal and adult tissues examined to date (Liston et al., 1996). This observation is consistent with *xiap* being a "house-keeping" gene potentially important in development, homeostasis and/or a viral defense mechanism. To facilitate studies of *xiap* as a prototype of human *iaps*, cloning and characterizing of its murine homologue was undertaken.

Sequence analysis from an approximately 3 kb cDNA contig (Fig. 2.2) revealed *miap*-3 with a coding sequence of 1491 bp (Fig. 2.3). Comparison of cDNA sequences and sequence data obtained from a 30 kb genomic contig along with Southern blot analysis revealed the structure of *miap*-3 with six exons and five intervening sequences (Fig. 2.8 and Table 2.2). Miap-3 contains three N-terminal BIR domains and a C-terminal RING zinc-finger motif. The RING zinc-finger motif including the 6 cysteine residues, which are likely involved in cation coordination, are all conserved (Fig 2.5). The mouse and the

human genes share 87% nucleotide similarity in the coding regions (Fig. 2.4), which at the amino acid level, the homology between proteins increases to 94% (Fig. 2.6). The DNA homology between the two genes falls below 60% outside the coding region. The high degree of conservation between mouse and human X-linked IAPs, especially in the BIR and RING zinc-finger domains suggests functional conservation. The strong conservation is observed both across species and within the human*iap* gene family (Liston et al. 1996).

The mouse *iap* transcript is detected as an approximately 8 kb mRNA band on northern blots containing poly $(A)^+$ or total RNA from newborn or adult mice (Fig 2.6). The presence of *miap*-3 message in all tissues tested is consistent with *miap*-3 being a "house-keeping" gene with possible roles in development as well as homeostasis. No evidence of alternative splicing has, however, been observed for *miap*-3 transcripts. The fact that *miap*-3 transcript is 6.5 kb larger than the coding region suggests the existence of large 5' and/or 3' UTRs. Further characterization of *miap*-3 has revealed a greater than 6 kb 5' UTR (Holcik, M., unpublished). Computer analysis shows that the region upstream *miap*-3 first exon extending to the 5' UTR bears two putative promoter sequences. The considerable divergence of the large 5' UTRs of *miap*-3 and *xiap* suggests that these regions may bear additional specific regulatory elements.

The genomic organization of *miap*-3 was determined by analyzing four phage clones isolated from a mouse liver genomic DNA. *miap*-3 has six exons ranging from 43 to greater than 1500 bp in size (Table 2.2; and Fig. 2.3). The 5' UTR, ATG translation initiation codon, two first BIR domains and a part of the third BIR domain are encoded

within the first exon. The remainder of the third BIR domain is encoded by the second and third exons. The RING zinc finger and TAG translation stop codon are encoded by the last exon extending to the 3' UTR. Preliminary evidence suggests that the exon containing the TAG translation termination codon is the last exon of the gene. No strong polyadenylation signal has as yet been detected. *miap*-3 six exons are intervened by five introns ranging from 1.0 to 2.5 kb in size (Table 2.2). Sequences of all the intron acceptor and donor sites match with conserved sequences.

The strong structural resemblance of the *miap*-3 gene to those of other *iaps* (Liston et al, 1977a) suggests that all of the *iaps* may have originated from a common progenitor gene. One interesting observation is that all mammalian IAPs cloned to date have three BIR domains instead of the two viral BIR domains. In *Drosophilia*, however, both versions of the protein are present (Hay et al., 1995). *Drosophilia* has two IAPs namely Diap-1 and Diap-2. Diap-1 has two BIR domains while Diap-2 has three. It is intriguing to speculate that this has been the point in the evolution at which proteins with three BIR domains have developed from a parental IAP containing two BIR domains perhaps by a duplication event of one of the already existing two BIR domains. Sequence comparison demonstrates that BIR 1 shows more homology to BIR 2 than to BIR 3 (Fig 2.10). This suggest that BIR 2 and BIR 3 had had more time through evolution to differ from each other. Duplication expansion events do not confine to BIR domains of *iaps*, but it is rather observed at the gene level as well. Such a recent event is probably responsible for the duplication of two genes encoding *iaps* i.e. *hiap*-1 and *hiap*-2 on chromosome 11 in a

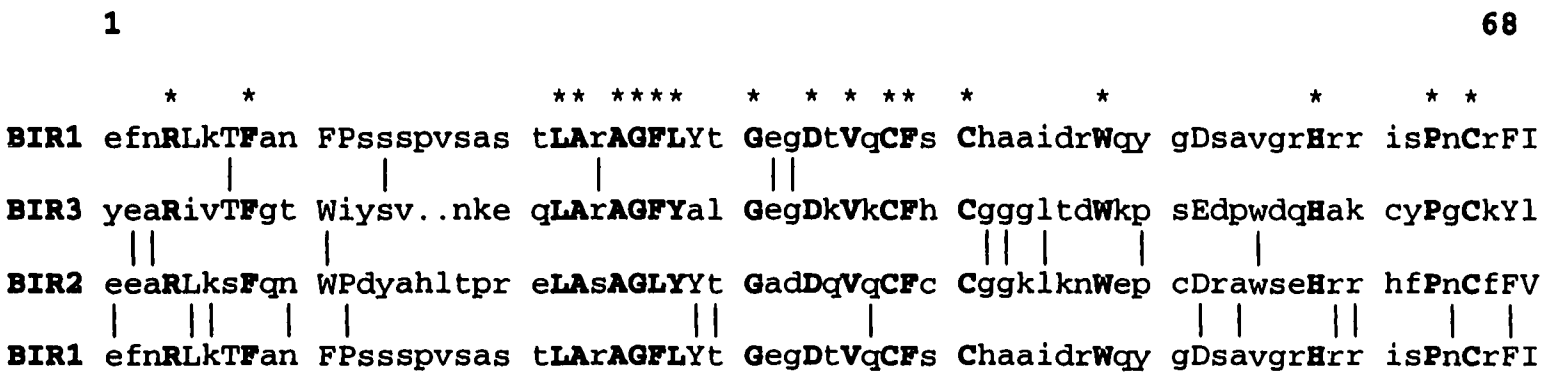
1
68
BIR1 efnRLkTFan FPssspvsas tLArAGFLYt GegDtVqCFs ChaaidrWqy gDsavgrHrr isPnCrFI
BIR3 yeaRivTFgt Wiysv..nke qLArAGFYal GegDkVkCFh CgggltdWkp sEdpwdqHak cyPgCkYl
BIR2 eeaRLksFqn WPdyahltpr eLAsAGLYYt GadDqVqCFc CggklknWep cDrawseHrr hfPnCfFV
BIR1 efnRLkTFan FPssspvsas tLArAGFLYt GegDtVqCFs ChaaidrWqy gDsavgrHrr isPnCrFI

Figure 2.10. Alignment of the three BIR Domains of *miap*-3.

Alignment of the three BIR domains of *miap*-3 shows that BIR 1 has more identity to BIR 2 than BIR 3. Residues that are similar in all the three BIR domains have been shown in bold capital letters and have been marked with an star; Identical residues in two of the BIR domains have been shown in capital letters and marked with |. BIR 1 shows 47% homology with BIR 2 while the homology between BIR 1 and three is 34% and between BIR 2 and BIR 3 is 38%.

tandem repeat arrangement. The functional significance of duplication in BIR domains as well as the significance of development of new genes encoding IAPs remain to be addressed. One speculation is that the four human *iap* genes may have tissue and/or developmental specificity. A second speculation is that because of the importance of apoptosis and proteins that function as apoptosis inhibitors, a higher degree of redundancy is required to provide better means of regulating this important machinery, the dysfunctioning of which may bear deleterious consequences. Comparison of the *miap*-3 genomic structure with that of the other *iaps* will not only be useful in determining the genomic structure and exon-intron arrangement of other members of *iap* family but it may as well prove to be useful in answering some of these questions.

To further characterize *miap*-3, its chromosomal location as well as cellular localization of its protein product was determined. Fluorescence *in situ* hybridization (FISH) on mouse lymphocyte metaphase spreads using a 15 kb *miap*-3 genomic clone was employed to determine the chromosomal location of the mouse X-linked *iap* gene. *miap*-3 mapping to mouse chromosome X in the region of A3-A5 (Fig. 2.9) was based on analysis of ten photomicrographs. Human *xiap* has also been mapped to human X chromosome in the region of q25 by FISH analysis (Rajcan-Separovic et al., 1996). Localization of *xiap* and *miap*-3 in human Xq25 and mouse X region A3-5 respectively may indicate that these two regions are syntenic containing other homologous genes. In this regard it is noteworthy that although the murine homologue of the human Xp11 *syp* (Fisher et al., 1995) is on XA3, the mouse homologue of Xq26 Hprt is on XA6 (Lyon et al., 1987).

Miap-3 protein localizes to cytoplasm with an accentuation around the nucleus (fig. 2.7). It is not possible to ascertain from the fluorescent micrographs whether the protein is present in the nucleus. In this regard it may be noteworthy that Miap-3 and Xiap do not appear to contain a nuclear localization signal. Interaction of Hiap-1 and Hiap-2 with membrane associated components of TNF signal transduction pathway, i.e. TRAF family (Rothe et al., 1995a, b), is in keeping with a cytoplasmic localization of the human Xiap and its murine homologue. Cellular localization of Xiap and Miap-3 was confirmed in further detail by functional characterization of the two proteins. Results of these findings will be presented and discussed in the following chapter.

In conclusion, the gene encoding *miap*-3 has been isolated and assigned to chromosome X of the mouse. The X-linked mouse gene encodes a protein with three N-terminal BIR domains and a C-terminal RING zinc finger. These results may aid in the production of useful resources such as animal models for further characterization of the *iap* genes, thereby clarifying their role in the inhibition of apoptosis. In addition to the analysis of its function in mouse development, *miap*-3 may also serve as a prototype in revealing the roles of mammalianIAPs in human development and associated disorders.

Chapter III

Functional characterization of Xiap and Miap-3

Introduction

Over a dozen different proteases have been identified in mammalian cells as cell death effectors (reviewed by Vaux and Strasser, 1996; Alnemri et al., 1996). All mammalian cell types appear to possess several of these proteases as inactive precursors. ICE, the prototype cysteine protease, appears to be the first protease that is activated during apoptosis by in-coming apoptosis signals (Fig. 1.4). ICE, in turn, can activate other proteases, thus initiating a downstream cascade of cysteine proteases that will cleave their targets ultimately causing cell death (Kaufmann, et al., 1993; Lazebnik et al., 1994; Tewari

et al., 1995b). This cascade of proteolytic activity can negatively be regulated by viral proteins such as baculovirus p35 and IAPs (reviewed by Clem and Miller, 1994a; White and Gooding, 1994). p35 interacts with ICE and to some extent with ICE-like proteases forming a stable complex with them upon its cleavage (Bump et al., 1995). This interaction and subsequent cleavage of the viral protein, thus, inhibits the protease from interacting with downstream targets .

IAPs are also capable of inhibiting apoptosis (Liston et al., 1996). Although, IAPs demonstrate functional similarity to p35, they share no significant structural similarity suggesting a different mechanism of action for IAPs. The molecular basis of apoptosis inhibition byIAPs is however, not known.

Viral IAPs consist of two structural motifs; an N-terminal 70 amino acid repeats known as BIR (baculovirus IAP repeat) domain and a C-terminus C_4HC_3 type RING zinc finger (Clem and Miller, 1994b). Early characterization of viral IAPs revealed that the anti-apoptotic ability of OpIAP and CpIAP is abolished by substitution of their RING zinc finger with that of AcIAP (Friesen and Miller, 1987; Clem et al., 1991) suggesting a regulatory role for RING zinc finger. The function of BIR domains, however, is still unknown.

To date over a dozen members of *iap* gene family have been identified in various organisms (Liston et al., 1997b). Members of the IAP family can be classified in three groups according to their structural motifs: 1. IAPs with three BIR domains and a RING

zinc finger. These include Xiap, Hiap-1, and Hiap-2 and their murine homologues; 2. IAPs with two BIR domains and a RING zinc finger; such as viral IAPs as well as *Drosophilia* Diap-1; and 3. IAPs with three BIR domains but no RING zinc finger. The SMA (spinal muscular atrophy)-associated NAIP appears to be the only member of this third group of IAPs. The other human IAPs contain three BIR domains as well as a RING zinc finger (Liston et al., 1996). All of the human IAPs have been shown to be generally capable of inhibiting apoptosis in a variety of cells and against different apoptotic stimuli. Liston and coworkers (1996), using pools of CHO expressing human IAPs in their death assay system, have demonstrated that X-linked *xiap* functions as the most potent one. It is, however, not clear how IAPs inhibit apoptosis and which region of these proteins (i.e. BIR domains or RING zinc finger) is responsible for their antiapoptotic function.

Enhanced rescue of a *Drosophilia* eyeless mutant using a truncated version of *Drosophilia* IAP Diap-1 possessing only two BIR domains and lacking the RING zinc finger (Hay et al., 1995) and also suppression of apoptosis by NAIP which lacks the RING zinc finger suggested that the BIR domains are responsible for the anti-apoptotic effect of IAPs. One possible model is that human IAPs, in a similar fashion to viral proteins, function as protease substrates thus inhibiting progression of the protease cascade of events.

In an attempt to address some of these issues, I have assessed the anti-apoptotic capability of various *xiap* and *miap*-3 constructs in protecting cells against apoptotic assaults. Results demonstrate that BIR domains are both necessary and sufficient for the anti-apoptotic function of IAPs. The RING zinc finger, however, appears to function as a

negative regulatory domain. I also examined cellular localization of Xiap and Miap-3 in normal cells and in apoptotic cells. Results demonstrate that while full-length IAPs as well as a truncated RING zinc finger protein localize exclusively to the cytoplasm, the BIR domains appear to localize to the nucleus in addition to the cytosol. I also show that BIR domains localize to the nucleus during apoptosis. This indicates that cleavage and release of BIR domains from the negative regulatory effect of RING zinc finger during apoptosis may be necessary for its exertion of anti-apoptotic effect.

Materials and Methods

Plasmid constructs. *xiap* deletion constructs were generated by PCR amplification (see Table 3.1 for a list of primers) and subsequent insertion downstream of an hemagglutinin (HA) epitope tag in the expression vectors pcDNA3 (Invitrogen). These include *xiap* full-length cDNA, BIR 1 deleted (xiap Δ1), BIR 1 and 2 deleted (xiap Δ2), BIR 1 and 2 and 3 deleted (xiap ΔBIRs) and/or RING zinc finger deleted (xiap ΔRZF) constructs (Fig. 3.1; and Fig. 3.3). *miap*-3 constructs includes *miap*-3 full-length coding region, or BIR domains or RING zinc finger (Fig. 3.2; and Fig. 3.3). Fragments were amplified by PCR using primer sets in which one primer contained a BamHI site and the second contained an EcoRI site (Table 2.1). PCR products were double digested with

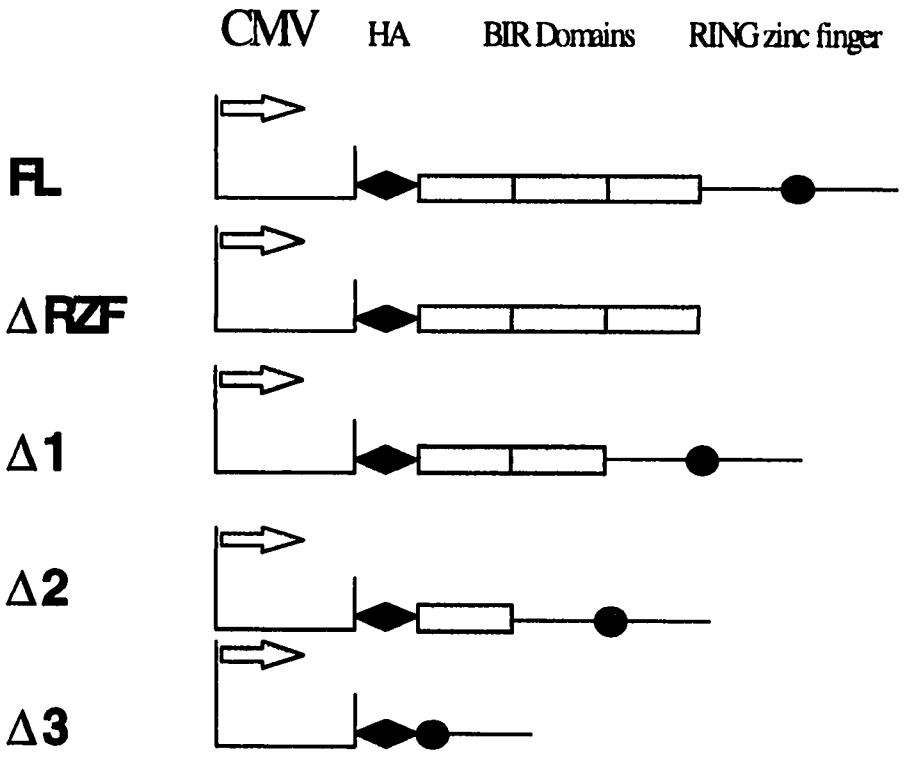
CMV
HA
BIR Domains
RING zinc finger
FL
ΔRZF
Δ1
Δ2
Δ3

Figure 3.1: *xiap* deletion constructs in the eucaryotic expression vector pCDNA3.

Schematic representation of *xiap* PCR amplified cDNA fragments, sub-cloned into expression vector pCDNA3, driven by a CMV promoter (arrow) downstream of an HA epitope tag (shown in purple diamonds). Primer sets 2486-2482, 2485-2482, 2484-2482, 2483-2482, 2486-2481 (Table 3.1) were used to amplify *xiap* full length (FL), BIR 1 deleted (Δ1), BIR 1+2 deleted (Δ2), BIR 1+2+3 deleted (Δ3) and RING zinc finger deleted (ΔRZF) cDNA respectively. BIR domains are shown in light pink boxes and RING zinc finger is shown in dark pink oval.

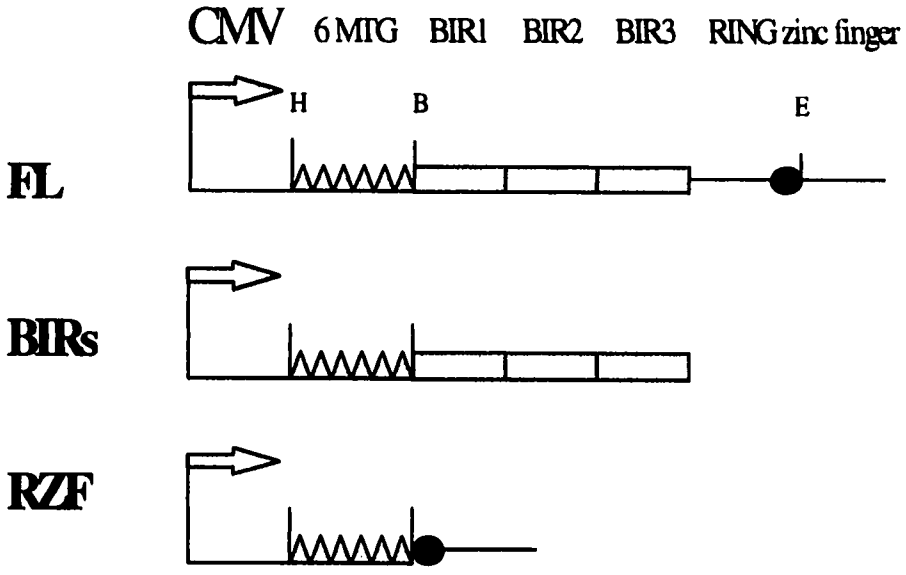
CMV
6 MTG
BIR1
BIR2
BIR3
RING zinc finger
H
B
E
FL
BIRs
RZF

Figure 3.2: *miap*-3 deletion constructs in pCDNA3.

Schematic representation of various *miap*-3 deletion fragments in pCDNA3 expression vector downstream a six repeat of the human *myc* epitope tag (purple triangles) driven by a CMV promoter (arrow). BIR domains are shown in pink boxes and RING zinc finger is shown in pink oval. Primer sets 2574-2575, 2574-2577 and 2576-2577 (Table 2.1) were used to amplify *miap*-3 BIR domains (BIRs), full length (FL) and RING zinc finger (RZF) respectively. MTG, *myc* epitope tag; H, HindIII; B, BamHI; and E, EcoRI.

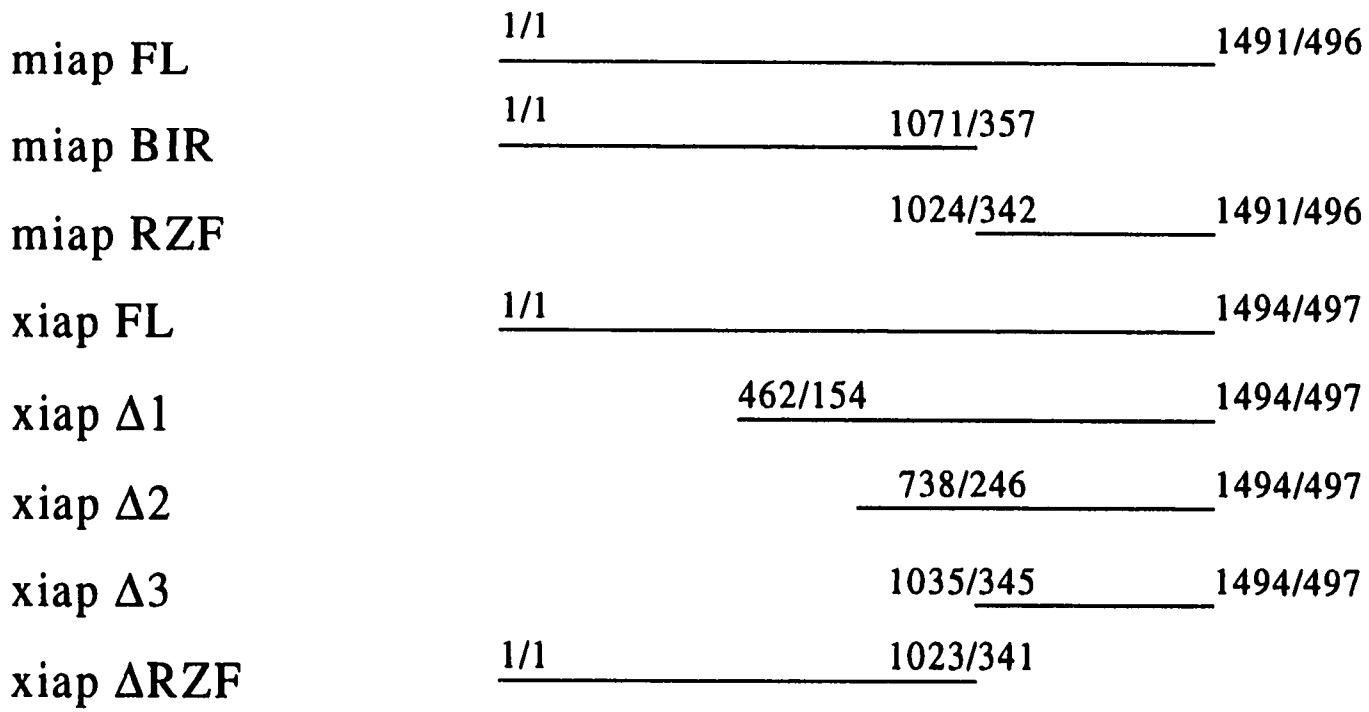
miap FL
1/1
1491/496
miap BIR
1/1
1071/357
miap RZF
1024/342
1491/496
xiap FL
1/1
1494/497
xiap Δ1
462/154
1494/497
xiap Δ2
738/246
1494/497
xiap Δ3
1035/345
1494/497
xiap ΔRZF
1/1
1023/341

Figure 3.3: *xiap* and *miap*-3 constructs in the eucaryotic expression vector pCDNA3.

xiap and *miap*-3 constructs explained in Fig. 3.1 and Fig. 3.2 have been summarized here. Solid bars represent each construct with its relative position in the respectivecDNA. Numbers indicate position of basesa.a.'s in their respective cDNA/protein.

primer number	primer sequence	primer orientation
2481	AGACACTCCTCAAGTGAATG	1065 R
2482	TACTATAGAGTTAGATTAAGAC	1510 R
2483	ATTCACTTGAGGAGTGTCTG	1036 F
2484	CTGATAGGTTTCCCAAATTC	736 F
2485	GTATCCAGAATGGTCAGTAC	330 F
2486	TGACTTTTAACAGTTTTGAAGG	1 F

Table 3.1: List of primers used in subcloning of *xiap* deletion fragments.

List of primers used to PCR amplify *xiap* deletion constructs. The cDNA sequence, to which every primer binds and the orientation of each primer have been indicated; forward (F) and reverse (R). Primer numbers are the identification number given to each primer in the Molecular Genetics Laboratory and stored in the data base.

BamHI and EcoRI and then sub-cloned into the BamHI/EcoRI restricted expression vector pcDNA3 (Invitrogen). A 300-bp human *myc* epitope tag encoding six repeats of the sequence MEQKLISEEDL allowing detection of Myc-IAP fusion proteins by monoclonal α-Myc antibody 9E10, also PCR amplified from a Bluescript clone using primers bearing a HindIII or a BamHI site. The PCR product was digested with HindIII and BamHI and sub-cloned upstream of the cDNA in the *miap*-3 pcDNA3 constructs in a HindIII-BamHI site. The full-length coding region of *xiap* was also PCR amplified using a primer set in which one primer contained a BamHI site and the second contained an EcoRI site. PCR products were double digested with BamHI and EcoRI and then sub-cloned into the BamHI/EcoRI restricted expression vectors pcDNA3 downstream of the human Myc epitope tag.

***In vitro* translation.** Two μg of the cesium chloride gradient purified pCDNA3 constructs were added to 50 μL of a reticulocyte lysate in the presence of ^{35}S labeled methionine (Promega TNT Kit) and incubated at 30 °C for over an hour. Fractionation of the labeled *in vitro* translated products on an 8% SDS-PAGE revealed bands of the expected sizes by autoradiography (Fig. 3.4).

Cell line establishment. CHO (Chinese hamster ovary) cells (ATCC) grown in Eagles medium supplemented with 10 % fetal calf serum (GibcoBRL) were transfected with 1-2 μg of cesium chloride gradient quality plasmid using 10 μL of Lipofectace or

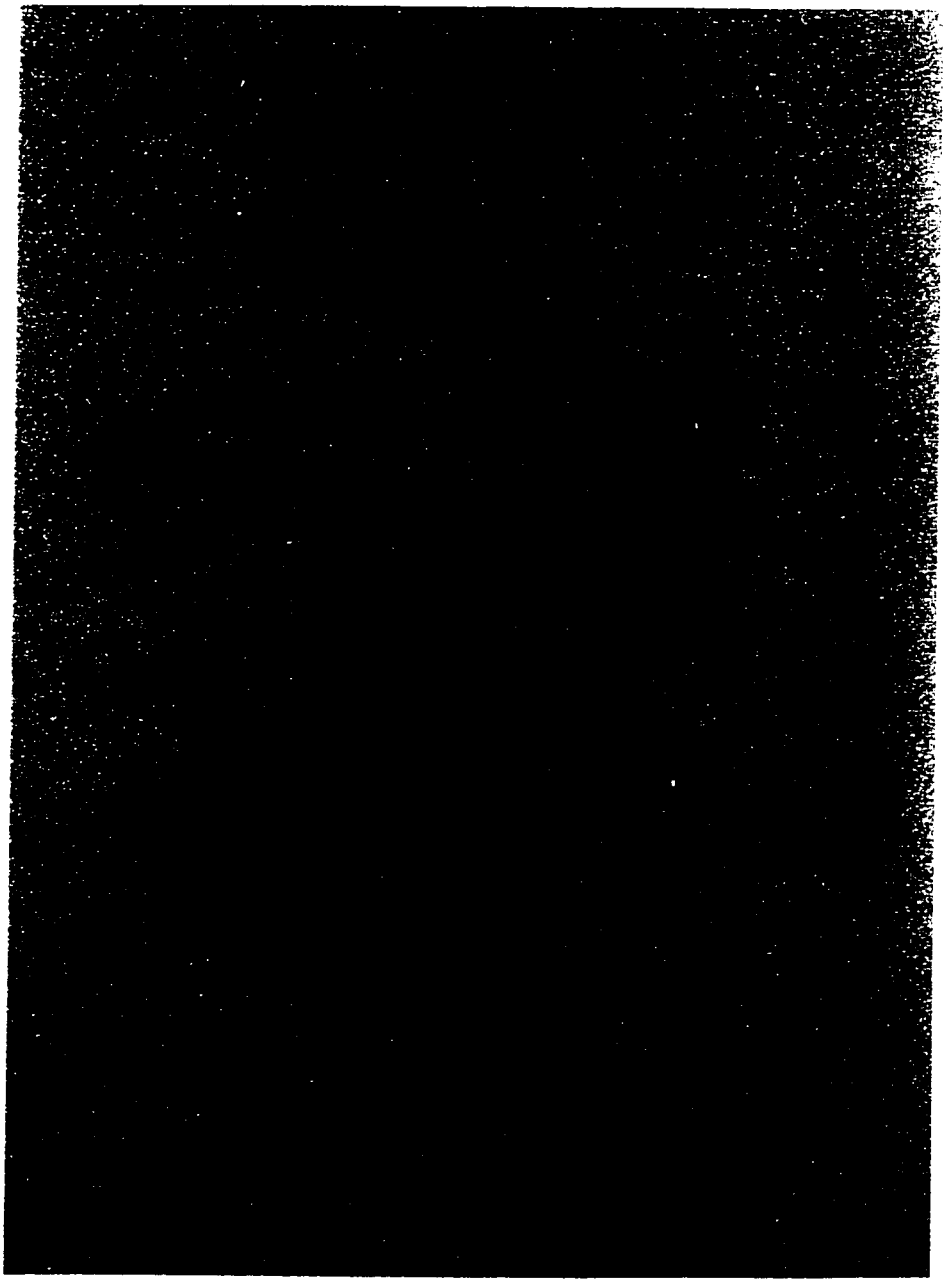

Figure 3.4: *In vitro* transcription and translation of *miap*-3 constructs in pCDNA3.

miap-3 constructs in pCDNA3 (Fig. 3.2) were tested for transcription and translation in an *in vitro* system as described in the Materials and Methods. The generated products were fractionated on an SDS-PAGE gel and exposed to film. Arrows indicated 66 and 26 kDa. The difference in the expected sizes is due to the 6MTG which has a calculated size of approximately 10 kDa. F, full length; B, BIR domains; R, RING zinc finger; and P,plasmid only with no insert.

Lipofectamine (GibcoBRL) per well in 6-well dishes for at least 5 hours. Transfected cultures were maintained under 450 μg/mL of Genetecin (G418) selection (GibcoBRL) for two weeks. Transformants were maintained in 250 μg/mL of G418 throughout the experiments. *xiap* transfected G418 resistant CHO cells were seeded at diluted concentration to obtain single cell colonies. Cell lysates from these colonies were used to identify Xiap expressing clones byimmunoblotting.

Death assays. For each death assay, cells were seeded in 24-well culture dishes at 0.5-1 x 10^5 mL-1 in triplicate. For serum deprivation assay, cells were washed three times in PBS and maintained in regular medium with no fetal calf serum supplement. Viable cells in each sample were counted by trypan blue exclusion at 0, 24, 48, or 72, hr after serum withdrawal using a haemocytometer. Survival was calculated as a percentage of initial viable cells counts (time 0). For menadione assays, transfected cells were washed three times in PBS and incubated in 10 and 20 μM menadione (Sigma) for 2 hours. After exposure to menadione, cells were washed five times in PBS and maintained in regular medium for 24 h. Viable cells were counted as described after 24 hours incubation post menadione exposure. Survival was calculated as a percentage of initial viable cell counts (time 0). Cells expressing Bcl-2 or full-length *xiap* coding cDNA (Liston et al., 1996) were used as positive controls. Untransfected CHO wild-type cells and CHO cells expressing pcDNA3 (Invitrogen) with no insert were used as negative controls. Each experiment was carried out 3 times independently (except for the β-gal (Fig 3.6c) which

was done only once). Results of the three experiment were pooled and subjected to statistical analysis.

For transient death assay, CHO cells were cotransfected with pcDNA3 plasmid carrying LacZ gene and one of *xiap* following constructs with a ratio of 1:3-5 (a total of 3-5 μg plasmid DNA) using Lipofectamine (Gibco BRL); pcDNA3-HA-BIR 1-BIR 2-BIR 3-RZF (full-length *xiap*), pcDNA3-HA-BIR 2-BIR 3-RZF (Δ1), pcDNA3-HA-BIR 3-RZF (Δ2), pcDNA3-HA-RZF (Δ3), pcDNA3-HA-BIR 1-BIR 2-BIR 3 (ΔRZF). Cells were grown in 6-well tissue culture dishes 24-48 hours after transfection and incubated overnight. Dishes containing cells which were 70-80% confluent were fixed with 0.25% glutaradehyde in PBS at 4 °C for 15-30 min and stained with 0.25 % X-Gal (5-bromo-4-chloro-3-indolyl β-D-galactoside)/5 mM potassium ferricyanide and 5 mM potassium ferrocyanide in PBS. Blue and clear cells were counted visually as transfected (expressing β-galactosidase) and non-transfected cells respectively. Efficiency of transformation was estimated as the ratio of blue cells to the total number of cells. The efficiency of transfection was approximately 75%. Membrane blebbing was used as an indicator to visually confirm apoptosis throughout death assay experiments (Fig 3.10).

Antibody generation. *xiap* or *miap*-3 coding sequences were PCR amplified and cloned in pGEX-2TK (Pharmacia) downstream frame of the sequence encoding Glutathione S-transferase (GST) (Fig. 3.5). The GST-fusion constructs were expressed *in vivo* by transforming and inducing *E. coli* with 0.5-1.0 M IPTG (Sigma) at 37 °C for 2

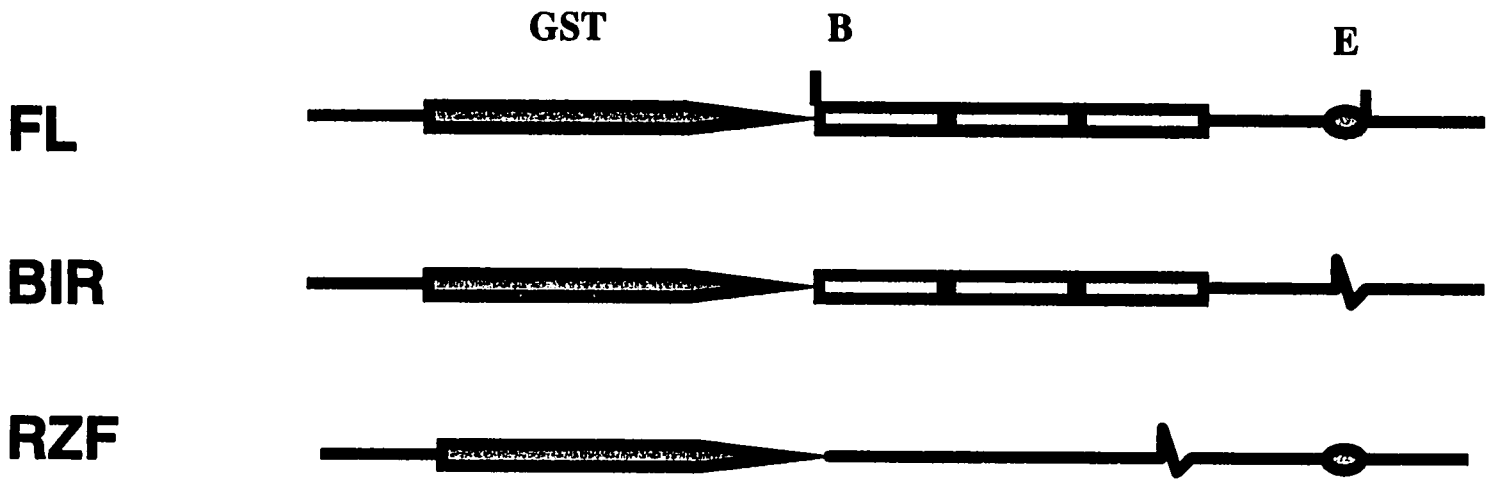
GST
B
E
FL
BIR
RZF

Figure 3.5: *miap*-3 constructs in the procaryotic expression vector pGEX-2TK.

miap-3 full length (FL), BIR domains (green boxes), and RING zinc finger (blue circle) were sub-cloned in the prokaryotic expression vector pGEX-2TK in downstream frame of GST (yellow arrow) by PCR amplifying each fragment as explained in Fig. 3.2.

hours. The resulting proteins were analyzed on an 8% SDS-PAGE. GST fusion proteins of the expected 81 kDa was detected (Not shown). Approximately 100 μg of gel purified Xiap/Miap-3 was used in complete Freunds adjuvant to immunize rabbits. Cleared serum from immunized rabbits was precipitated by ammonium sulfate and dialyzed against PBS. α-Xiap and α-Miap-3 immunoglobins were purified with column immobilized GST-Xiap and GST-Miap respectively.

Immunoblotting. Cells grown to nearly confluence were lysed in loading buffer (50 mM Tris, 2% SDS, 100 μM dithiothreitol, 0.1% bromophenol blue, 10% glycerol and a mixture of protease inhibitors). Total protein extracts from tissues were collected by homogenizing (Polytron homogenizer) fresh specimen in lysis buffer (150 mM NaCl, 50 mM Tris-Cl pH 8.0, and 5% SDS and a mixture of protease inhibitors) and subsequent boiling for five min and sonication. Protein samples were resolved on 12% SDS-PAGE gels and electrophoretically transferred (BioRad TransBlot) to immobilon membranes (Millipore). Western blotting was performed as described (Sambrook et al., 1989). Briefly, blots were blocked in 5% Skim milk in PBST (phosphate buffer PH 7.4 + 0.1% Tween 20) and then incubated with the primary antibody for an hour. Following extensive wash, blots were incubated in the secondary antibody conjugated to HRP for an additional one hour. Blots were then washed with 1xPBST. Signals were detected using ECL kit (Amersham).

Immunofluorescent microscopy. COS (African Green Monkey Kidney) cells were transfected using *xiap* or *miap*-3 pCDNA3 constructs as described above and

maintained in regular medium for 24 hours post transfection. COS or CHO cells expressing *xiap* or *miap*-3 constructs were grown on cover slips in 6-well dishes, fixed with cold methanol for 10-30 min, air dried and incubated with primary antibody in PBST for one hour at room temperature. Slides were then incubated with secondary antibody conjugated to either FITC or CY3 (Amersham or Sigma) following extensive washes. Negative controls were prepared using similar method without incubating slides with primary antibody. Slides were examined under aZeiss immunofluorescent microscope.

Results

Anti-apoptotic capability of *xiap* and *miap*-3 resides in the BIR domains.

In previous studies, we have demonstrated that IAPs are capable of inhibiting apoptosis in variety of cells (Liston et al., 1996). To find out what region of IAPs confer this anti-apoptotic effect, death assays were performed using pools of CHO cells expressing various deletion constructs of either *xiap* or *miap*-3 (Fig. 3.1; Fig. 3.2; 3.3; and Fig. 3.6). The full-length coding sequence of *xiap* or *miap*-3 provided a modest protection to CHO cells against serum withdrawal (approximately 25% after 72 hours). BIR domains, however, had an enhanced protection (approx. four folds over controls) while cells expressing RING zinc finger survived at the level of controls (Fig. 3.6a). Similar results were obtained from death assay experiments in which CHO cells expressing various *xiap* deletion constructs were used (Fig. 3.6b). In these death assay experiments, only

e

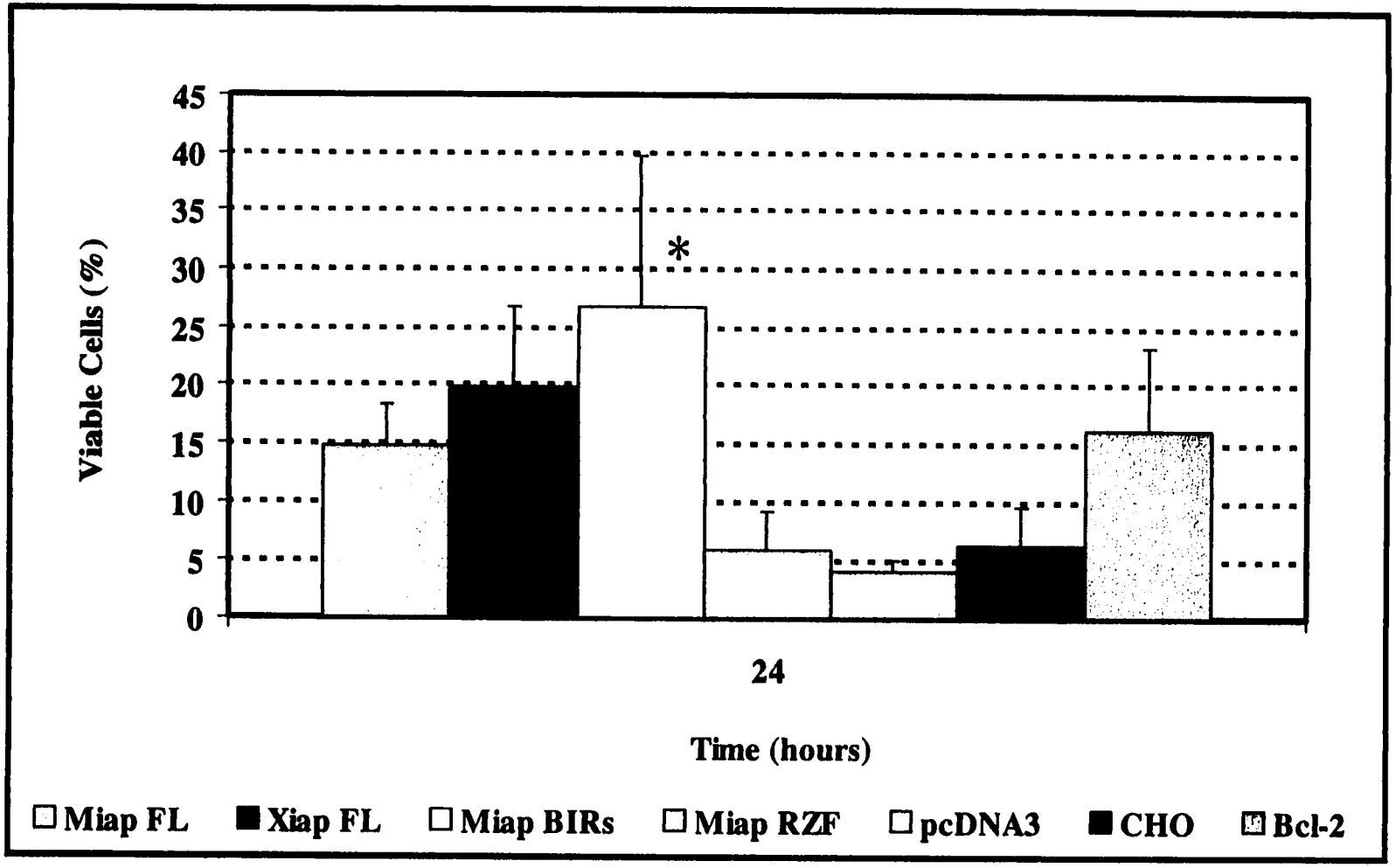
45
40
35
30
25
20
15
10
5
0
Viable Cells (%)
*
24
Time (hours)
Miap FL
Xiap FL
Miap BIRs
Miap RZF
pcDNA3
CHO
Bcl-2

d

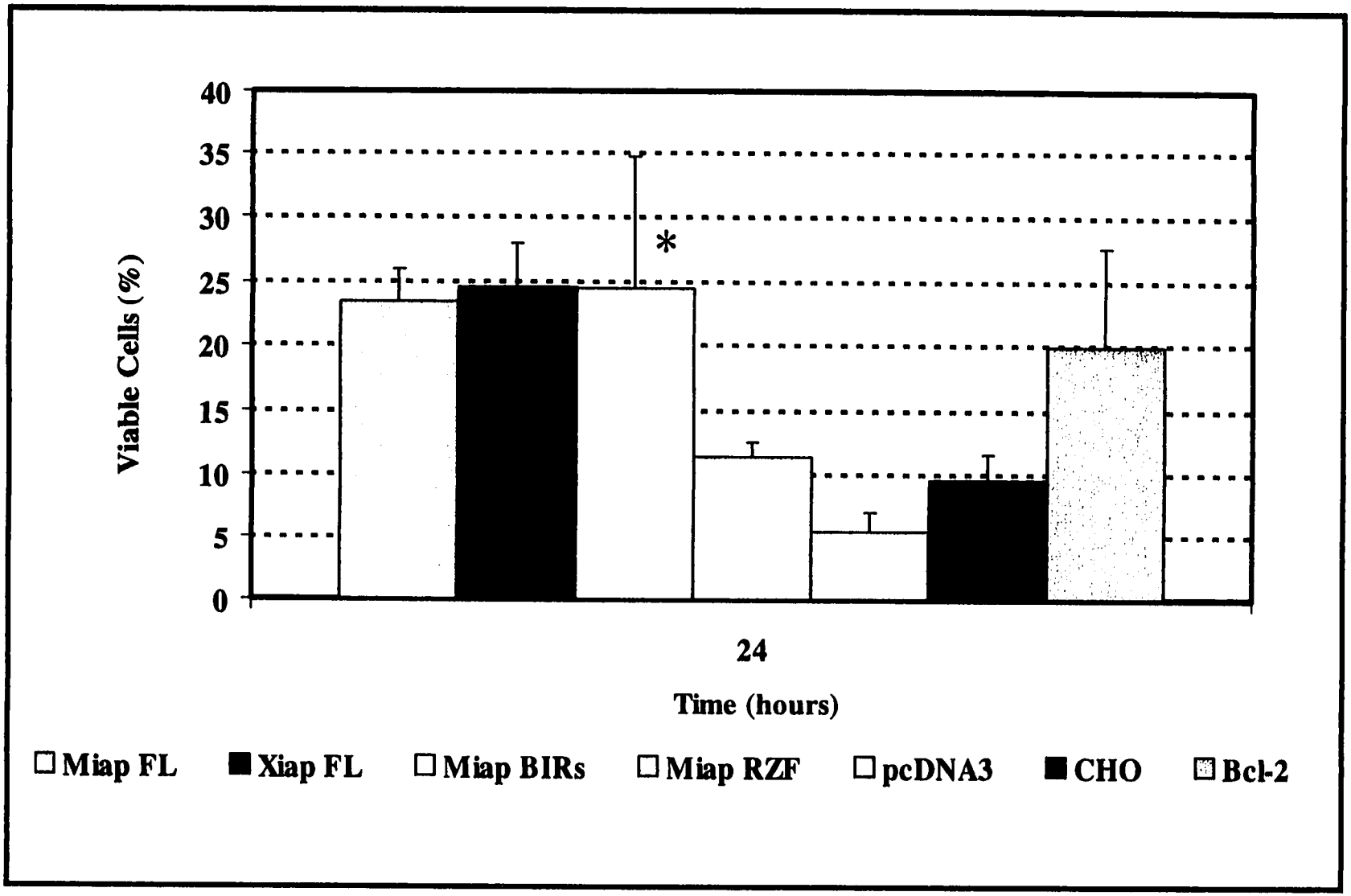
40
35
30
25
20
15
10
5
0
Viable Cells (%)
*
24
Time (hours)
Miap FL
Xiap FL
Miap BIRs
Miap RZF
pcDNA3
CHO
Bcl-2

c

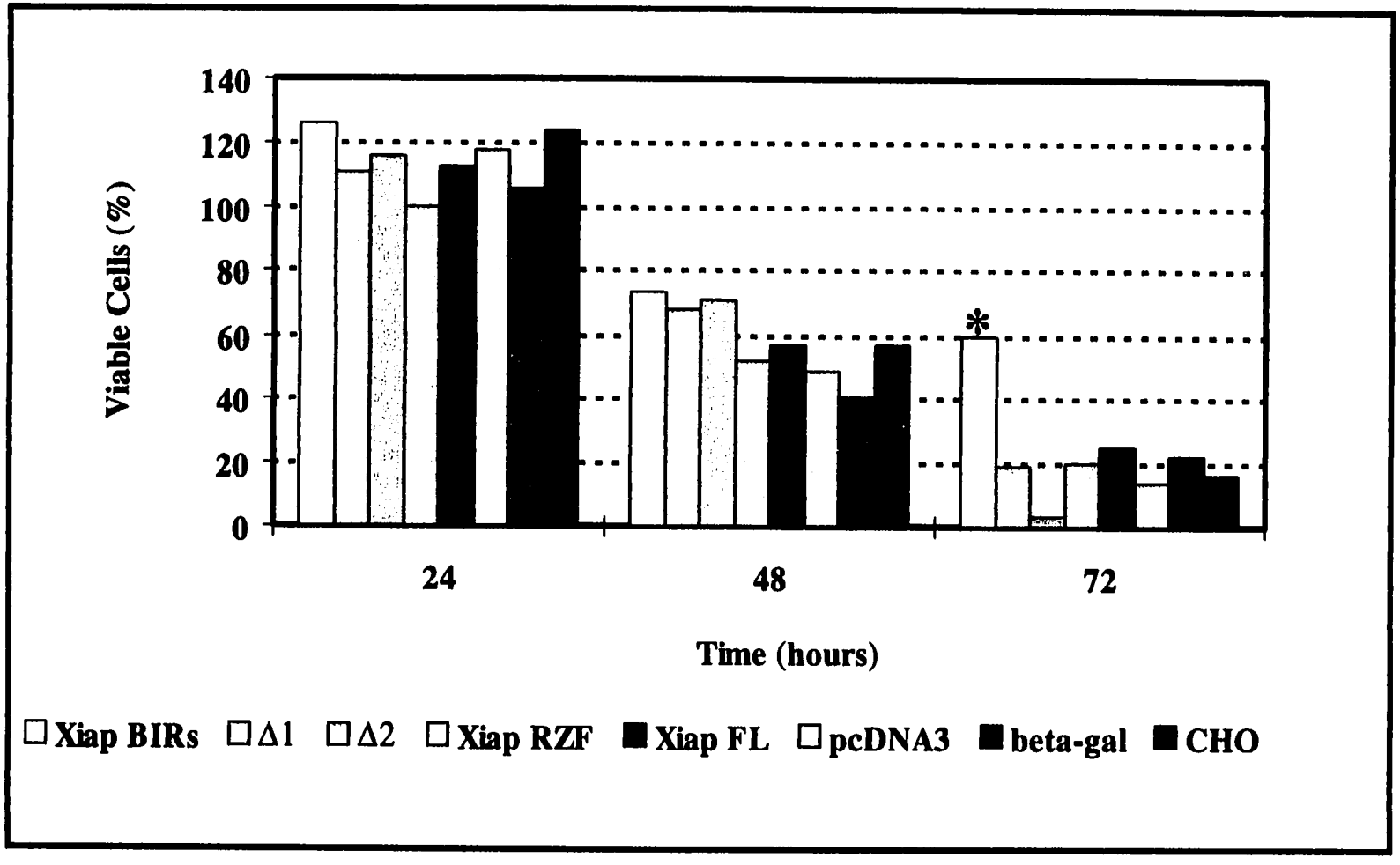
140
120
100
80
60
40
20
0
Viable Cells (%)
*
24
48
72
Time (hours)
Xiap BIRs
Δ1
Δ2
Xiap RZF
Xiap FL
pcDNA3
beta-gal
CHO

b

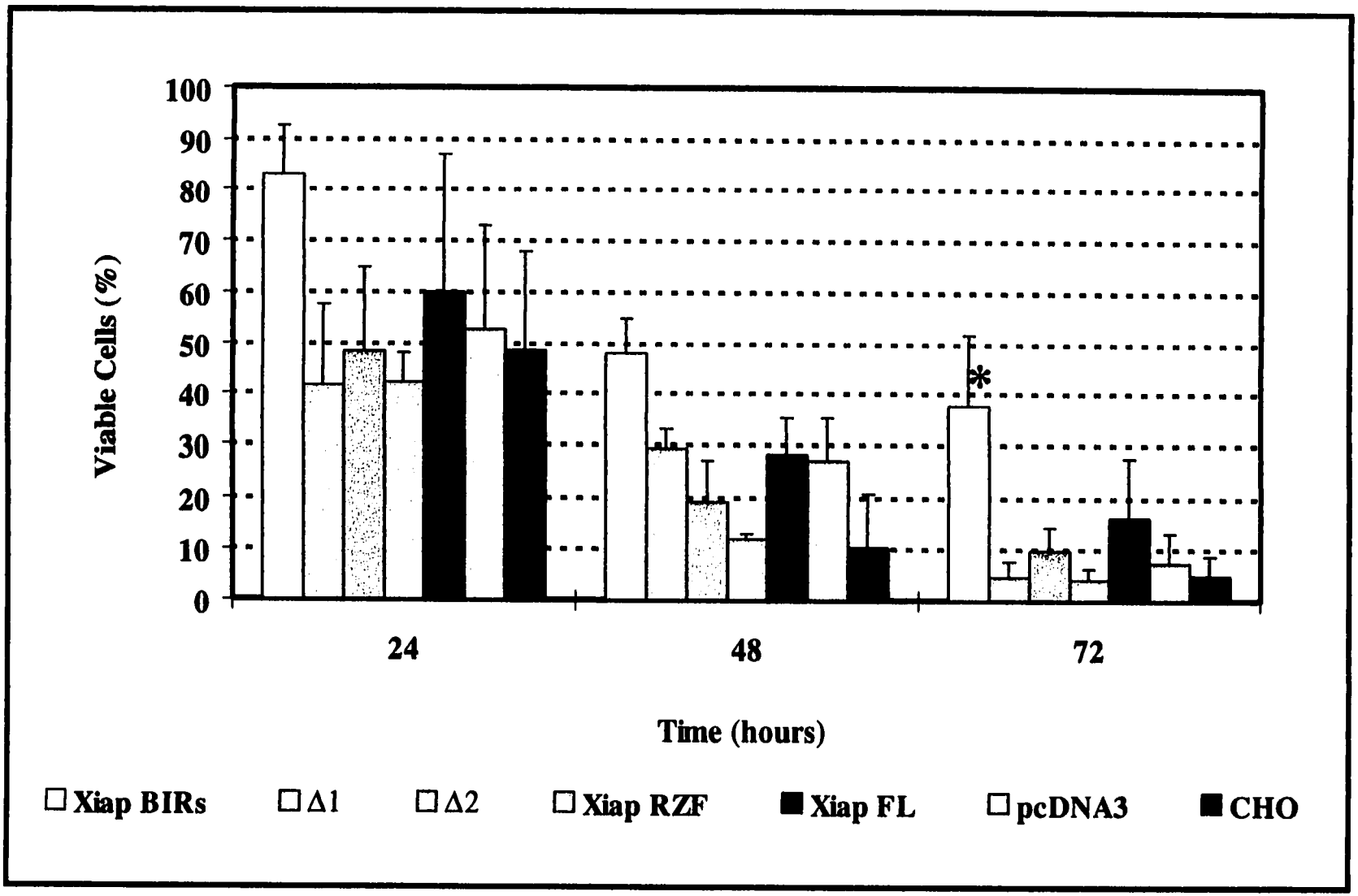
100
90
80
70
60
50
40
30
20
10
0
Viable Cells (%)
24
48
72
Time (hours)
*
Xiap BIRs
Δ1
Δ2
Xiap RZF
Xiap FL
pcDNA3
CHO

a

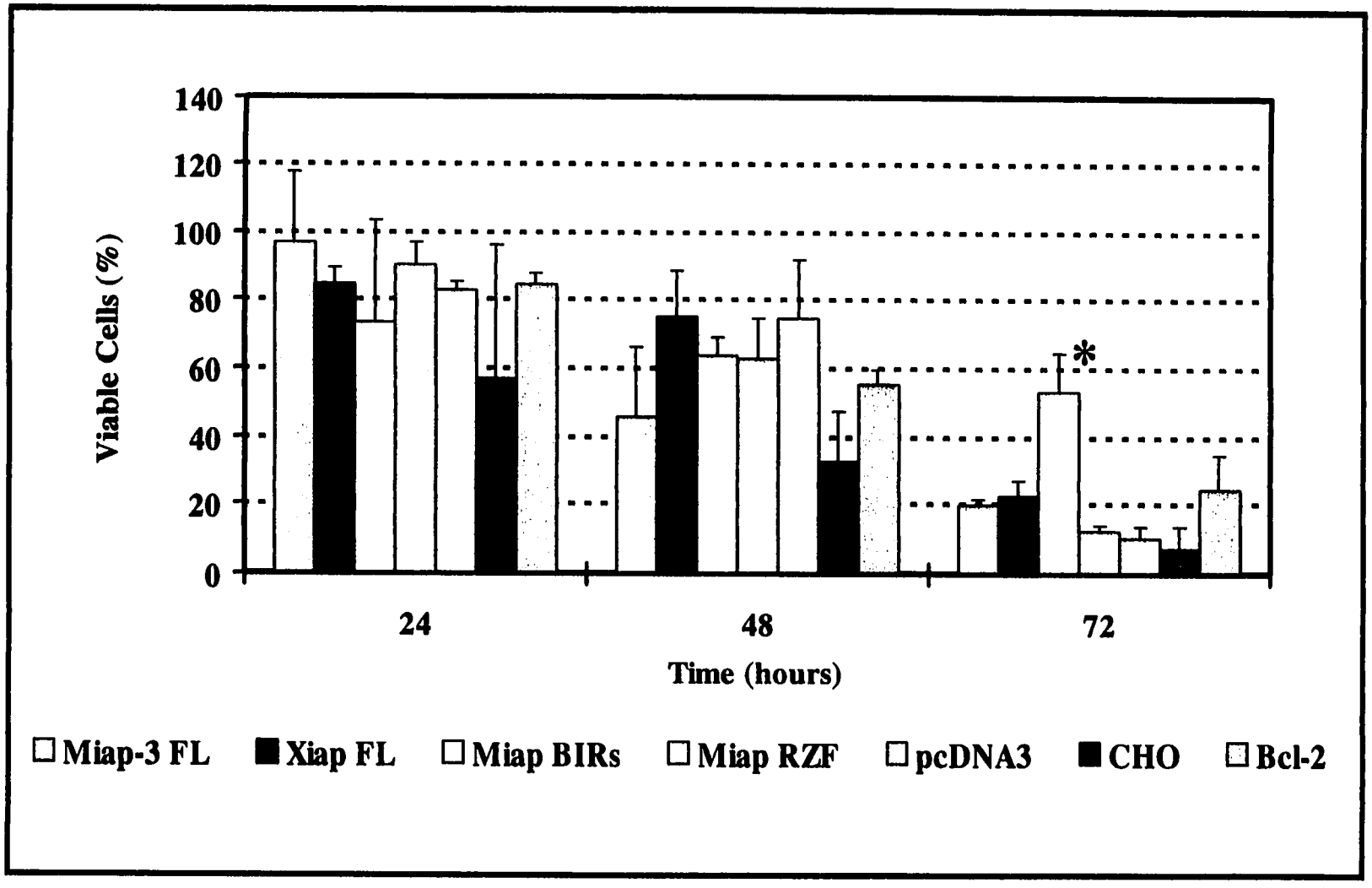
140
120
100
80
60
40
20
0
Viable Cells (%)
24
48
72
Time (hours)
*
Miap-3 FL
Xiap FL
Miap BIRs
Miap RZF
pcDNA3
CHO
Bcl-2

Figure 3.6: Results of death assay experiments in CHO cells expressing *miap*-3 or *xiap* deletion constructs.

On the X axis time after serum withdraw (where apoptosis is induced by serum withdrawal; **a**, **b**, and **c**) or time after two hr menadione exposure (where apoptosis is induced by menadione; **d**, 10 μM, and **e**, 20 μM) is shown in hours. On the Y axis percentage of viable cells are shown. Results are pooled from three (for *miap*-3) and four (for *xiap*) independent assays. Black bars show standard deviation. FL, full length; BIRs, BIR domains; RZF, Δ3; pcDNA3, vector with no insert; CHO, untransfected CHO cells; Bcl-2, *bcl*-2 coding sequence; Δ1, *xiap* BIR 1 deleted; Δ2, *xiap* BIR1+2 deleted; β-gal, cell transfected with a pcDNA3 vector carrying β-gal gene. β-gal co-transfection results demonstrate outcome of a single round of experiment.

* See Appendix A for significance and statistical analysis of death assays data.

those cells that expressed *xiap* with RING zinc finger deleted (therefore containing BIR domains only) showed enhanced survival over controls as well as over cells expressing full-length *xiap* coding sequence which showed probable moderate protection. Deletion of any of the BIR domains resulted in the inability of the construct to protect against apoptosis (Fig. 3.6 b, and c). Statistical analysis and significance of these finding are included in Appendix A.

In the death assay experiments where the free radical inducer menadione was used to induce apoptosis, the level of protection provided by *miap*-3 BIR domains was comparable to that conferred by the full-length protein (Fig. 3.6d, and e).

Changes in the cellular localization pattern of IAPs during apoptosis.

Immunofluorescence analysis of Xiap and Miap-3 cellular localization had previously shown cytoplasmic localization (Fig. 2.7) (Farahani et al., 1997, P. Liston, unpublished). BIR domains anti-apoptotic capability of Xiap and Miap-3 prompted an analysis of changes in the cellular localization pattern of IAPs. To study effect of apoptotic stress on IAPs' cellular localization, CHO cell line expressing full-length Xiap was plated on coverslips and incubated in regular medium overnight. Apoptosis was induced by serum deprivation as described under Materials and Methods. The cellular localization pattern of Xiap was examined by immunoflouroscent detection of protein species using polyclonal α-Xiap or α-Myc antibodies. In control cells, maintained in serum supplemented medium, Xiap was detected in the cytoplasm (Fig. 3.7a). But in the absence of serum, staining began to appear in the nucleus as well (Fig. 3.7b). The nuclear staining can be seen as

early as 10-15 hours post serum withdrawal. No evidence of hallmarks of apoptosis such as blebbing was observed at this stage. Only some nuclear and cytoplasmic condensation can be observed especially as apoptosis proceeds. Staining begins to disappear after 24 h of serum withdrawal. By 40 hours most of the cells appear to have lost their integrity.

Localization of BIR domains to nucleus during apoptosis.

The next question to be asked was whether it was the full-length protein or a portion of it that was translocalized to the nucleus during apoptosis. immunofluorescent microscopic examination of COS cells transiently expressing full-length Xiap or Miap-3 or one of their deletion constructs revealed that Xiap and Miap-3 full-length proteins and RING zinc-finger protein concentrate in the cytoplasm with some accentuation in the peri-nuclear zone (Fig. 3.8b). The distribution of full-length protein or RING zinc finger was similar to that observed for the full-length Xiap under non-apoptotic conditions (Fig. 3.7a). In contrast, BIR domains appeared to localize both in the cytoplasm as well as in the nucleus (Fig. 3.8c). In some cases, BIR domains localized mainly to the nucleus with little or no staining detected in the cytoplasm (Fig. 3.8d). Expression of a construct in COS cells containing BIR domains produced a cellular localization pattern much like the one observed in the CHO cell line expressing full length Xiap under apoptotic conditions (Fig. 3.7b). Further immunostaining using α-human Myc monoclonal antibody, which specifically identifies the sequence tag fused to the N-terminus of full-length *xiap*, confirmed that it was indeed the N-terminal portion of the proteins, i.e. BIR domains that was translocated to the nucleus during apoptosis. Level of signals in negative controls prepared as described in the Materials and Methods section without incubating the slides

with primary antibody, were low and could not be detected with Immunofluorescent microscopy.

Miap-3 tissue distribution.

α-Miap polyclonal antibody detects a 55 kDa protein in all of the mouse tissues tested including brain, lung, kidney, heart, spleen, liver and skeletal muscle (Fig. 3.9a). An extra band with the estimated size of 37 KDa is also present in all of the mouse tissues tested. The ratio of intensity of the lower band to the higher band varies from tissue to tissue.

To find out whether appearance of the lower molecular weight protein species identified by α-Miap polyclonal antibody correlates with apoptosis, fibroblast NIH3T3 cells were grown in regular medium until they were nearly confluent. Serum was withdrawn from the medium and whole cell extracts were collected after 24 hours. Immunoblotting shows that under normal condition α-Miap antibody detected one protein species with the expected size of 55 kD corresponding to endogenous Miap-3. But the 55 kDa protein gradually decreases as serum deprivation continues and a lower 37 kDa species begin to appear. After 24 hours post serum deprivation, the 37 kDa protein species is dominant and the 55 kDa band is not detected any longer (Fig. 3.9b).

Figure 3.7: Immunofluorescent detection of Xiap in CHO cells under normal and apoptotic conditions.

a. CHO cells expressing Xiap FL were stained with CY3 (Sigma) and examined for Xiap localization. Under normal conditions, Xiap appears to localize exclusively to the cytoplasm.

b. The same CHO cells were stained after 10 h of serum withdrawal. Under apoptotic conditions i.e. serum deprivation, staining appears in the nucleus as well as cytoplasm indicating protein translocation to the nucleus (Mag. 1000x).

Level of signals in negative controls prepared as described in the Materials and Methods section without incubating the slides with primary antibody, were low and could not be detected with Immunofluorescent microscopy.

c

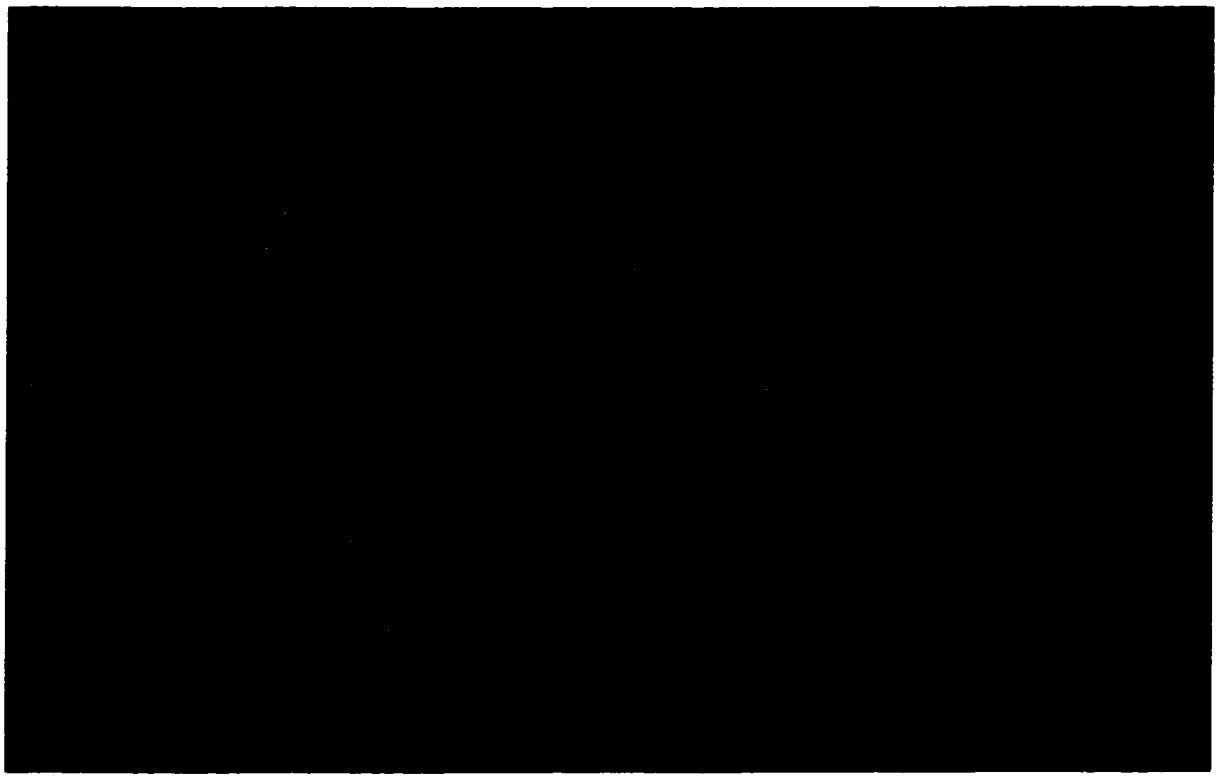

d

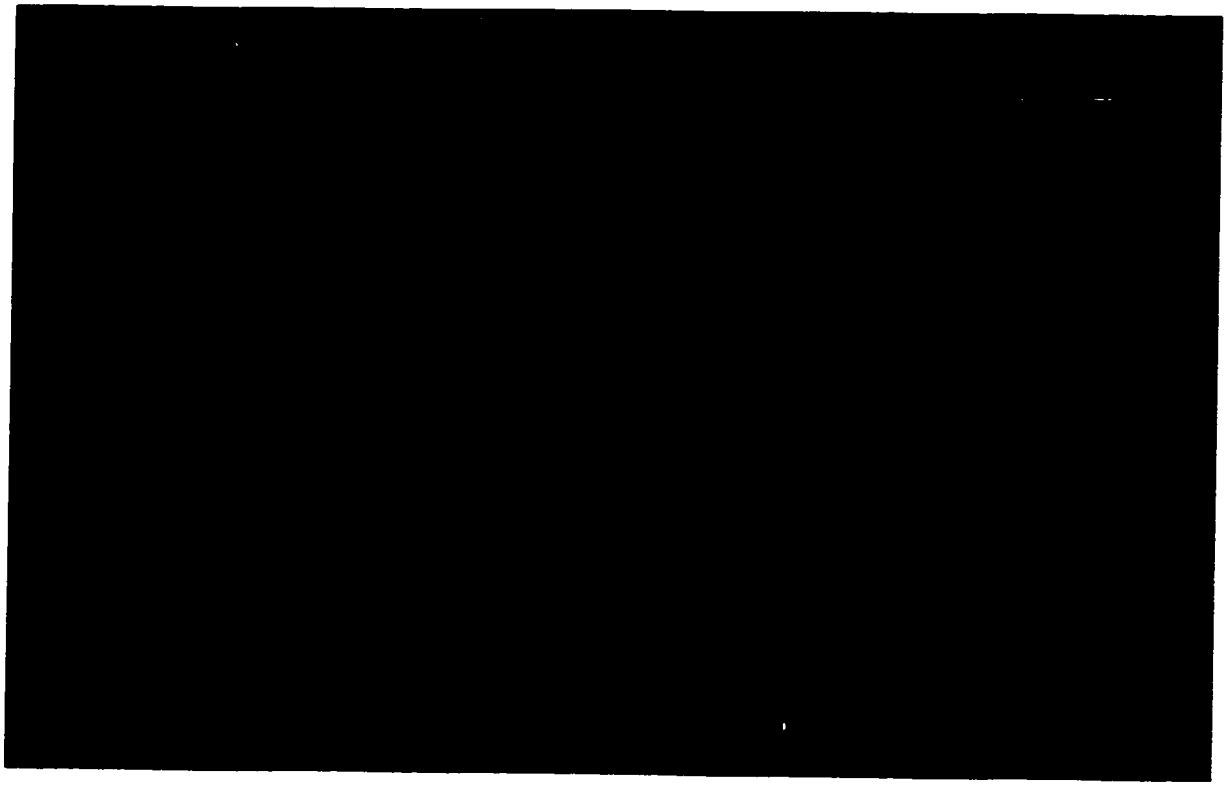

Figure 3.8: Immunofluorescent detection of the X-linked IAPs' cellular localization in COS cells.

COS cells were transiently transfected with *miap*-3 cDNA constructs in pcDNA3. Cells were stained with primary α-Myc antibody and secondary total Ig antibody conjugated to FITC. Slides were examined and photographed using a Zeiss fluorescent microscope (photographs show cells transfected with *miap* constructs).

FL and RZF are only detected in the cytoplasm (a and b respectively) while BIR domains are detected in the nucleus as well (c and d). *miap*-3 photos are included (mag 1000x). Detectable level of fluoresce were not observed in the negative controls were primary antibody was not used.

b

Construct	Base/a.a.	Viable cells % serum withdrawal			Cellular localization
		24 h	48 h	72 h	
No insert	NA	52.69	27.11	7.37	ND
Xiap Δ1	462-1494/154-497	41.71	29.33	4.66	ND
Xiap Δ2	738-1494/246-497	48.51	19.14	9.64	ND
Xiap FL	1-1494/1-497	59.69	28.21	16.24	cytoplasmic
Xiap BIRs	1-1023/1-341	83.09	48.16	37.64	cytoplasmic Nuclear
Xiap RZF	1035-1494/345-497	42.12	11.89	4.13	cytoplasmic

a

Construct	Base/a.a.	Viable cells %					Cellular localization
		serum withdrawal			menadione		
		24 h	48 h	72 h	10 μM	20 μM	
No insert	NA	82.49	74.21	10.06	05.40	04.14	ND
Miap-3 FL	1-1491/1-496	96.82	45.93	19.52	23.42	15.42	cytoplasmic
Miap-3 BIRs	1-1071/1-357	73.07	63.33	53.40	24.49	26.91	cytoplasmic Nuclear
Miap-3 RZF	1029-1491/342-496	89.86	62.44	11.90	11.33	05.87	cytoplasmic

Table 3.2: Anti-apoptotic effect and cellular distribution of full-length Xiap or Miap-3 and their truncated versions under normal and apoptotic conditions.

Effect of various **a.** Miap-3 and **b.** Xiap constructs in protecting CHO cells against apoptosis induced by serum deprivation or menadione exposure (for miap-3 constructs only) as well as their cellular localization (in COS cells) have been summarized. In column two position beginning and end of each construct has been shown.

d

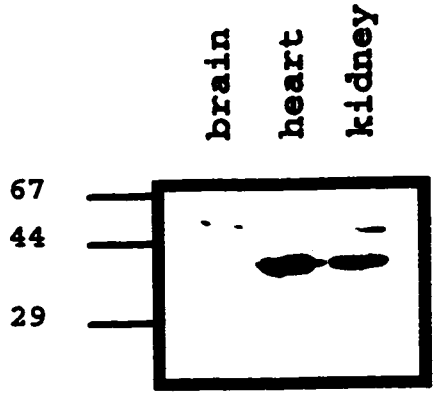

e

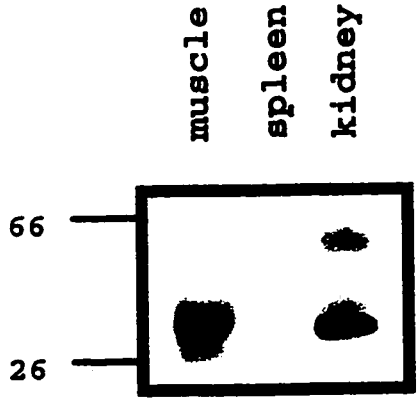

a

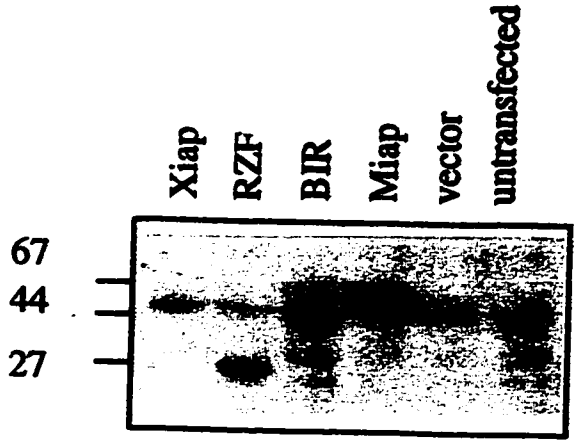
Xiap
RZF
BIR
Miap
vector
untransfected
67
44
27

b

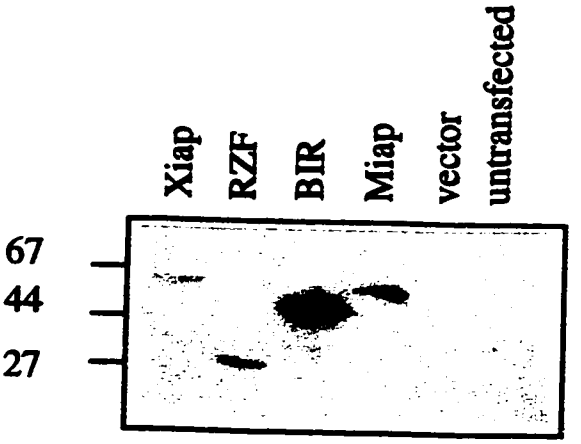
Xiap
RZF
BIR
Miap
vector
untransfected
67
44
27

c

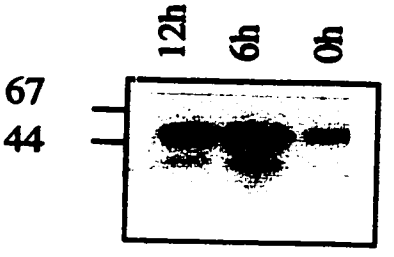
12h
6h
0h
67
44

Figure 3.9: Detection of Miap-3.

(a) *miap*-3 polyclonal antibody detects two species of proteins in various mouse tissues; M; muscle; S, spleen; K, kidney; H, heart; L, liver; and B, brain. Arrows show 66 and 26 kDa. Relative intensity of the two detected bands vary from tissue to tissue. In skeletal muscle, for instance, the intensity of the higher band is very low while the intensity of the lower band is greater contrary to spleen where the intensity of the higher band is greater than the lower band. Intensity of the two protein species in liver and brain appear to be identical.

(b) *miap*-3 polycolonal antibody detects a protein species of approximately 55 kDa in NIH 3T3 fibroblasts. Under apoptotic conditions, i.e. serum deprivation, the 55 kDa protein is no longer detected, instead, a lower size protein species of approximately 37kDa appears.

Figure 3.10. Phase contrast microscopy of apoptotic CHO cells.

CHO cells develop membrane blebbing, and condensation indicating apoptosis caused by serum withdrawal.

a. A CHO cell demonstrating pronounced membrane (arrowheads) blebbing and condensation after approximately 20 h of serum withdrawal (mag 400x).

b. Micrograph of apoptotic CHO cell (arrowhead) demonstrating nuclear and cytoplasmic condensation caused by serum deprivation for approximately 20 hr (mag 1000x).

Discussion

IAPs have two distinct domains: the N-terminal BIR domains and the C-terminal RING zinc finger. Although all of human IAPs i.e. NAIP, Xiap, Hiap-1 and Hiap-2 have generally been shown to protect a variety of cell lines against apoptosis induced by a number of different triggers, the mechanism of this function is by large unknown. Moreover, it has not been established whether the anti-apoptotic capability of IAPs is conferred by BIR domains or the RING zinc finger. I have employed death assays to address some of these questions. Expression constructs containing full length IAP cDNA, or BIR domains, or RING zinc finger, as well as deleted forms of human and/or murine X-linked *iaps* (i.e. *xiap/miap-3*) were transiently or stably expressed in CHO cell lines. Apoptosis was induced by serum withdrawal or treatment with menadione.

Expression of full-length Xiap confers modest protection to CHO cells. More than 20% of CHO cells expressing full-length Xiap are viable after 72 hours of serum deprivation. Expression of BIR domains, however, provides enhanced protection against serum withdrawal induced apoptosis. In fact over 50% of CHO cells expressing BIR domains but not the RING zinc finger, are still viable 72 hours after serum deprivation (Fig 3.6b). Similar results have been observed with Miap-3, the murine homologue of Xiap (Fig. 3.6a). Expression of the full-length Miap-3 protects approximately 25% of CHO cells following 72 hours of serum deprivation. Removal of the RING zinc finger, however, enhances this anti-apoptotic effect with greater than 60% viability observed for CHO cells following 72 hours of serum deprivation. Removal of one or more of the BIR domains or

the RING zinc finger in isolation results in a loss of apoptotic suppression as reflected in a decreased number of surviving cells (Fig. 3.6a; and 3.6b; and Table 3.2a and 3.2b).

Results of these death assay experiments, thus, demonstrate that three BIR domains are sufficient and necessary for suppression of apoptosis. These results suggest a negative regulatory function for the RING zinc finger. In fact, similar type RING zinc fingers have been implicated to function as regulatory elements in dozens of proteins possessing such motifs (Reviewed by Saurin et al., 1996; Evans and Hollenberg, 1988; Lovering et al., 1993). These proteins function by interacting with other proteins through their RING zinc fingers.

Observation of the BIR domains conferring apoptotic suppression is consistent with the anti-apoptotic activity observed for the zinc finger-less SMA NAIP (Roy et al., 1995) and also is in keeping with findings of Hay and his co-workers who demonstrated that expression of *Drosophila* Diap-1 which possess only two BIR domains and no RING zinc finger is more effective than the full-length protein in rescuing an eyeless mutant (Hay et al., 1995). Examination of anti-apoptotic capability of truncated mammalian IAPs possessing two BIR domains i.e. BIR 1+2 or BIR 2+3 and no RING zinc finger should provide useful information on whether all three BIR domains are necessary for anti-apoptosis function of IAPs in various cellular background and also against various apoptotic triggers.

Sequence comparison of BIR elements in mammalian IAPs show that BIR 1 and BIR 2 are more identical to each other than to BIR 3 (Fig. 2.10). It appears that the third BIR is a recent duplication of one of the already existing two BIR elements. This may have provided a slight functional advantage to the IAPs with three BIR domains and/or introduced another level of redundancy which appears to be the inseparable element of apoptosis signaling pathway components. A clear example of this redundancy can be seen in the evolution of each protein that functions in the apoptosis signaling pathway in the lower animals such as in the nematode *Caenerohabditis elegans* to a family of proteins in the higher animals (see introduction of the thesis).

I also evaluated the effect of full length and truncated version of Miap-3 in protecting CHO cells against menadione induced apoptosis. Interestingly, I have noticed that in death assays where apoptosis is induced by menadione, the enhanced effect of BIR domains are no longer observed. In fact expression of both BIR domains and full length Miap-3 protect CHO cells against menadione induced apoptosis at a similar level (Fig. 3.6d and e). In these experiments, CHO cells were exposed to two different concentrations of menadione. Results of both experiments using 10 or 20 μM of menadione are comparable. Over 95% of control CHO cells die of apoptosis after 24 hours when exposed to 10 or 20 μM menadione for 2 hours. Approximately 25% of CHO cells exposed to menadione are viable after 24 hours when they are expressing full-length Miap-3 or Miap-3 BIR domains (Fig. 3.6d and e; and Table 3.2).

Ability of BIR domains to provide an enhanced protection against apoptosis induced by serum deprivation but not against menadione induced apoptosis, may suggest that IAPs function downstream from the point where various apoptotic signals merge resulting in the subsequent activation of downstream proteases. These observations also suggest that menadione may override the enhanced protection of BIR domains by affecting components that function in parallel signaling pathways leading toapoptosis.

Immunofluorescent microscopy of Xiap expressing CHO cell lines revealed that Xiap is expressed in the cytoplasm (Fig. 3.7a). Localization examination of CHO cell lines expressing Xiap revealed nuclear staining after 10 hours post serum withdrawal, suggesting translocation of either full-length or a portion of Xiap to the nucleus upon apoptosis induction (Fig. 3.7b). Translocation of Xiap to the nucleus, in fact, occurs prior to appearance of apoptosis hallmarks such as membrane blebbing and cytoplasmic condensation. All CHO cells expressing Xiap demonstrate a degree of nuclear staining after 10 hours of serum deprivation. It is noteworthy that even at 24 hours post serum deprivation, the number of viable CHO cells expressing Xiap is comparable to that of controls expressing no IAPs (3.6b; and Table 3.2). It takes approximately 48 hours to observe a clear difference in the percentage of viable cells expressing no IAPs and those that express full-length IAPs or BIR domains in death assays where apoptosis is induced by serum withdrawal. Therefore, it appears that nuclear translocation of Xiap occurs before apoptosis enters into a phase where cells have been committed to death and apoptosis becomes irreversible, due to perhaps extensive structural damage ultimately developing into cellular condensation and cytoskeleton collapse. Translocation of BIR

domains to the nucleus should be deemed as a part of an anti-apoptotic mechanism that can protect the cell. This, however, may not be sufficient for rescuing the cell and apoptosis may still proceed. By 48 hours post serum deprivation, staining becomes difficult to detect. Light microscopy examination of cells show pronounced membrane blebbing, cellular condensation and cell death (Fig. 3.10). By this time, a clear difference in the percentage of viable cells between IAP protected and non-protected cultures emerges (Fig. 6a and b; and Table 3.2).

Translocation of Xiap to the nucleus during apoptosis was evident from fluorescent microscopy examination of CHO cell lines expressing Xiap (Fig. 3.7b). However, it was not clear whether the nuclear translocation during apoptosis included the intact protein. Fluorescent microscopy of COS cells transiently expressing Xiap or Miap-3 deletion constructs revealed that the full-length Xiap and Miap-3 localize to the cytoplasm with an accentuation in the peri-nuclear zone (Fig. 3.8a). Cells expressing the RING zinc finger domain only demonstrate similar cytoplasmic localization pattern (Fig. 3.8b). Fluorescent microscopy reveals a different localization pattern in cells expressing BIR domains (Fig. 3.8c). In these cells, BIR domains protein appears to localize to both cytoplasm and nucleus. The degree of accentuation of proteins in the cytoplasm or nucleus varies from one cell to the next. In some cases, BIR protein mainly localizes to the nucleus and very little or no protein is left in the cytoplasm (Fig. 3.8d). These results suggest that Xiap RING zinc finger is removed by a cleavage activity during apoptosis, releasing BIR domains for nuclear translocation while RING zinc finger remains in the cytoplasm of apoptotic cells.

One model for the IAPs anti-apoptotic function is that under normal conditions i.e. absence of apoptosis signal, IAPs are present in the cytoplasm. Upon increase in or introduction of death signal and subsequent activation of proteases responsible for the execution of cell death, IAPs bind these active proteases and prevent them from interacting with their targets. Reed and his coworkers have recently demonstrated that Xiap and its BIR domains can bind several active caspases and inhibit apoptosis (Deveraux et al., 1997). Interaction with active proteases probably results in the cleavage of IAPs and release of their BIR domain. This allows BIR domains to be translocated to the nucleus in complex with other proteins since no NLS has been identified in Miap-3 or Xiap. BIR domains may function as transcription regulators once in the nucleus. In keeping with this, J. Tanner has shown that Xiap BIR domain can bind regulatory elements in the promoter region of the transcription factor NFkB and regulate expression of a downstream reporter genes (Tanner, J., personal comm.).

The implication of IAPs cleavage during apoptosis was first discovered by Miayazaki, T. who demonstrated a cleavage product of endogenous Xiap in α-Fas antibody treated Jurkat cells (unpublished data). Xiap cleavage product is approximately 26 kDa in size. This corresponds to the size of two BIR domains. It is interesting to note that Xiap appears to contain a putative aspartic acid protease cleavage site between BIR 2 and BIR 3. Cleavage of Xiap at this site can potentially generate an approximately 26 kDa product. The aspartic acid residue is the only gap when Xiap and Miap-3 are aligned. Absence of this particular Asp Acid residue (Fig. 2.5) makes Miap-3 one residue shorter than Xiap. Therefore, Miap-3 may be cleaved at another site which has yet to be identified. Cleavage

of Miap-3 at another site may produce a BIR containing cleavage product which is different in size compared to Xiap cleavage product. If true, this may suggest that the primary aim of interaction of IAPs with active proteases is to produce a complex that sequesters the protease active site. Generation of a cleavage product containing BIR domains may only be a secondary result of this interaction. Nevertheless, generation of a cleavage product containing a variable number of BIR domains may confer specificity for the further possible function of these motifs.

Generation of a Miap-3 cleavage product containing BIR domains is confirmed by western blot analysis. α-Miap-3 polyclonal antibody detects two bands with the sizes of 55 kDa corresponding to the full length Miap-3 and a 37 kDa protein species that could potentially correspond to three BIR domains in various mouse tissues (Fig. 3.9). There is, however, clear difference in the ratio of the full length protein and the cleavage product in various tissues. The ratio of the two protein species is lower in brain and heart and much higher in kidney and skeletal muscle (Fig. 3.9a). α-Miap-3 polyclonal antibody detects a 55 kDa protein in mouse fibroblast cell line NIH3T3 maintained under normal conditions. The lower size protein becomes dominant after 24 hours of serum deprivation and the full length protein is no longer detectable (Fig. 3.9b). Therefore, production of a smaller size protein species which is believed to be a cleavage product of Miap-3 does not appear to be the result of α-Miap non-specific cross reactivity.

In conclusion, it appears that in response to apoptotic signals, IAPs, localizing to the cytoplasm, are cleaved and their BIR domains are translocated to the nucleus while the

RING zinc finger remains in the cytoplasm. The significance of IAPs BIR domains translocation to the nucleus in protecting cells against apoptosis is currently under investigation. In the present work, I have shown that IAPs anti-apoptotic capability is conferred by BIR domains which are possibly cleaved and translocated to the nucleus in response to apoptotic induction. I believe that these findings are important in understanding the mechanism ofIAPs function in protecting cells against cell death.

Conclusion

Significance of findings

In this work, a novel mammalian gene encoding Miap-3, the Murine homologue of the human X-linked IAP (Xiap) was cloned and characterized. *miap*-3 has a coding sequence of 1491 bp encoding 496 amino acids. *miap*-3 has six exons spanning approximately 25 kb of genomic DNA assigned to mouse chromosome X in the region A3-A5. Moreover, the ability of various portions of Xiap and Miap-3 in suppressing apoptosis was assessed. Results of these experiments suggest, in at least some cellular contexts, that the anti-apoptotic capability of IAPs is conferred by BIR domains with a negative regulatory function for the RING zinc finger. These results support the observation that expression of *Drosophila* Diap-1, which possesses only two BIR domains, is more effective than the

full-length protein in rescuing an eyeless mutant (Hay et al., 1995). These results also demonstrate that the RING zinc finger is unnecessary for the suppression of apoptosis consistent with the anti-apoptotic role documented for NAIP (Liston et al., 1996). In an effort to define the minimal functional sequences necessary for apoptosis inhibition, the ability of truncated mammalian IAPs with two BIR domains i.e. BIR 1+2 or BIR 2+3 and no RING zinc finger to protect cells against apoptosis should be investigated. These truncated version of Miap-3/Xiap are useful in delineating the anti-apoptotic capability of two BIR domains. It would also be of interest to show whether the RING zinc finger is dispensable when two mammalianBIR domains with anti-apoptotic capability are present.

IAPs that have been identified to date can be divided in two groups: IAPs that possess two BIR domains and the RING zinc finger. This includes the sub-groups of IAPs with two BIR domains (i.e. the viral IAPs and Diap-1) or IAPs with three BIR domains (i.e. mammalian IAPs). NAIP is the sole member of the second group of IAP which possess three BIR domains but no RING zinc finger. It appears that at least in insect cells when IAPs possess two BIR domains, the RING zinc finger becomes an indispensable motif in suppression of apoptosis. This has been supported by the original work of Clem and Miller (1994b) when they exchanged various viral protein RING zinc fingers. They showed that fusion of the AcIAP RING zinc finger with OpIAP or CpIAP BIR domains abolishes the anti-apoptotic capability of viral IAPs, suggesting a critical role for the RING zinc finger. Site directed mutagenesis will help to delineate such important sequences.

The *Drosophila* genome has encoded a second IAP, namely Diap-2 which possesses three BIR domains as well as a RING zinc finger. This may indicate that IAPs with three BIR domains have developed later in the evolution in higher animals. This implies a common ancestral gene that has served as the progenitor of all IAPs. To further characterize various sub-groups of IAPs, it is important to delineate their specificity. It has been shown that *xiap* which is expressed in all tissues, functions more like a ubiquitously expressed "house keeping" gene. *naip* however is expressed in a tissue specific manner. The developmental expression profile of these genes may help answer some of the questions concerning their specialization. It is conceivable that during development, anti-apoptotic protection is provided by one IAP such as Xiap. This function may be provided by other IAPs once development is completed; NAIP, for instance, may have developed further specificity to function in theCNS.

The *iap* genes contain either short (e.g. NAIP approximately 200 bases) or long (e.g. *xiap*, and *miap*-3) untranslated regions (UTRs). *xiap* and *miap*-3 have coding sequences of approximately 1.5 kb (Farahani, et al., 1997; and M. Lagace, unpublished) and unusually large messages of 9.5 and 8 kb respectively suggesting an 8 and a 6.5 kb 5' and/or 3' UTRs. In mammals, cis-acting elements have been identified in both 5' and 3' UTRs (reviewed in Schafer et al., 1995). These elements are both important for transcriptional as well as translational regulation (Weiss and Liebhaber, 1994; Weiss and Liebhaber, 1995; Russell and Liebhaber, 1996; Wang and Liebhaber, 1996; Roy et al., 1992). An example of such regulation is observed in AML-1 (acute myeloid leukemia 1) (Ghozi et al., 1996). AML1 has an approximately 7 kb 5' UTR with two transcription activation sites

containing regulatory elements. Transcription of AML1 gene is regulated by both promoters generating mRNA species ranging from 2-8 kb. AML1 5' UTR has been shown to play an important role in the AML1 post transcription regulation as well. On the other hand, 3' UTR has been shown to play an important role in stabilizing mRNA messages as well as regulating its translation. α-globin gene, for instance, the 3' UTR plays an important role in stabilizing the mRNA and regulating its translation (Weiss and Liebhaber, 1994; Weiss and Liebhaber, 1995). Analysis of 7 kb sequence mapping upstream of *miap*-3 first coding exon has revealed two potential promoter regions and several known regulatory elements such as SP1 sites (Holcik, M. personal comm.). These sequences may be important in transcription regulation of miap-3.

The remaining *iap* genes, however, do not appear to possess long 5' or 3' UTRs. NAIP with a coding region of over 5 kb has an mRNA of 6.1 kb in size (unpublished). The significance of the difference in the size of *iaps* UTRs is unknown. Characterization of *iaps* UTRs may provide information in determining their developmental as well as tissue specificity. This information may be useful in the development of clinical strategies aiming at altering the expression levels of*iaps* as required (see below).

How do IAPs inhibit apoptosis?

Data presented in this work demonstrate that during apoptosis BIR domains are translocated to the nucleus, whereas the RING zinc finger or the full-length protein remains primarily in the cytosol. Fragments containing BIR domains may be produced by a proteolytic cleaves of IAPs. This cleaves may be the result of IAPs interaction with active

caspases. IAPs may interact with active caspases and as a result be cleaved. Interaction of IAPs with active caspases and their subsequent proteolytic cleavage may result in a complex where the caspase active site is sequestered by IAPs. This may be one of the mechanism by which IAPs inhibit apoptosis and also transported to the nucleus. Our observation of cleavage and translocation of BIR domains to the nucleus during apoptosis is compatible with the documentation that Xiap is cleaved and its N-terminal cleavage product containing BIR domains is detected in the nucleus during apoptosis (Miyazaki, T. unpublished data). The important question then is " how do IAPs inhibit apoptosis and what is the relevance of BIR domain nuclear translocation to its anti-apoptotic function?" In the non-apoptotic situation, IAPs are distributed throughout cytoplasm. Upon induction of apoptosis, IAPs are recruited into the apoptosis signaling pathway, probably by components of TNF (tumor necrosis factor) signaling pathway (Rothe et al., 1995b). Rothe et al., (1995a) have shown that IAPs can interact with the complexes formed at the cytosolic domains of TNF receptors. These complexes may be recognized by proteases which cleave IAPs. Formation of a complex between proteases and cleavage product of IAPs may be the mechanism through which specific proteases involved in cell death execution are inactivated. This is in keeping with the recently demonstrated interaction and inhibition of caspases by Xiap (Deveraux, et al., 1997). Another possibility is that the IAP cleavage product not only blocks protease activity, but it also produces a BIR domain containing cleavage product that is translocated to the nucleus where it performs a second function. The significance of BIR domains translocation to the nucleus is the subject of current investigation. BIR domains function in the nucleus may directly or indirectly be involved in promoting transcription of genes important in cell survival and/or whose

products are capable of inhibiting apoptosis. It has been demonstrated that Xiap BIR domains can transactivate NFkB driven promoters and upregulate their expression (Tanner, J. unpublished data). NFkB, which is a common transcription factor, in turn can bind to its cognate recognition sites in the promoter regions of many genes and activate their transcription. Overexpression of NFkB has been shown to increase cellular resistance to apoptosis and promote cell survival (Reviewed byThanos and Maniatis, 1995).

Clinical importance of these findings

In a multicellular organism, cells are constantly exposed to environmental factors. The presence or absence of these factors stimulate cellular responses which are subject to multiple levels of monitoring and regulation (Reviewed by Williams and Smith, 1993). Regulation of cell death by apoptosis inhibitors and promoters generates a balance that dictates survival or death of a particular cell in a particular circumstance. Structural and/or functional defects in the apoptosis promoters and inhibitors can lead to various pathological proliferative or degenerative disorders (Thompson, 1995). Disorders caused by dysregulation of apoptosis machinery could be classified into two primary groups: first, the disorders that arise due to an abnormal accumulation of cells; and second, the disorders that are caused by abnormal loss of cells through apoptosis (Thompson, 1995). Studies focused on the cellular and molecular basis of immune system associated diseases have provided a number of examples for both types of proliferative and degenerative disorders, the underlying cause of which is dysregulation of apoptosis (see May et al., 1995; Hale et al., 1996). Overproduction and/or persistence of unnecessary lymphocytes in the immune system may result in autoimmune disorders such as lupus erythematosus,

rheumatoid arthritis and autoimmune diabetes (see Mountz et al., 1994; Emlen et al., 1994; Penha-Goncalves et al., 1995; Firestein et al., 1995). Accumulation of B cells can also lead to disorders such as a rare type of leukemia called XLP (an X-linked proliferative disease)(see May et al., 1995). It has been now documented that XLP arises due to abnormal proliferation of B cell that somehow have become resistant to apoptosis. On the other hand, enhanced apoptosis in the T cell population can render the immune system without a competent defense machinery. Such rapid depletion of T cells can be seen in individuals infected with HIV (immunodefeciency virus) (Ameisen and Capron, 1991). Depletion of T cell repertoire can lead to the rise of secondary opportunistic infections characteristics of AIDS (Acquired Immuno-Deficiency Syndrome) patients. Apoptosis resistance or loss of apoptosis sensitivity are also observed in many tumor cells (reviewed by Sinkovics, 1991; Bosman et al., 1996). In fact the tumorigenecity of cancer cells to some extent depends on how defective cells are in their apoptosis machinery. In other words, it appears that tumor cells suffer from the inability to die.

Recent information concerning apoptosis and its importance in development and homeostasis (Bosman et al., 1996; Dixon et al., 1997) is in favour of a new model of oncogenesis. The new model considers abrogation in the apoptosis machinery as the underlying cause of transformed cells survival and their subsequent development as cancers, in addition to enhancement in cellular proliferation. Strasser et al., (1990) and Evan and his coworkers (1992) have demonstrated that transformation of fibroblasts by *myc* results in apoptosis of the transformed cells (Fanidi, et al., 1992). This apoptosis can be prevented by expression of bcl-2. Schulte-Herman and his coworkers (1993) have

demonstrated that generation of neoplastic tissues by cancer promoting agents such as Phenobarbital depends on its capability to block apoptosis in the neoplastic foci in hepatic cancer (Grasl-Kraupp, et al., 1993). Transformed cells are otherwise eliminated through apoptosis.

Enhanced cell death is the primary cause of another group of degenerative disorders which occur in the central nervous system (CNS). During development of the CNS, over 50% of originally produced neurons die through apoptosis, particularly those that fail to establish proper synaptic connections (Oppenhiem, 1991). Neurons that survive developmental stages normally persist for the individual's life span. Any post development loss of neurons can potentially cause CNS disorders such as in neurodegenerative diseases (Bosman et al., 1996). Such abnormal loss of neurons through apoptosis is implicated in SMA (spinal muscular atrophies), ALS (amyotrophic lateral sclerosis) and Alzheimer's disease as well as post ischemia injuries.

Understanding the molecular basis of apoptosis is of utmost importance in delineating the underlying pathogenecity of clinically important disorders such as AIDS, ALS, Alzheimer's disease, SMA, Parkinson's disease as well as in circumventing post ischemia dehabilitating consequences. Information acquired from these investigations will prove to be invaluable in planning therapeutic strategy and drug design to treat and probably prevent apoptosis-associated disorders. Our ability in manipulating apoptosis machinery will provide us with the necessary medical tools and technology to increase or decrease

the turnover rate of cells appropriately. It is, indeed needless to emphasize on potentials of such capability which will revolutionize the field of medicine as we know it today.

The delineation of the apoptotic mechanisms and their role in malignancies is beginning to shed light on the problem of resistance in cancer cells to various chemotherapeutic agents. Analysis of the apoptotic mechanism may aid in the development of clinical tools to alter the level of susceptibility of cells to apoptosis and/or to activate intrinsic apoptosis machinery. The IAPs may therefore provide ideal targets for chemotherapeutic pharmacological intervention. Further characterization of these proteins may permit a control of apoptotic regulation with a potential in clinical procedures. Increasing cellular resistance to apoptosis may provide a mechanistically simple means of treating degenerative diseases such as AIDS, SMA, ALS. Robertson and his coworkers (Xu et al, 1997) have recently demonstrated that high levels of NAIP can protect neurons in the rat hippocampus against postischemia apoptosis. These workers have been able to increase levels of NAIP in the neurons of these rats by treating them with the neuroprotective compound K525A. Preliminary results from other groups have shown that NAIP level is also subject to increase in cells treated with compound such as dexamethazone (Sikorsky, A., personal communication). Selective increase in the level of IAPs in apoptosis prone cells that constitute the underlying cause of many neurodegenerative disorders may prevent depletion of cells and alleviate postischemia and post stroke neuronal death.

Progress in the field of diseases caused by dysregulation of apoptosis has been undoubtedly significant. Translation of this knowledge to therapeutic language remains

perhaps the most challenging step. Treatment and cure for the diseases caused by enhancement of proliferation and/or apoptosis is, however, no longer remote, although not imminent.

References

Akao, Y., Otsuki, Y., Kataoka, S., Ito, Y., and Tsujimoto, Y. (1994). Multiple subcellular localization of Bcl-2: Detection in nuclear outer membrane, endoplasmic reticulum membrane, and mitochondrial membranes. Cancer Res., **54**: 2468-2471.

Allsopp, T.E., Wyatt, S., Paterson, H.F., Davis, A.M. (1993). The proto-oncogene bcl-2 can selectively rescue neurotrophic factor dependent neurons from apoptosis. Cell, **73**: 295-307.

Alnemri, E.S., Livingston, D.J., Nicholson, D.W., Salvesen, G., Thornberry, N.A., Wong, W.W., and Yuan, J. (1996). Human ICE/CED-3 protease nomenclature. Cell, **87**: 171.

Ameisen, J.C., and Capron, A. (1991). Cell dysfunction and depletion in AIDS: The programmed cell death hypothesis. Immunol. Today, **12**: 102-105.

Batistou, A., Merry, D.E., Korsmeyer, S.J., Greene, L.A. (1993). Bcl-2 affects survival but not neuronal differentiation of PC12 cells. J.Neurosci., **13**: 4422-4428.

Birnbaum, M.J., Clem, R.J., Miller, L.K. (1994). An apoptosis inhibiting gene from a nuclear polyhedrosis virus encoding a peptide with Cys/His sequence motifs. J. Virol., **68**: 2521-2528.

Boise, L.H., Gonzalez-Garcia, M., Postema, C.E., Ding, L., Lindsten, T., Turka, L.A., Mao, X., Nunez, G., and Thompson, C.B. (1993). Bcl-x, a Bcl-2 related gene that functions as a dominant regulator of apoptotic cell death. Cell, **74**: 597-608.

Boldin, M.P., Varfolomeev, E.E., Pancer, Z., Mett, I.L., Camonis, J.H., Wallach, D. (1995). A novel protein that interacts with the death domain of Fas/Apo1 contains a sequence motif related to the death domain. J Biol Chem., **270**: 7795-7798.

Bosman, F.T., Visser, B.C., and van Oeveren, J. (1996). Apoptosis: Pathophysiology of programmed cell death. Pathol Res Pract., **192**: 676-683.

Braunagel, S.C., Daniel, K.D., Reilly, L.M., Guarino, L.A., Hong, T., and Summers, M.D. (1992). Sequence, genomic organization of the EcoRI-A fragment of *Autographa californica* nuclear polyhedrosis virus, and identification of a viral-encoded protein resembling the outer capsid protein VP8 of rotavirus. Virology, **191**: 1003-1008.

Breathnach, R., Benoist, C., O'Hare, K., Gannon, F., and Chombon, P. (1987). Ovalbumin gene: Evidence for a leader sequence in mRNA and DNA sequences at the exon-intron boundaries. PNAS., **75**: 4853-4857.

Brunner, T., Yoo, N.J., Griffith, T.S., Ferguson, T.A., and Green, D.R. (1996). Regulation of CD95 ligand expression: A key element in immune regulation. Behring Inst Mitt., **7**:161-174.

Bump, N.J., Hackett, M., Hugunin, M., Seshagiri, S., Brady, K., Chen, P., Ferenz, C., Franklin, S., Ghayur, T., Li, P., Licari, P., Mankovich, J., Shi, L., Greenburgm, A.H., Miller, L.K., Wong, W.W. (1995). Inhibition of ICE family proteases by baculovirus antiapoptotic protein p35. Science, **269**:1885-1888.

Cheng, E.H., Levine, B., Boise, L.H., Thompson, C.B., Hardwick, J.M. (1996). Bax-independent inhibition of apoptosis by Bcl-XL. Nature, **379**: 554-556

Cheng, G., Baltimore, D. (1996). TANK, a co-inducer with TRAF2 of TNF- and CD40L-mediated NF-kB activation. Genes Dev., **10**: 963-973.

Chinnaiyan, A.M., Tewari, K.O., Dixit, V.M. (1995). FADD: A novel death domain-containing protein, interacts with the death domain of Fas and initiates apoptosis. Cell, **81**: 505-512.

Chittenden, T., O'Connor, R., Flemington, C., Lutz, R.J., Evan, G.I., and Guild, B.C. (1995). Induction of apoptosis by the Bcl-2 homolog Bak. Nature, **374**: 733-736.

Clem, R.J., Fechheimer, M., Miller, L.K. (1991). Prevention of apoptosis by a baculovirus gene during infection of insect cells. Science, **254**: 1388-1390.

Clem, R.J., and Miller, L.K. (1993). Apoptosis reduces both the *in vitro* replication and the *in vivo* infectivity of a baculovirus. J. Virol., **67**: 3730-3738.

Clem, R.J., Miller, L.K. (1994a). Induction and inhibition of apoptosis by insects viruses. In Tomei, L.D. and Cope, F.O. (eds), Apoptosis II: The molecular basis of apoptosis in diseases. Cold Spring Harbor Laboratory Press, Cold Spring Harbor, NY, pp. 111-141.

Clem, R.J., Miller, L.K. (1994b). Control of programmed cell death by the baculovirus genes *p35* and *iap*. Mol. Cell. Biol., **14**: 5212-5222.

Clem, R.J., Hardwick, J.M., Miller, L.K. (1996). Antiapoptotic genes of baculoviruses. Cell Death Differ., **3**: 9-16.

Clouston, W.M., and Kerr, J.F. (1985). Apoptosis, Lymphocytotoxicity and the containment of viral infection. Med Hypotheses., **18**: 399-404.

Cohen, P.L., and Eisenberg, R.A. (1991). *Lpr* and *Gld*: Single gene models of systemic autoimmunity and lymphoproliferative disease. Annu Rev Immunol., **9**: 243-269.

Crook, N.E., Clem, R.J., Miller, L.K. (1993). An apoptosis-inhibiting baculovirus gene with a zinc finger-like motif. J.Virol., **67**: 2168-2174.

De Meyts, P., Urso, B., Christoffersen, C.T., and Shymko, R.M. (1995a). Mechanism of insulin and IGF-I receptor activation and signal transduction specificity. Receptor dimer cross-linking, Bell-shaped curves, and sustained versus transient signaling. Ann., N Y Acad Sci., **766**: 388-410.

De Meyts, P., Christoffersen, C.T., Urso, B., Wallach, B., Gronskov, K, Yakushiji, F., and Shymko, R.M. (1995b). Role of the time factor in signaling specificity: Application to mitogenic and metabolic signaling by the insulin and insulin-like growth factor-I receptor tyrosine kinases. Metabolism, **44**: 2-11.

Deveraux, Q.L., Takahashi, R., Salvesen, G.S., and Reed, J.C. (1997). X-linked IAP protein directly inhibits protease effectors of cell death. Nature, **388**: 300.

Digby, M.R., Kimpton, W.G., York, J.J., Connick, T.E., Lowenthal, J.W. (1996). ITA: A vertebrate homolog of IAP that is expressed in T lymphocytes. DNA Cell Biol., **15**: 981-988.

Dixon, S.C., Soriano, B.J., Lush, R.M., Borner, M.M., and Figg, W.D. (1997). Apoptosis: Its role in the development of malignancies and its potential as a novel therapeutic target. Ann Pharmacother., **311**: 76-82.

Driscoll, M., and Chalfie, M. (1992). Developmental and abnormal cell death in *C. elegans*. TINS, **15**: 15-19.

Duan, H., Chinnaiyan, A.M., Hudson, P.L., Wing, J.P., He, W., Dixit, V.M. (1996). ICE-LAP3, a novel mammalian homolog of the *Caenorhabditis elegans* cell death protein CED-3, is activated during Fas- and tumor necrosis-factor induced apoptosis. J. Biol. Chem., **271**: 35013-35035.

Duckett, C.S., Nava, V.E., Gedrich, R.W., Clem, R.J., Van Dongen, J.L., Gilfilan, M.C., Sheils, H., Hardwick, J.M., Thompson, C.B. (1996). A conserved family of cellular genes related to the baculovirus *iap* gene and encoding apoptosis inhibitors. EMBO J., **15**: 685-2694.

Ellis, H.M., and Horvitz, H.R. (1986). Genetic control of programmed cell death in the nematode *C. elegans*. Cell, **44**: 817-829.

Ellis, H.M., Jacobsen, D.M., and Horvitz, H.R. (1991). Genes required for the engulfment of cell corpses during programmed cell death in *Caenorhabditis elegans*. Genetics, **129**: 79-94.

Emlen, W., Niebur, J., and Kadera, R. (1994). Accelerated *in vitro* apoptosis of lymphocytes from patient with systemic lupus erythematosus. J Immunol., **152**: 3685-3692.

Espevik, T., Shalaby, R., Liabakk, N.B., Waage, A., and Sundan, A. (1990). The role of TNF in regulation of cell function. Scand L Clin Lab invest Suppl., **202**: 160.

Evans, R.M., and Hollenberg, S.M. (1988). Zinc fingers: Gilt by association. Cell, **52**: 1-3.

Fang, G.S., Shen, R., Heng, H.H.Q., Tsui, L.-C., Kazlauskas, A. and Pawson, T. (1994a). Receptor binding, tyrosine Phosphorylation and chromosome localization of the mouse SH2-containing phosphotyrosine Syp. Oncogene, **9**: 1745-1750.

Fang. W., Rivard, J.J., Mueller, D.L., and Behrens, T.W. (1994b). Cloning and molecular characterization of mouse *bcl-x* in B and T lymphocytes. J Immunol., **153**: 4388-4398.

Fanidi, A., Harrington, E.A., and Evan, G.I. (1992). Cooperative interaction between *c-myc* and *bcl*-2 proto-oncogenes. Nature, **359**: 554-556.

Farahani, R., Fong, W.G., Korneluk, R.G., and MacKenzie, A.E. (1997). Genomic organization and primary characterization of *miap*-3: The homologue of human X-linked IAP. Genomics, **42**: 514-518.

Farrow, S.N., White, J.H.M., Martinou, I., Raven, T., Pun, K.-T., Grinham, C.J., Martinou, J.-C., Brown, R. (1995). Cloning of a *bcl*-2 homolog by interaction with adenovirus E1B 19K. Nature, **374**: 731-733.

Faucheu, C., Diu, A., Chan, A.W.E., Blanchet, A.-M., Miossec, C., Herve, F., Collard-Dutilleul, V., Gu, Y., Aldape, R.A., Lippke, J.A., Rocher, C., Su, M.S.-S., Livingston, D.J., Hercend, T., Lalanne, J.-L. (1995). A novel protease similar to the interleukin-1 β converting enzyme inducesapoptosis in transfected cells. EMBO J., **14**: 1914-1922.

Fernandes-Alnemri, T., Litwack, G., and Alnemri, E.S. (1994). CPP32, a novel human apoptotic protein with homology to *Caenorhabditis elegans* cell death protein Ced-3 and mammalian interleukin-1β-converting enzyme. J. Biol. Chem., **269**: 30761-30764.

Fernandes-Alnemri, T., Litwack, G., Alnemri, E.S. (1995a). Mch-2, a new member of the apoptotic CED-3/ICE cysteine protease gene family. Cancer Res., **55**: 2737-2742.

Fernandes-Alnemri, T., Takahashi, A., Armstrong, R., Krebs, J., Fritz, L., Tomaselli, K.J., Wang, L., Yu, Z., Croce, C.M., Salveson, G., Earnshaw, W.C., Litwack, G., Alnemri, E.S. (1995b). Mch-3, a novel human apoptotic cysteine protease highly related to CPP-32. Cancer Res., **55**: 6045-6052.

Fernandes-Alnemri, T., Armstrong, R., Krebs, J., Srinivasula, S.M., Wang, L., Bullrich, F., Fritz L., Trapani, J.A., Tomaselli, K.J., Litwack, G., and Alnemri, E.S. (1996). *In vitro* activation of CPP32 and Mch3 by Mch4, a novel human apoptotic cysteine protease containing two FADD-like domains. PNAS., **93**: 7464-7469.

Firestein, G.S., Yeo, M., and Zvaifler, N.J. (1995). Apoptosis in rheumatoid arthritis synovium. J Clin Invest., **96**: 1631-1638.

Fisher, S.E. (1994). Apoptosis in cancer therapy: Crossing the threshold. Cell, **78**: 539-542.

Fisher, S.E., Hatchwell, E., Chand, A., Ockenden, N., Monaco, A.P., and Craig, I.W. (1995). Construction of two YAC contigs in human Xp11.23-p11.22, one encompassing the loci OATL1, GATA, TFE3, and SYP, the other linking DXS255 to DXS146. Genomics, **29**: 496-502.

Friesen, P.D., and Miller, L.K. (1987). Divergent transcription of early 35- and 94-kilodalton protein genes encoded by the HindIII K genome fragment of the baculovirus *Autographa californica* nuclear polyhedrosis virus. J Virol., **61**: 2264-2272.

Garcia, I., Martinou, I., Tsujimoto, Y. and Martinou, J.C. (1992). Prevention of Programmed cell death of sympathetic neurons by the *bcl*-2 proto-oncogene. Science, **258**: 302-304.

Ghozi, M.C., Bernstein, Y., Negreanu, V., Levanon, D., and Groner, Y. (1996). Expression of the human acute myeloid leukemia gene AML1 is regulated by two promoter regions. PNAS., **93**: 1935-1940.

Goldstein, P., Marguet, D., Depraetere, V. (1995). Homology between reaper and the cell death domains of Fas and TNFR1. Cell, **81**: 185-186.

Gorlich, D., (1997). Nuclear protein import. Curr Opin Cell Biol., **9** : 412-419.

Grasl-Kraupp, B., Waldhor, T., Huber, W., and Schulte-Hermann, R. (1993). Glutathione S-transferase isoenzyme patterns in different subtypes of enzyme-altered rat liver foci treated with the peroxisome proliferator nafenopin or with Phenobarbital. Carsinogenesis, **14**: 2407-2412.

Grell, M., Douni, E., Wajant, H., Lohden, M., Clauss, M., Maxeiner, B., Georgopoulos, S., Lesslauer, W., Kollias, G., Pfizenmaier, K., Scheurich, P. (1995). The transmembrane

form of tumor necrosis factor is the prime activating ligand of the 80 kDa tumor necrosis factor receptor. Cell, **83**: 793-802.

Gruss, H.J., Dower, S.K. (1995). Tumor necrosis factor ligand superfamily: Involvement in the pathology of malignant lymphomas. Blood, **85**: 3378-3404.

Hale, A.J., Smith, C.A., Sutherland, L.C., Stoneman, V.E.A., Longthorne, V.L., Culhane, A.C., Williams, G.T. (1996). Apoptosis: Molecular regulation of cell death. Eur. J. Biochem., **236**: 1-26.

Hawkins, C.J., Uren, A.G., Hacker, G., Medcalf, R. L., and Vaux, D.L. (1996). Inhibition of interleukin 1 beta-converting enzyme-mediated apoptosis of mammalian cells by baculovirus IAP. PNAS., **93**: 13786-13790.

Hay, B.A., Wassarman, D.A., Rubin, G.M. (1995). *Drosophilia* homologs of baculovirus inhibitor of apoptosis proteins function to block cell death. Cell, **83**: 1253-1262.

Henderson, S., Rowe, M., Gregory, C., Croom-Carte, D., Wang, F., Longnecker, R., Kieff, E., and Rickinson, A. (1991). Induction of *bcl-2* expression by Epstein-Barr virus latent membrane protein 1 protects infected B cells from programmed cell death. Cell, **65**: 1107-1115.

Henderson, S., Huen, D., Rowe, M., Dawson, C., Johnson, G., Rickinson, A. (1993). Epstein-Barr virus-encoded BHRF1 protein, a viral homolog of Bcl-2, protects human B cells from programmed cell death. PNAS., **90**: 8479-8483.

Heng, H.H.Q., Squire, J., and Tsui, L.-C. (1992). High resolution mapping of mammalian genes by *in situ* hybridization to free chromatin. PNAS., **89**: 9509-9513.

Heng, H.H.Q., and Tsui, L.-C. (1993). Mode of DAPI banding and simultaneous in *in situ* hybridization. Chromosome, **102**: 325-332.

Hengartner, M.O., Ellis, R,E. and Horvitz, R.H. (1992) *Caenorhabditis elegans* gene *ced-9* protects cells from programmed cell death. Nature, **356**: 494-499.

Hengartner, M.O. and Horvitz, R.H. (1994). *C. elegans* cell survival gene *ced-9* encodes a functional homolog of the mammalian proto-oncogene *bcl-2*. Cell, **76**: 665-676.

Hershberger, P.A., Dickson, J.A., and Friesen, P.D. (1992). Site-directed mutagenesis of the 35-kilodalton protein gene encoded by *Autographa californica* nuclear polyhedrosis virus: cell line-specific effects on virus replication. J Virol., **66**: 5525-5533.

Hershberger, P.A., LaCount, D.J., and Friesen, P.D. (1994). The apoptotic suppressor P35 is required early during baculovirus replication and is targeted to the cytosol of infected cells. J Virol., **68**: 3467-3477.

Hockenbery, D., Nunez, G., Milliman, C.L., Schreiber, R.D., and Korsmeyer, S.J. (1990). Bcl-2 is an inner mitochondrial membrane protein that blocks programmed death. Nature, **348**: 334-336.

Hockenbery, D., Oltvai, Z.N., Yin, X.M., Milliman, C.L., and Korsmeyer, S.J. (1993). Bcl-2 functions in an antioxidant pathway to prevent apoptosis. Cell, **75**: 2411-251.

Hsu, H., Xiong, J., Goeddel, D.V. (1995). The TNF receptor 1-associated protein TRADD signals cell death and NF-kB activation. Cell, **81**: 495-504.

Hsu, H., Shu, H.-B., Pan, M.-G., Goeddel, D.V. (1996). TRADD-TRAF2 and TRADD-FADD interactions define two distinct TNF receptor 1 signal transduction pathways. Cell, **84**: 299-308.

Itoh, N., Yonehara, S., Ishii, A., Yonehara, M., Mizushima, S.-I., Sameshima, M., Hase, A.., Seto, Y., and Nagata, S. (1993). The polypeptide encoded by the cDNA for human cell surface antigen Fas can mediate apoptosis. Cell, **66**: 233-243.

Itoh, N., Nagata, S. (1993). A novel protein domain required for apoptosis. J. Biol. Chem., **268**: 10932-10937.

Jacobson, M.D., Burne, J.F., Raff, M.C. (1994) Programmed cell death and bcl-2 protection in the absence of a nucleus. EMBO J., **13**: 1899-1910.

Jacobson, M.D., Raff, M.C. (1995). Programmed cell death and *bcl*-2 protection in very low oxygen. Nature, **374**: 814-816.

Ju, S.T., Panka, D.J., Cui, H., Ettinger, R., el-Khatib, M., Sherr, D.H., Stanger, B.Z., and Marshak-Rothstein, A. (1995). Fas (CD95)/FasL interactions required for program cell death after T-cell activation. Nature, **373**: 444-448.

Kamada, S., Shinto, A.A., Tsujimura, Y., Takahshi, T., Noda, T., Kitamura, Y., Kondoh, H., and Tsujimoto, Y. (1995). *Bcl*-2 deficiency in mice leads to pleiotrophic abnormalities: Accelerated lymphoid cell death in the thymus and spleen, polycystic kidney, hair hypopigmentation and distorted small intestine. Cancer Res., **55**: 354-359.

Kamens, J., Paskind, M., Hugunin, M., Talanian, R.V., Allen, H., Banach, D., Bump, N., Hackett, M., Johnston, C.G., Li, P., and Mankovich, J., Terranova, M., Ghayur, T. (1995). Identification and characterization of ICH-2, a novel member of the interleukin-1β-converting enzyme family ofcysteine proteases. J. Biol. Chem., **270**: 15250-15256.

Kamita, S.G., Majima, K., Maeda, S. (1993). Identification and characterization of the p35 gene of *Bombyx mori* nuclear polyhedrosis virus that prevent virus-induced apoptosis. J Virol., **67**: 455-463.

Kaufmann, S.H., Desnoyers, S., Ottaviano, Y., Davidson, N.E., and Poirier, G.G. (1993). Specific proteolytic cleavage of poly (ADP-ribose) polymerase: An early maker of chemotherapy-induced apoptosis. Cancer Res., **5**: 3976-3985.

Kayalar, C., Ord, T., Testa, M.P., Zhong, L.T., and Bredesen, D.E. (1996). Cleavage of actin by interleukin 1 beta-converting enzyme to reverse DNase I inhibition. PNAS., **93**: 2234-2238.

Kerr, J.F.R., Wyllie, A.H., Currie, A.R. (1972). Apoptosis: A basic biological phenomenon with wide ranging implications in tissue kinetics. J. Br. Cancer., **26**: 239-257.

Kiefer, M.C., Brauer, M.J., Powers, V.C., Wu, J.J., Umansky., S.R., Tomei, L.D., Barr, P.J. (1995). Modulation of apoptosis by the sidely distributed Bcl-2 homologue Bak. Nature, **374**: 736-739.

Komiyama, T., Ray, C.A., Pickup, D.J., Howard, A.D., Thornberry, N.A., Peterson, E.P., Salveson, G. (1994). Inhibition of interleukin-1 β converting enzyme by the cowpox virus serpin CrmA. J. Biol. Chem., **269**: 19331-19337.

Korsmeyer, S.J., Shutter, J.R., Veis, D.J., Merry, D.E., and Oltivai, Z.N. (1993). Bcl-2/Bax; a rheostat relates an anti-oxidant pathway and cell death. Semin Cancer Biol., **4**: 327-337.

Krajewski, S., Mai, J.K., Krajewska, M., Sikorska, M.J., Mossakowski, M.J. and Reed, J.C. (1995). Upregulation of Bax protein levels in neurons following cerebral ischemia. J. Neurosci., **15**: 6364-6376.

Kuida, K., Lippke, J.A., Ku, G., Harding, M.W., Livingston, D.J., Su, M.S.-S., and Flavell, R.A. (1995). Altered cytokine export and apoptosis in mice deficient in interleukin-1β converting enzyme. Science, **267**: 2000-2003.

Kumar, S., Kinshita, M., Noda, M., Copeland, N.G., and Jenkins, N.A. (1994). Induction of apoptosis by the mouse *Nedd2* gene, which encodes a protein similar to the product of *Caenorhabditis elegans* cell death gene ced-3 and mammalian IL-1β converting enzyme. Genes & Dev., **8**: 1613-1626.

Lazebnik, Y.A., Kaufmann, S.H., Desnoyers, S., Poirier, G.G., and Earnshaw, W.C. (1994). Cleavage of poly(ADP-ribose) polymerase by a proteinase with properties like ICE. Nature, **371**: 346-347.

Li, P., Allen, H., Banerjee, S., Franklin, S., Herzo, L., Johnston, C., McDowell, J., Paskind, M., Rodman, L., and Salfeld, J. (1995). Mice deficient in IL-1 beta-converting

enzyme are defective in production of mature IL-1 beta and resistant to endotoxic shock. Cell, **80**: 401-411.

Lippke, J.A., Gu, Y., Sarnecki, C., Caron, P.R., Su, M.S.-S. (1996). Identification and characterization of CPP-32/Mch-2 homolog 1, a novel cystein protease similar to CPP-32. J. Biol. Chem., **271**: 1825-1828.

Liston, P., Lefebvre, C., Fong, W.G., Xuan, J.Y., Korneluk, R.G. (1997a). Genomic characterization of the mouse inhibitor of apoptosis protein 1 and 2 genes. Genomics, **46**: 495-503.

Liston, P., Young, S.S., Mackenzie, A.E., and Korneluk, R.G. (1997b). Life and death decisions: The role of the IAPs in modulating programmed cell death. Apoptosis, **2**: 423-441.

Liston, P., Roy, N., Tamai, K., Lefebvre, C., Baird, S., Cherton-Horvat, G., Farahani, R., McLean, M., Ikeda, J.-E., MacKenzie, A., Korneluk, R.G. (1996). Suppression of apoptosis in mammalian cells by NAIP and a related family of IAP genes. Nature, **379**: 349-353.

Lithgow, T., van Driel, R., Nertram, J.F., and Strasser, A. (1994). The protein product of the oncogene *bcl*-2 is a component of the nuclear envelope, the endoplasmic reticulum, and the out mitochondrial, membrane. Cell Growth Differ., **5**: 411-417.

Loetscher, H., Schlaeger, E.J., Lahm, H.W., Pan, Y.C., Lesslauer, W., and Brockhaus, M. (1990). Purification and partial amino aid sequence analysis of two distinct tumor necrosis factor receptors from HL60 cells. J Biol Chem., **365**: 20131-20138.

Lovering, R., Hanson, I.M., Borden, K.L.B., Martin, S., O'Reilly, N.J., Evans, G.I., Rahman, D., Pappin, D.J.C., Trowsdale, J., amd Freemont, P.S. (1993). Identification and preliminary characterization of a protein motif related to the zinc finger. PNAS., **90**: 2112-2116.

Lyon, F.M., Zenthon, J., Burteshaw, M.D., and Evans, E.P. (1987). Localization of the Hprt locus by in situ hybridization and distribution of loci on the mouse X-chromosome. Cytogenet Cell Genent., **44**: 163-166.

Mah, S.P., Zhong, L.T., Liu, Y., Roghani, A., Edwards, R.H., Bredesen, D.E. (1993). The protooncogene **bcl**-2 inhibits apoptosis in PC12 cells. J. Neurochem., **60**: 1183-1186.

May. P., May, E., Schwartz, L., and Yonish-Rouach, E. (1995). Apoptosis and cancer. Rev Prat., **45**: 1903-1908.

McDonnell, T.J., Deane, N., Platt, F.M., Nunez, G., Jaeger, U., McKearn, J.P., and Korsmeyer, S.J. (1989). Bcl-2-immunoglobulin transgenic mice demonstrate extended B cell survival and follicular lymphoproliferation. Cell, **57**: 79-88.

Milligan, C.E., Prevette, D., Yaginuma, H., Homma, S.A., Cardwell, C., Fritz, L.C., Tomaselli, K.J., Oppenheim, R.W., and Schwartz. L.M. (1995). Peptide inhibitors of the ICE protease family arrest programmed cell death of motoneurons *in vivo* and *in vitro*. Neuron, **15**: 385-393.

Miura, M., Zhu, H., Rotello, R., Hartwieg, E.A., and Yuan, J. (1993). Induction of apoptosis in fibroblasts by IL-1β converting enzyme, a mammalian homolog of the *C. elegans* cell death gene *ced-3*. Cell, **75**: 653-660.

Mountz, J. D., Wu, J., Cheng, J., and Zhou, T. (1994). Autoimmune disease. A problem of defective apoptosis. Arthritis Rheum., **37**: 1415-1420.

Munday, N.A., Vaillancourt, J.P., Ali, A., Casano, F.J., Miller, D.K., Molineaux, S.M., Yamin, T.T., Yu, V.L., Nicholson, D.W. (1995). Molecular cloning and proapoptotic activity of ICE rel-II and ICE rel-III, members of the ICE/CED-3 family of cysteine proteases. J. Biol. Chem., **270**: 15870-15878.

Muzio, M., Chinnaiyan, A.M., Kischkel, F.C., O'Rourke, K., Shevchenko, A., Ni, J., Scaffidi, C., Bretz, J.D., Zhang, M., Gentz, R., Mann, M., Krammer, P.H., Peter, M.E., Dixit, V.M. (1996). FLICE, a novel FADD-homologous ICE/CED-3-like protease, is recruited to the CD95 (Fas/Apo-1) death-inducing signaling complex. Cell, **85**: 817-827.

Nagata, S., and Golstein, P. (1995). The Fas death factor. Science, **267**: 1449-1456.

Neamati, N., Fernandez, A., Wright, S., Kiefer, J., and McConkey, D.J. (1995). Degradation of lamin B1 precedes oligonucleosomal DNA fragmentation in apoptotic thymocytes and isolated thymocyte nuclei. J Immunol., **154**: 3788-3795.

Neilan, J.G., Lu, Z., Afonzo, C.L., Kutish, G.F., Sussman, M.D., Rock, D.L. (1993). An African swine fever virus gene with similarity to the proto-oncogene *bcl-2* and Epstein-Barr virus gene BHRF1. J Virol., **67**: 4391-4394.

Nicholson, D.W., Ali, A., Thornberry, N.A., Vaillancourt, J.P., Ding, C.K., Gallant, M., Gareau, Y., Griffin, P.R., Labelle, M., Lazebnik, Y.A., Munday, N.A., Raju, S.M., Smulson, M.E., Yamin, T.T., Yu, V.L., Miller, D.K. (1995). Identification and inhibition of the ICE/CED-3 protease necessary for mammalian apoptosis. Nature, **376**: 37-43.

Nunez, G., London, L., Hockenbery, D., Alexander, m., McKearn, J.P., and Korsmeyer, S.J. (1990). Deregulated *bcl-2* gene expression selectively prolongs survival of growth factor-deprived hemopoietic cell lines. J Immunol., **144**: 3602-3610.

Oehm, A., Behrmann, I., Falk, W., Pawlita, M., Maier, G., Klas, C., Li-Weber, M., Richards, S., Dhein, J., and Trauth, B.C. (1992). Purification and molecular cloning of the APO-1 cell surface antigen, a member of the tumor necrosis factor/nerve growth receptor superfamily. Sequence identity with theFas antigen. J Biol Chem., **267**: 10709-10715.

Oltvai, Z.N., Milliman, C.L. and Korsmeyer, S.J. (1993). Bcl-2 heterodimerizes *in vivo* with a conserved homolog, Bax, that accelerates cell death. Cell, **74:** 609-619.

Oltvai, Z.N., Korsmeyer, S.J. (1994). Checkpoints of dueling dimers foil death wishes. Cell, **79**: 189-192.

Opipari, A.W., Hu, H.M., Yabkowitz, R., Dixit, V.M. (1992). The A20 zinc finger protein protects cells from tumor necrosis factor cytotoxicity. J. Biol. Chem., **267**: 12424-12427.

Oppenheim, R.W. (1991). Cell death during development of the nervous system. Ann. Rev. Neurosci., **14:** 253-501.

Oudejan, J.J., Van den Brule, A.j., Jiwa, N.M., de Bruin, P.C., Ossenkoppele, G.J., van der Valk, P., Walbooers, J.M. and Meijer, C.J. (1995). BHRF1, the Epstein-Barr virus (EBV) homologue of the *bcl*-2 proto-oncogene, is transcribed in EBV-associated B-cell lymphomas and in reactive lymphocytes. Blood, **86**: 1893-1902.

Penha-Goncalves, C., Leijon, K., Persson, L., and Holmberg, D. (1995). Type 1 diabetes and the control of dextamethazone-induced apoptosis in mice maps to the same region on chromosome 6. Genomics, **28**: 398-404.

Pfeffer, L., Marsuyama, T., Kundig, T.M., Waleham, A., Kishihara, K., Shahinian, A., Wiegmann, K., Ohashi, P.S., Kronke, M., and Mak, T.W. (1993). Mice deficient for the 55 kD tumor necrosis factor receptor are resistant to endotoxic shock, yet succumb to L. monocytogenes infection. Cell, **73**: 457-467.

Rabizadeh, S., LaCount, D.J., Friesen, P.D., and Bredesen, D.E. (1993). Expression of the baculovirus p35 gene inhibits mammalian neural cell death. J. Neurochem., **61**: 2318-2321.

Rajcan-Separovic, E., Liston, P., Lefebvre, C., Korneluk, R.G. (1996). Assignment of human inhibitor of apoptosis protein (IAP) genes *xiap*, *hiap-1*, and *hiap-2* to chromosomes Xq25 and 11q22-23 by fluorescence *in situ* hybridization. *Genomics*, **37**: 404-406.

Ray, C.A., Black, R.A., Kronheim, S.R., Greenstreet, T.A., Sleath, P.R., Salvesen, G.S., Pickup, D.J. (1992). Viral inhibition of inflammation: Cowpox virus encodes an inhibitor of the interleukin-1 β converting enzyme. Cell, **69**: 597-604.

Rothe, M., Wong, S.C., Henzel, W.J., Goeddel, D.V. (1994). A novel family of putative signal transducers associated with the cytoplasmic domain of the 75 kDa tumor necrosis factor receptor. Cell, **78**: 681-692.

Rothe, M., Pan, M.-G., Henzel, W.J., Ayres, T.M., Goeddel, D.V. (1995a). The TNFR2-TRAF signaling complex contains two novel proteins related to baculoviral inhibitor or apoptosis proteins. Cell, **83**: 1243-1252.

Rothe, M., Sarma, V., Dixit, V.M., Goeddel, D.V. (1995b). TRAF2-mediated activation of NF-kB by TNF receptor 2 and CD40. Science, **269**: 1424-1426.

Roy, N. Laflamme, G., and Raymond, V. (1992). 5' untranslated sequences modulate rapid mRNA degradation mediated by 3' AU-rich element in v-/c-fos recombinants. Nucleic Acids Res., **20**: 5753-5762.

Roy, N., Mahadevan, M.S., McLean, M., Shutler, G., Yaraghi, Z., Farahani, R., Baird, S., Besner-Johnston, A., Lefebvre, C., Kang, X., Salih, M., Aubry, H., Tamai, K., Guan, X., Ioannou, P., Crawford, T.O., de Jong, P.J., Surh, L., Ikeda, J.-E., Korneluk, R.G., MacKenzie, A. (1995). The gene for neuronal apoptosis inhibitory protein is partially deleted in individuals with spinal muscular atrophy. Cell, **80**: 167-178.

Russell, J.E., and Liebhaber, S.A. (1996). The stability of human beta-globin mRNA is dependent on structural determinants positioned in its 3' untranslated region. Blood, **87**: 5314-5323.

Sambrook, J., Fritsch, E.F., and Maniatis, T. (1989). Molecular cloning: A laboratory manual. 2nd ed. Cold Spring Harbor Laboratory Press.

Sarin, A., Adams, D.H., and Henkart, P.A. (1993). Protease inhibitors selectively block T cell receptor-triggered programmed cell death in a murine T cell hybridoma and activated peripheral T cell. J Exp Med., **178**: 1693-1700.

Sarma, V., Lin, Z., Clark, L., Rust, B.M., Tewari, M., Noelle, R.J., Dixit, V.M. (1995). Activation of the B-cell surface receptor CD40 induces A20, a novel zinc finger protein that inhibits apoptosis. J. Biol. Chem., **270**: 12343-12346.

Sato, T., Hanada, M., Bodrug, S., Irie, S., Iwama, N., Boise, L.H., Thompson, C.B., Golemis, E., Fong, L., Wang, H.G. (1994). Interaction among members of the Bcl-2 protein family analyzed with a yeast two-hybrid system.PNAS., **91**: 9238-9242.

Sato, T., Iris, S., Kitada, S., Reed, J.C. (1995). FAP-1: A protein tyrosine phosphatase that associates with Fas. Science, **268**: 411-415.

Saurin, A.J., Borden, K.L.B., Boddy, M.N., Freemont, P.S. (1996). Does this have a familiar RING? Trends Biochem. Sci., **21**: 197-235.

Schafer, M., Nayernia, K., Engel, W., and Schafer, U. (1995). Translation control in spermatogenesis. Dev Biol., **172**: 344-352.

Schendel, S.L., Xie, Z., Montal M.O., Matsuyama, S., Montal, M., and Reed, J.C. (1997). Channel formation by antiapoptotic protein Bcl-2. PNAS., **94**: 5113-5118.

Sentman, C.L., Shutter, J.R., Hockenbery, D., Kanagawa, O., and Korsmeyer, S.J. (1991). Bcl-2 inhibits multiple forms of apoptosis but not negative selection in thymocytes. Cell, **67**: 879-888.

Seto, M., Jaeger, U., Hockett, R.D., Graninger, W., Bennett, S., Goldman, P., and Korsmeyer, S.J. (1988). Alternative promoters and exons, somatic mutation and deregulation of the Bcl-2-Ig fusion gene in lymphoma. EMBO J., **7**: 123-131.

Seshagiri, S., and Miller, L.K. (1997). *Caenorhabditis elegans* CED-4 stimulates CED-3 processing and CED-3 induced apoptosis. Curr. Biol., **7**: 455-460.

Shi, L., Kraut, R.P., Aebersold, R., amd Greenberg, A.H. (1992). A natural killer cell granule protein that induces DNA fragmentation and apoptosis. J Exp Med., **175**: 553-566.

Simbulan-Rosenthal, C.M., Rosenthal, D.S., Ding, R., Jackman, J., and Smulson, M. E. (1996). Depletion of nuclear poly(ADP-ribose) polymerase by antisense RNA expression: Influence on genomic stability, chromatin organization, DNA repair, and DNA replication. Prog Nucleic Acid res Mol Biol., **5**: 135-156.

Shimizu, S., Eguchi, Y., Kosaka, H., Kamiike W., Matsuda, H., and Tsujimoro, Y. (1995). Prevention of hypoxia-induced cell death by Bcl-2 and Bcl-xL. Nature, **374**: 811-813.

Sinkovics, J.G. (1991). Programmed cell death (apoptosis): Its virological and immunological connections (a review). Acta Microbio Hung., **38**: 321-334.

Smith, C.A. Davis, T., Anderson, D., Solam, L., Beckmann, M.P., Jerzy, R., Dower, S.K., Cosman, D., Goodwin, R.G. (1990). A receptor for tumor necrosis factor defines an unusual family of cellular and viral proteins. Science, **28**: 1019-1023.

Smith, C.A., Farrah, T., Goodwin, R.G. (1994). The TNF receptor superfamily of cellular and viral proteins: Activation,costimulation, and death. Cell, **76**: 7959-962.

Song, H.Y., Rothe, M., Goeddel, D.V. (1996). The tumor necrosis factor-inducible zinc finger protein A20 interacts with TRAF1/TRAF2 and inhibits NF-kB activation. PNAS., **93**: 6721-6725.

Sorenson, C.M., Rogers, S.A., Korsmeyer, S.J., and Hammerman, M.R. (1995). Fulminant metanephoric apoptosis and abnormal kidney development in *bcl*-2-deficient mice. Am J Physiol., **268**: F73-F81.

Steller, H. (1995). Mechanisms and genes in cellular suicide. Science,**267**: 1445-1449.

Stranger, B.Z., Leder, P., Lee, T.-H., Kim, E., Seed, B. (1995). RIP: A novel protein containing a death domain that interacts with Fas/APO-1 CD95 in yeast and causes cell death. Cell, **81**: 513-523.

Strasser, A., Harris, A.W., Bath, M.L., and Cory, S. (1990). Novel primitive lymphoid tumors induced in transgenic mice by cooperation between *myc* and *bcl*-2. Nature, **348**: 331-333.

Sulston, J.E., and Horvitz, H.R. (1977). Post-embryonic cell lineage of the nematode, *Caenorhabditis elegans*. Dev Biol., **56**: 110-156.

Sulston, J.E. (1983). Neuronal cell lineage in the nematode, *Caenorhabditis elegans*. Cold Spring Harb Symp Quant Biol., **48**: 443-452.

Takahashi, T., Tanaka, M., Brannan, C.I., Jenkins, N.A., Copeland, N.G., Suda, T., and Nagata, S. (1994). Generalized lymphoproliferative disease in mice, caused by a point mutation in the Fas ligand. Cell, **76**: 969-976.

Takata, Y., and Kobayashi, M. (1994). Insulin-like growth factor I signaling through heterodimers of insulin and insulin-like growth factor I receptors. Dianete Metab., **20**: 31-36.

Tartaglia, L.A., Weber, R.F., Figari, I.S., Reynolds, C., Palladino, M.A., Goeddel, D.V. (1991). The two different receptors for tumor necrosis factor mediate distinct cellular responses. PNAS., **88**: 9292-9296.

Tartaglia, L.A., Pennica, D., Goeddel, D.V. (1993). Ligand passing: The 75-kD tumor necrosis factor (TNF) receptor recruits TNF for signaling by the 55-kD TNF receptor. J. Biol. Chem., **268**: 18542-18548.

Tewari, M., and Dixit, V.M. (1995a). Fas- and TNF-induced apoptosis is inhibited by the poxvirus *crmA* gene product. J. Biol. Chem., **270**: 3255-3260.

Tewari, M., Quan, L.T., O'Rourke, K., Desnoyers, S., Zeng, Z., Beidler, D.R., Poirer, G., Salvasen, G.S., and Dixit, V.M. (1995b). Yama/CPP32, a mammalian homolog of CED-3, is a CrmA-inhibitable protease that cleaves the death substrate poly(ADP-ribose) polymerase. Cell, **81**: 801-809.

Thanos, D., and Maniatis, T. (1995). NFkB: A lesson in family values. Cell, **80**: 529-532.

Thompson, C.B.,(1995). Apoptosis in the pathogenesis and treatment of disease. Science, **267**: 1456-1462.

Thornberry, N.A. (1994). Interleukin-1β converting enzyme. In Methods in enzymology, 224. Academic Press, Inc.

Ting, A.T., Pimentel-Muinos, F.X., and Seed, B. (1996). RIP mediates tumor necrosis factor receptor 1 activation of NF-kappaB but not Fas/Apo-1-initiated apoptosis. EMBO J., **15**: 6189-6196.

Tsujimoto, Y., and Croce, C.M. (1986). Analysis of the structure, transcript, and protein products of *bcl*-2, the gene involved in human follicular lymphoma. PNAS., **83**: 5214-5218.

Uren, A.G., Pakusch, M., Hawkins, C.J., Puls, K.L., Vaux, D.L. (1996). Cloning and expression of apoptosis inhibitory protein homologs that functions to inhibit apoptosis and/or bind tumor necrosis factor receptor-associated factors. PNAS., **93**: 4974-4978.

Vaux, D.L., Cory, S., and Adams, L.M. (1988). *bcl*-2 gene promotes hemopoietic cell survival and cooperates with *c-myc* to immortalize pre-B cells. Nature, **335**: 440-442.

Vaux, D.L., Weissman, I.L., ad Kim, S.k. (1992). Prevention of programmed cell death in *Caenorhabditis elegans* by human *bcl*-2. Science, **258**: 1955-1957.

Vaux, D.L., Haecker, G., Strasser, A. (1994). An evolutionary perspective on apoptosis. Cell, **76**: 777-779.

Vaux, D.L., and Stasser, A. (1996). The molecular biology of apoptosis. PNAS., **93**: 229-2244.

Veis, D.J., Sorenson, C.M., Shutter, J.R., and Korsmeyer, S.J. (1993). *bcl*-2 deficient mice demonstrate fulminant lymphoid apoptosis, polycystic kidneys and hypopigmented hair. Cell, **75**: 229-240.

Wang, L., Muira, M., Bergeron, L., Zhu, H., Yuan, J. (1994). *ich*-1, an *ice/ced*-3-related gene, encodes both positive and negative regulators of programmed cell death. Cell, **78**: 739-750.

Wang, Z.Q., Auer, B., Stingl, L., Berghammer, H., Haidacher, D., Schweiger, M., and Wagner, E.F. (1995). Mice lacking ADPRT and poly(ADP-ribosl)ation develop normally but are susceptible to skin disease. Gene Dev., **9**: 509-520.

Wang, X., and Liebhaber, S.A. (1996). Complementary change in cis determinants and trans factor in the evolution of an mRNA stability complex. EMBO J., **15**: 5040-5051.

Watanabe-Fukunagata, R., Brannan, C.I., Copeland, N.G., Jenkins, N.A., and Nagata, S. (1992). Lymphoproliferation disorder in mice explained by defect in Fas antigen that mediates apoptosis. Nature, **346**: 314-317.

Weiss, I.M., and Liebhaber, S.A. (1994). Erythroid cell-specific determinants of alpha-globin mRNA stability. Mol Cell Biol., **14**: 8123-8132.

Weiss, I.M., and Liebhaber, S.A. (1995). Erythroid cell-specific mRNA stability elements in the alpha 2-globin 3' nontranslated region. Mol Cell Biol., **15**: 247-2465.

White, E. (1993). Regulation of apoptosis by the transforming gene of the DNA tumor virus adenovirus. Proc Soc Exp Biol Med., **204**: 30-39.

White, E., and Gooding, L.R. (1994). Regulation of apoptosis by human adenoviruses. In Tomei, L.D. and Cope, F.O. (eds), Apoptosis II: The molecular basis of apoptosis in diseases. Cold Spring Harbor Laboratory Press, Cold Spring Harbor, NY, pp.111-141.

White, E. (1996). Life, death, and the pursuit of apoptosis. Genes Dev., **10**: 1-15.

Williams, G.T., and Smith, C.A. (1993). Molecular regulation of apoptosis: Genetic controls on cell death. Cell, **74**: 777-779.

Wilson, K.P., Black, J.A., Thompson, J.A., Kim, E.E., Griffith, J.P., Navia, M.A., Murcko, M.A., Chambers, S.P., Aldape, R.A., and Raybuck, S.A. (1994). Structure and mechanism of interleukin-1 beta converting enzyme. Nature, **370**: 270-275.

Wong, G.H., Tartaglia, L.A., Lee, M.S., and Goeddel, D.V. (1992). Antiviral activity of tumor necrosis factor is signaled through the 55-kDa type I TNF receptor. J Immunol., **149**: 3350-3353.

Xu, D.G., Crocker, S.J., Doucet, J.P., St-Jean, M., Tamai, K., Hakim, A.M., Ikeda, J.E., Liston, P., Thompson, C.S., Korneluk, R.G., MacKenzie, A., Robertson, G.S. (1997). Elevation of neuronal expression of NAIP reduces ischemic damage in the rat hippocampus. Nat Med., **3**: 997-1004

Yang, E., Zha, J., Jockel, J., Boise, L.H., Thompson, C.B., and Korsmeyer, S. (1995). Bad, a heterodimeric partner for Bcl-xL and Bcl-2, displaces Bax and promotes cell death. Cell, **80**: 285-291.

Yin, X-M, Oltvai, Z.N. and Korsmeyer, S.J. (1994). BH1 and BH2 domains of Bcl-2 are required for inhibition of apoptosis and heterodimerization with Bax. Nature, **369**: 321-321.

Yuan, J., and Horvitz, H.R. (1992). The *Caenorhabditis elegans* genes *ced*-3 and *ced*-4 act cell autonomously to cause programmed cell death. Dev Biol., **138**: 33-41.

Yuan, J., Shaman, S., Ledoux, S., Ellis, H.M., and Horvitz, H.R. (1993). The *C. elegans* cell death gene *ced-3* encodes a protein similar to mammalian interleukin-1β-converting enzyme. Cell, **75**: 641-652.

Yuan, J. (1995). Molecular control of life and death. Curr Opin Cell Biol., **7**: 211-214.

Zha, H., Fisk, H.A., Yaffe, M.P., Mahajan, N., herman, B., and Reed, J.C. (1996). Structure-function comparison of the proapoptotic protein Bax in yeast and mammalian cells. Mol Cell Biol., **16**: 6494-6408.

Zhong, L.T., Sarafian, T., Kane, D.J., Charles, A.C., Mah, S.P., Edwards, R.H., and Bredesen, D.E. (1993). Bcl-2 inhibits death of central neural cells induced by multiple agents. PNAS., **90**: 4533-4537.

Zou, H., Henzel, W.J., Liu, X., Lutschg, A., and Wang, X. (1997). Apaf-1, a human protein homologous to *C. elegans* CED-4, participates in cytochrome c-dependent activation of caspase-3. Cell, **90**: 405-413.

Appendix A

Statistical analysis of the death assays data

Statistical analysis of the death assay data was performed using Prism software (GraphPad Inc.). All the obtained data was subjected to ANOVA (analysis of variance), repeated measures with Tukey multiple comparison post test with confidence variance of 95%.

a. Statistical analysis of death assay experiments in CHO cells expressing *miap*-3 FL, *xiap* FL, *miap*-3 BIRs, *miap*-3 RZF, bcl-2, and pCDNA3. Based on this analysis, percentage of viable CHO cells expressing various *miap*-3 constructs at 24 hr is not significantly different. However, at 48 and 72 hr, the means obtained demonstrate a significance compared to 24 hr with a P value of <0.0017, 0.0001, 0.5112, 0.0001, 0.0001, 0.0274, and 0.0001 for cells expressing *miap*-3 FL, *xiap* FL, *miap*-3 BIR, *miap*-3 RZF, pCDNA3, untransfected CHO cells, and bcl-2 respectively.

miap-3 FL statistical analysis

Parameter	Value	Data Set-B	Data Set-C	Data Set-D
Table Analyzed				
miap				
Repeated Measures ANOVA				
P value	0.0017			
P value summary	**			
Are means signif. different? (P < 0.05)	Yes			
Number of groups	4			
F	19.63			
R squared	0.9075			
Was the pairing significantly effective?				
R squared	0.004936			
F	0.1609			
P value	0.8549			
P value summary	ns			
Is there significant matching? (P < 0.05)	No			
ANOVA Table	SS	df	MS	
Treatment (between columns)	15490	3	5162	
Individual (between rows)	84.64	2	42.32	
Residual (random)	1578	6	263.0	
Total	17150	11		
Tukey's Multiple Comparison Test	Mean Diff.	q	P value	95% CI of diff
24 vs 48	50.90	5.436	P < 0.05	5.055 to 96.74
24 vs 72	77.30	8.256	P < 0.01	31.46 to 123.1
24 vs 96	95.33	10.18	P < 0.01	49.49 to 141.2
48 vs 72	26.40	2.820	P > 0.05	-19.44 to 72.24
48 vs 96	44.43	4.745	P > 0.05	-1.411 to 90.27
72 vs 96	18.03	1.925	P > 0.05	-27.81 to 63.87

xiap FL statistical analysis

Parameter	Value	Data Set-B	Data Set-C	Data Set-D
Table Analyzed				
xiap				
Repeated Measures ANOVA				
P value	P<0.0001			
P value summary	***			
Are means signif. different? (P < 0.05)	Yes			
Number of groups	4			
F	58.55			
R squared	0.9670			
Was the pairing significantly effective?				
R squared	0.0005830			
F	0.05298			
P value	0.9488			
P value summary	ns			
Is there significant matching? (P < 0.05)	No			
ANOVA Table	SS	df	MS	
Treatment (between columns)	14080	3	4693	
Individual (between rows)	8.494	2	4.247	
Residual (random)	480.9	6	80.16	
Total	14570	11		
Tukey's Multiple Comparison Test	Mean Diff.	q	P value	95% CI of diff
24 vs 48	9.407	1.820	P > 0.05	-15.90 to 34.71
24 vs 72	61.91	11.98	P < 0.001	36.61 to 87.22
24 vs 96	81.13	15.69	P < 0.001	55.82 to 106.4
48 vs 72	52.51	10.16	P < 0.01	27.20 to 77.81
48 vs 96	71.72	13.87	P < 0.001	46.41 to 97.03
72 vs 96	19.21	3.717	P > 0.05	-6.094 to 44.52

miap-3 BIRs statistical analysis

Parameter	Value	Data Set-B	Data Set-C	Data Set-D
Table Analyzed				
bir				
Repeated Measures ANOVA				
P value	0.5112			
P value summary	ns			
Are means signif. different? (P < 0.05)	No			
Number of groups	4			
F	0.8594			
R squared	0.3006			
Was the pairing significantly effective?				
R squared	0.0009259			
F	0.003975			
P value	0.9960			
P value summary	ns			
Is there significant matching? (P < 0.05)	No			
ANOVA Table	SS	df	MS	
Treatment (between columns)	1111	3	370.4	
Individual (between rows)	3.427	2	1.713	
Residual (random)	2586	6	431.0	
Total	3701	11		
Tukey's Multiple Comparison Test	Mean Diff.	q	P value	95% CI of diff
24 vs 48	9.737	0.8123	P > 0.05	-48.95 to 68.42
24 vs 72	19.67	1.641	P > 0.05	-39.02 to 78.36
24 vs 96	25.16	2.099	P > 0.05	-33.52 to 83.85
48 vs 72	9.933	0.8287	P > 0.05	-48.75 to 68.62
48 vs 96	15.43	1.287	P > 0.05	-43.26 to 74.11
72 vs 96	5.493	0.4583	P > 0.05	-53.19 to 64.18

miap-3RZF statistical analysis

Parameter	Value	Data Set-B	Data Set-C	Data Set-D
Table Analyzed				
RZF				
Repeated Measures ANOVA				
P value	P<0.0001			
P value summary	***			
Are means signif. different? (P < 0.05)	Yes			
Number of groups	4			
F	145.6			
R squared	0.9864			
Was the pairing significantly effective?				
R squared	0.01036			
F	2.317			
P value	0.1797			
P value summary	ns			
Is there significant matching? (P < 0.05)	No			
ANOVA Table	SS	df	MS	
Treatment (between columns)	15150	3	5048	
Individual (between rows)	160.7	2	80.35	
Residual (random)	208.1	6	34.68	
Total	15510	11		
Tukey's Multiple Comparison Test	Mean Diff.	q	P value	95% CI of diff
24 vs 48	27.43	8.066	P < 0.01	10.78 to 44.07
24 vs 72	77.97	22.93	P < 0.001	61.32 to 94.61
24 vs 96	85.73	25.21	P < 0.001	69.08 to 102.4
48 vs 72	50.54	14.86	P < 0.001	33.89 to 67.19
48 vs 96	58.30	17.15	P < 0.001	41.65 to 74.95
72 vs 96	7.760	2.282	P > 0.05	-8.887 to 24.41

pCDNA3 statistical analysis

Parameter	Value	Data Set-B	Data Set-C	Data Set-D
Table Analyzed				
pcdna3				
Repeated Measures ANOVA				
P value	P<0.0001			
P value summary	***			
Are means signif. different? (P < 0.05)	Yes			
Number of groups	4			
F	64.06			
R squared	0.9697			
Was the pairing significantly effective?				
R squared	0.008700			
F	0.8697			
P value	0.4659			
P value summary	ns			
Is there significant matching? (P < 0.05)	No			
ANOVA Table	SS	df	MS	
Treatment (between columns)	16050	3	5350	
Individual (between rows)	145.3	2	72.64	
Residual (random)	501.1	6	83.52	
Total	16700	11		
Tukey's Multiple Comparison Test	Mean Diff.	q	P value	95% CI of diff
24 vs 48	8.277	1.569	P > 0.05	-17.56 to 34.11
24 vs 72	72.43	13.73	P < 0.001	46.60 to 98.27
24 vs 96	81.15	15.38	P < 0.001	55.31 to 107.0
48 vs 72	64.16	12.16	P < 0.001	38.32 to 89.99
48 vs 96	72.87	13.81	P < 0.001	47.04 to 98.70
72 vs 96	8.713	1.651	P > 0.05	-17.12 to 34.55

untransfected CHO cells statistical analysis

Parameter	Value	Data Set-B	Data Set-C	Data Set-D
Table Analyzed				
cho				
Repeated Measures ANOVA				
P value	0.0274			
P value summary	*			
Are means signif. different? (P < 0.05)	Yes			
Number of groups	4			
F	6.332			
R squared	0.7600			
Was the pairing significantly effective?				
R squared	0.1789			
F	2.724			
P value	0.1440			
P value summary	ns			
Is there significant matching? (P < 0.05)	No			
ANOVA Table	SS	df	MS	
Treatment (between columns)	5901	3	1967	
Individual (between rows)	1692	2	846.2	
Residual (random)	1864	6	310.7	
Total	9457	11		
Tukey's Multiple Comparison Test	Mean Diff.	q	P value	95% CI of diff
24 vs 48	24.10	2.368	P > 0.05	-25.72 to 73.92
24 vs 72	49.69	4.883	P > 0.05	-0.1328 to 99.51
24 vs 96	55.84	5.487	P < 0.05	6.017 to 105.7
48 vs 72	25.59	2.515	P > 0.05	-24.23 to 75.41
48 vs 96	31.74	3.119	P > 0.05	-18.08 to 81.56
72 vs 96	6.150	0.6043	P > 0.05	-43.67 to 55.97

bcl-2 statistical analysis

Parameter	Value	Data Set-B	Data Set-C	Data Set-D
Table Analyzed				
bcl-2				
Repeated Measures ANOVA				
P value	P<0.0001			
P value summary	***			
Are means signif. different? (P < 0.05)	Yes			
Number of groups	4			
F	86.97			
R squared	0.9775			
Was the pairing significantly effective?				
R squared	0.02246			
F	3.066			
P value	0.1210			
P value summary	ns			
Is there significant matching? (P < 0.05)	No			
ANOVA Table	SS	df	MS	
Treatment (between columns)	6360	3	2120	
Individual (between rows)	149.4	2	74.72	
Residual (random)	146.2	6	24.37	
Total	6655	11		
Tukey's Multiple Comparison Test	Mean Diff.	q	P value	95% CI of diff
24 vs 48	28.93	10.15	P < 0.01	14.97 to 42.88
24 vs 72	60.18	21.11	P < 0.001	46.22 to 74.13
24 vs 96	49.98	17.53	P < 0.001	36.02 to 63.93
48 vs 72	31.25	10.96	P < 0.01	17.29 to 45.21
48 vs 96	21.05	7.385	P < 0.01	7.094 to 35.01
72 vs 96	-10.20	3.578	P > 0.05	-24.16 to 3.755

b. Statistical analysis of death assay experiments in CHO cells expressing *xiap* FL, *xiap* Δ1, *xiap* Δ2, *xiap* Δ3, *xiap* BIRs, bcl-2, and pCDNA3. Based on this analysis, percentage of viable CHO cells expressing *xiap* various constructs at 24 hr is not significantly different. However, at 48 and 72 hr, the means obtained demonstrate a significance compared to 24 hr with a P value of <0.0340, 0.0247, 0.0084, 0.0008, 0.0246, 0.0296 and 0.0167 for cells expressing *xiap* FL, *xiap* Δ1, *xiap* Δ2, *xiap* Δ3, *xiap* BIRs,, and pCDNA3 and untransfected CHO cell respectively.

xiap FL statistical analysis

Parameter	Value	Data Set-B	Data Set-C	Data Set-D
Table Analyzed				
xiap				
Repeated Measures ANOVA				
P value	0.0340			
P value summary	*			
Are means signif. different? (P < 0.05)	Yes			
Number of groups	3			
F	8.845			
R squared	0.8156			
Was the pairing significantly effective?				
R squared	0.2371			
F	3.371			
P value	0.1387			
P value summary	ns			
Is there significant matching? (P < 0.05)	No			
ANOVA Table	SS	df	MS	
Treatment (between columns)	3049	2	1524	
Individual (between rows)	1162	2	581.0	
Residual (random)	689.4	4	172.3	
Total	4900	8		
Tukey's Multiple Comparison Test	Mean Diff.	q	P value	95% CI of diff
24 vs 48	31.66	4.177	P > 0.05	-6.543 to 69.86
24 vs 72	43.63	5.756	P < 0.05	5.427 to 81.83
48 vs 72	11.97	1.579	P > 0.05	-26.23 to 50.17

xiap Δ1 statistical analysis

Parameter	Value	Data Set-B	Data Set-C	Data Set-D
Table Analyzed				
d1				
Repeated Measures ANOVA				
P value	0.0247			
P value summary	*			
Are means signif. different? (P < 0.05)	Yes			
Number of groups	3			
F	10.73			
R squared	0.8428			
Was the pairing significantly effective?				
R squared	0.05611			
F	0.7566			
P value	0.5264			
P value summary	ns			
Is there significant matching? (P < 0.05)	No			
ANOVA Table	SS	df	MS	
Treatment (between columns)	2135	2	1067	
Individual (between rows)	150.6	2	75.28	
Residual (random)	398.0	4	99.50	
Total	2683	8		
Tukey's Multiple Comparison Test	Mean Diff.	q	P value	95% CI of diff
24 vs 48	12.38	2.150	P > 0.05	-16.65 to 41.41
24 vs 72	37.05	6.433	P < 0.05	8.024 to 66.08
48 vs 72	24.67	4.284	P > 0.05	-4.356 to 53.70

xiap Δ2 statistical analysis

Parameter	Value	Data Set-B	Data Set-C	Data Set-D
Table Analyzed				
d2				
Repeated Measures ANOVA				
P value	0.0084			
P value summary	**			
Are means signif. different? (P < 0.05)	Yes			
Number of groups	3			
F	19.81			
R squared	0.9083			
Was the pairing significantly effective?				
R squared	0.1428			
F	3.634			
P value	0.1260			
P value summary	ns			
Is there significant matching? (P < 0.05)	No			
ANOVA Table	SS	df	MS	
Treatment (between columns)	2464	2	1232	
Individual (between rows)	452.0	2	226.0	
Residual (random)	248.8	4	62.19	
Total	3165	8		
Tukey's Multiple Comparison Test	Mean Diff.	q	P value	95% CI of diff
24 vs 48	29.37	6.451	P < 0.05	6.425 to 52.32
24 vs 72	38.87	8.538	P < 0.01	15.93 to 61.82
48 vs 72	9.500	2.086	P > 0.05	-13.45 to 32.45

xiap Δ3 statistical analysis

Parameter	Value	Data Set-B	Data Set-C	Data Set-D
Table Analyzed				
d3				
Repeated Measures ANOVA				
P value	0.0008			
P value summary	***			
Are means signif. different? (P < 0.05)	Yes			
Number of groups	3			
F	69.03			
R squared	0.9718			
Was the pairing significantly effective?				
R squared	0.006255			
F	0.4471			
P value	0.6680			
P value summary	ns			
Is there significant matching? (P < 0.05)	No			
ANOVA Table	SS	df	MS	
Treatment (between columns)	2418	2	1209	
Individual (between rows)	15.66	2	7.830	
Residual (random)	70.05	4	17.51	
Total	2503	8		
Tukey's Multiple Comparison Test	Mean Diff.	q	P value	95% CI of diff
24 vs 48	30.23	12.51	P < 0.01	18.06 to 42.41
24 vs 72	37.99	15.73	P < 0.001	25.82 to 50.17
48 vs 72	7.760	3.212	P > 0.05	-4.417 to 19.94

xiap BIRs statistical analysis

Parameter	Value	Data Set-B	Data Set-C	Data Set-D
Table Analyzed				
bir				
Repeated Measures ANOVA				
P value	0.0246			
P value summary	*			
Are means signif. different? (P < 0.05)	Yes			
Number of groups	3			
F	10.75			
R squared	0.8431			
Was the pairing significantly effective?				
R squared	0.01257			
F	0.1624			
P value	0.8555			
P value summary	ns			
Is there significant matching? (P < 0.05)	No			
ANOVA Table	SS	df	MS	
Treatment (between columns)	3396	2	1698	
Individual (between rows)	51.29	2	25.64	
Residual (random)	631.8	4	157.9	
Total	4079	8		
Tukey's Multiple Comparison Test	Mean Diff.	q	P value	95% CI of diff
24 vs 48	34.93	4.814	P > 0.05	-1.640 to 71.50
24 vs 72	45.44	6.263	P < 0.05	8.873 to 82.01
48 vs 72	10.51	1.449	P > 0.05	-26.06 to 47.08

pCDNA3 statistical analysis

Parameter	Value	Data Set-B	Data Set-C	Data Set-D
Table Analyzed				
pcdna3				
Repeated Measures ANOVA				
P value	0.0296			
P value summary	*			
Are means signif. different? (P < 0.05)	Yes			
Number of groups	3			
F	9.632			
R squared	0.8281			
Was the pairing significantly effective?				
R squared	0.08750			
F	1.115			
P value	0.4121			
P value summary	ns			
Is there significant matching? (P < 0.05)	No			
ANOVA Table	SS	df	MS	
Treatment (between columns)	3097	2	1548	
Individual (between rows)	358.6	2	179.3	
Residual (random)	643.1	4	160.8	
Total	4099	8		
Tukey's Multiple Comparison Test	Mean Diff.	q	P value	95% CI of diff
24 vs 48	25.57	3.493	P > 0.05	-11.32 to 62.47
24 vs 72	45.31	6.190	P < 0.05	8.418 to 82.21
48 vs 72	19.74	2.697	P > 0.05	-17.15 to 56.63

untransfected CHO cells statistical analysis

Parameter	Value	Data Set-B	Data Set-C	Data Set-D
Table Analyzed				
cho				
Repeated Measures ANOVA				
P value	0.0167			
P value summary	*			
Are means signif. different? (P < 0.05)	Yes			
Number of groups	3			
F	13.47			
R squared	0.8707			
Was the pairing significantly effective?				
R squared	0.1057			
F	1.828			
P value	0.2729			
P value summary	ns			
Is there significant matching? (P < 0.05)	No			
ANOVA Table	SS	df	MS	
Treatment (between columns)	3410	2	1705	
Individual (between rows)	462.8	2	231.4	
Residual (random)	506.3	4	126.6	
Total	4379	8		
Tukey's Multiple Comparison Test	Mean Diff.	q	P value	95% CI of diff
24 vs 48	38.38	5.908	P < 0.05	5.640 to 71.11
24 vs 72	43.69	6.727	P < 0.05	10.96 to 76.43
48 vs 72	5.317	0.8185	P > 0.05	-27.42 to 38.05

c. Statistical analysis of *miap*-3 and *xiap* death assay data at 72 hr:

i. Analysis of data obtained at 72 hours from the death assay experiments where serum deprivation was used to induce apoptosis in CHO cells expressing *miap*-3 FL, *xiap* FL, *miap*-3 BIRs, *miap*-3 RZF, bcl-2, and pCDNA3 demonstrated that data obtained for CHO cells expressing *miap*-3 BIRs is statistically different from cells expressing *miap*-3 FL, *xiap* FL, *miap*-3 RZF, bcl-2, pCDNA3 or controls (untransfected CHO cells) with a P value of 0.0001.

ii. Analysis of data obtained at 72 hours from the death assay experiments where serum deprivation was used to induce apoptosis in CHO cells expressing *xiap* FL, *xiap* Δ1, *xiap* Δ2, *xiap* Δ3, *xiap* BIRs, and pCDNA3 demonstrated that data obtained for CHO cells expressing *xiap* BIRs is statistically different from cells expressing *xiap* FL, *xiap* Δ1, *xiap* Δ2, *xiap* Δ3, bcl-2, pCDNA3 or controls (untransfected CHO cells) with a P value of 0.0023.

Statistical analysis of *miap*-3 death assay data at 72 hours post serum withdrawal

Parameter	Value	Data Set-B	Data Set-C	Data Set-D
Table Analyzed				
miap-3 72 hr				
Repeated Measures ANOVA				
P value	P<0.0001			
P value summary	***			
Are means signif. different? (P < 0.05)	Yes			
Number of groups	7			
F	15.87			
R squared	0.8881			
Was the pairing significantly effective?				
R squared	0.009502			
F	0.5143			
P value	0.6105			
P value summary	ns			
Is there significant matching? (P < 0.05)	No			
ANOVA Table	SS	df	MS	
Treatment (between columns)	4378	6	729.7	
Individual (between rows)	47.30	2	23.65	
Residual (random)	551.8	12	45.98	
Total	4977	20		
Tukey's Multiple Comparison Test	Mean Diff.	q	P value	95% CI of diff
miap-3 vs xiap	-2.567	0.6556	P > 0.05	-21.95 to 16.81
miap-3 vs BIR	-33.87	8.652	P < 0.001	-53.25 to -14.49
miap-3 vs RZF	7.627	1.948	P > 0.05	-11.75 to 27.01
miap-3 vs pCDNA3	9.467	2.418	P > 0.05	-9.913 to 28.85
miap-3 vs CHO	12.46	3.182	P > 0.05	-6.923 to 31.84
miap-3 vs bcl-2	-4.623	1.181	P > 0.05	-24.00 to 14.76
xiap vs BIR	-31.31	7.997	P < 0.01	-50.69 to -11.93
xiap vs RZF	10.19	2.604	P > 0.05	-9.186 to 29.57
xiap vs pCDNA3	12.03	3.074	P > 0.05	-7.346 to 31.41
xiap vs CHO	15.02	3.837	P > 0.05	-4.356 to 34.40
xiap vs bcl-2	-2.057	0.5253	P > 0.05	-21.44 to 17.32
BIR vs RZF	41.50	10.60	P < 0.001	22.12 to 60.88
BIR vs pCDNA3	43.34	11.07	P < 0.001	23.96 to 62.72
BIR vs CHO	46.33	11.83	P < 0.001	26.95 to 65.71
BIR vs bcl-2	29.25	7.471	P < 0.01	9.871 to 48.63
RZF vs pCDNA3	1.840	0.4700	P > 0.05	-17.54 to 21.22
RZF vs CHO	4.830	1.234	P > 0.05	-14.55 to 24.21
RZF vs bcl-2	-12.25	3.129	P > 0.05	-31.63 to 7.129
pCDNA3 vs CHO	2.990	0.7637	P > 0.05	-16.39 to 22.37
pCDNA3 vs bcl-2	-14.09	3.599	P > 0.05	-33.47 to 5.289
CHO vs bcl-2	-17.08	4.363	P > 0.05	-36.46 to 2.299

Statistical analysis of *xiap* death assay data at 72 hours post serum withdrawal

Parameter	Value	Data Set-B	Data Set-C	Data Set-D
Table Analyzed				
Xiap 72 hr				
Repeated Measures ANOVA				
P value	0.0023			
P value summary	**			
Are means signif. different? (P < 0.05)	Yes			
Number of groups	7			
F	6.939			
R squared	0.7763			
Was the pairing significantly effective?				
R squared	0.02325			
F	0.6384			
P value	0.5452			
P value summary	ns			
Is there significant matching? (P < 0.05)	No			
ANOVA Table	SS	df	MS	
Treatment (between columns)	2592	6	432.0	
Individual (between rows)	79.49	2	39.74	
Residual (random)	747.1	12	62.26	
Total	3419	20		
Tukey's Multiple Comparison Test	Mean Diff.	q	P value	95% CI of diff
BIR vs d1	32.98	7.240	P < 0.01	10.43 to 55.53
BIR vs d2	28.00	6.147	P < 0.05	5.454 to 50.55
BIR vs d3	33.24	7.297	P < 0.01	10.69 to 55.79
BIR vs Xiap	21.41	4.699	P > 0.05	-1.143 to 43.96
BIR vs pCDNA3	30.27	6.645	P < 0.01	7.720 to 52.82
BIR vs CHO	32.71	7.181	P < 0.01	10.16 to 55.26
d1 vs d2	-4.980	1.093	P > 0.05	-27.53 to 17.57
d1 vs d3	0.2600	0.05707	P > 0.05	-22.29 to 22.81
d1 vs Xiap	-11.58	2.541	P > 0.05	-34.13 to 10.97
d1 vs pCDNA3	-2.713	0.5956	P > 0.05	-25.26 to 19.84
d1 vs CHO	-0.2700	0.05927	P > 0.05	-22.82 to 22.28
d2 vs d3	5.240	1.150	P > 0.05	-17.31 to 27.79
d2 vs Xiap	-6.597	1.448	P > 0.05	-29.15 to 15.95
d2 vs pCDNA3	2.267	0.4976	P > 0.05	-20.28 to 24.82
d2 vs CHO	4.710	1.034	P > 0.05	-17.84 to 27.26
d3 vs Xiap	-11.84	2.598	P > 0.05	-34.39 to 10.71
d3 vs pCDNA3	-2.973	0.6527	P > 0.05	-25.52 to 19.58
d3 vs CHO	-0.5300	0.1163	P > 0.05	-23.08 to 22.02
Xiap vs pCDNA3	8.863	1.946	P > 0.05	-13.69 to 31.41
Xiap vs CHO	11.31	2.482	P > 0.05	-11.24 to 33.86
pCDNA3 vs CHO	2.443	0.5363	P > 0.05	-20.11 to 24.99

iii. Analysis of data obtained at 24 hours from the death assay experiments where 10 or 20 μM menadione was used to induce apoptosis in CHO cells expressing *miap*-3 FL, *xiap* FL, *miap*-3 BIRs, *miap*-3 RZF, bcl-2, and pCDNA3 demonstrated that data obtained for CHO cells expressing *miap*-3 FL, *xiap* FL, *maip*-3 BIRs is statistically different from cells expressing *miap*-3 RZF, pCDNA3 or controls (untransfected CHO cells) with a P value of 0.0008 and 0.0056 respectively.

Statistical analysis of death assay data for CHO cells exposed to 10μM menadion

Parameter	Value	Data Set-B	Data Set-C	Data Set-D
Table Analyzed				
menadion10				
Repeated Measures ANOVA				
P value	0.0008			
P value summary	***			
Are means signif. different? (P < 0.05)	Yes			
Number of groups	7			
F	8.804			
R squared	0.8149			
Was the pairing significantly effective?				
R squared	0.08093			
F	2.854			
P value	0.0968			
P value summary	ns			
Is there significant matching? (P < 0.05)	No			
ANOVA Table	SS	df	MS	
Treatment (between columns)	1149	6	191.6	
Individual (between rows)	124.2	2	62.10	
Residual (random)	261.1	12	21.76	
Total	1535	20		
Tukey's Multiple Comparison Test	Mean Diff.	q	P value	95% CI of diff
miap-3 vs xiap	-1.190	0.4419	P > 0.05	-14.52 to 12.14
miap-3 vs BIR	-1.067	0.3961	P > 0.05	-14.40 to 12.26
miap-3 vs RZF	12.09	4.489	P > 0.05	-1.241 to 25.42
miap-3 vs pCDNA3	17.96	6.669	P < 0.01	4.629 to 31.29
miap-3 vs CHO	13.83	5.134	P < 0.05	0.4955 to 27.16
miap-3 vs bcl-2	3.627	1.347	P > 0.05	-9.705 to 16.96
xiap vs BIR	0.1233	0.04580	P > 0.05	-13.21 to 13.45
xiap vs RZF	13.28	4.931	P > 0.05	-0.05117 to 26.61
xiap vs pCDNA3	19.15	7.111	P < 0.01	5.819 to 32.48
xiap vs CHO	15.02	5.576	P < 0.05	1.686 to 28.35
xiap vs bcl-2	4.817	1.788	P > 0.05	-8.515 to 18.15
BIR vs RZF	13.16	4.885	P > 0.05	-0.1745 to 26.49
BIR vs pCDNA3	19.03	7.065	P < 0.01	5.695 to 32.36
BIR vs CHO	14.89	5.530	P < 0.05	1.562 to 28.22
BIR vs bcl-2	4.693	1.743	P > 0.05	-8.638 to 18.02
RZF vs pCDNA3	5.870	2.180	P > 0.05	-7.461 to 19.20
RZF vs CHO	1.737	0.6448	P > 0.05	-11.59 to 15.07
RZF vs bcl-2	-8.463	3.143	P > 0.05	-21.79 to 4.868
pCDNA3 vs CHO	-4.133	1.535	P > 0.05	-17.46 to 9.198
pCDNA3 vs bcl-2	-14.33	5.322	P < 0.05	-27.66 to -1.002
CHO vs bcl-2	-10.20	3.787	P > 0.05	-23.53 to 3.131

Statistical analysis of death assay data for CHO cells exposed to 20μM menadion

Parameter	Value	Data Set-B	Data Set-C	Data Set-D
Table Analyzed				
menadion20				
Repeated Measures ANOVA				
P value	0.0056			
P value summary	**			
Are means signif. different? (P < 0.05)	Yes			
Number of groups	7			
F	5.588			
R squared	0.7364			
Was the pairing significantly effective?				
R squared	0.1068			
F	2.723			
P value	0.1059			
P value summary	ns			
Is there significant matching? (P < 0.05)	No			
ANOVA Table	SS	df	MS	
Treatment (between columns)	1150	6	191.7	
Individual (between rows)	186.9	2	93.44	
Residual (random)	411.7	12	34.31	
Total	1749	20		
Tukey's Multiple Comparison Test	Mean Diff.	q	P value	95% CI of diff
miap-3 vs xiap	-0.9833	0.2908	P > 0.05	-17.72 to 15.76
miap-3 vs BIR	-9.530	2.818	P > 0.05	-26.27 to 7.210
miap-3 vs RZF	10.63	3.144	P > 0.05	-6.107 to 27.37
miap-3 vs pCDNA3	12.61	3.729	P > 0.05	-4.130 to 29.35
miap-3 vs CHO	9.033	2.671	P > 0.05	-7.707 to 25.77
miap-3 vs bcl-2	-0.8200	0.2425	P > 0.05	-17.56 to 15.92
xiap vs BIR	-8.547	2.527	P > 0.05	-25.29 to 8.194
xiap vs RZF	11.62	3.435	P > 0.05	-5.124 to 28.36
xiap vs pCDNA3	13.59	4.019	P > 0.05	-3.147 to 30.33
xiap vs CHO	10.02	2.962	P > 0.05	-6.724 to 26.76
xiap vs bcl-2	0.1633	0.04830	P > 0.05	-16.58 to 16.90
BIR vs RZF	20.16	5.962	P < 0.05	3.423 to 36.90
BIR vs pCDNA3	22.14	6.547	P < 0.01	5.400 to 38.88
BIR vs CHO	18.56	5.489	P < 0.05	1.823 to 35.30
BIR vs bcl-2	8.710	2.575	P > 0.05	-8.030 to 25.45
RZF vs pCDNA3	1.977	0.5845	P > 0.05	-14.76 to 18.72
RZF vs CHO	-1.600	0.4731	P > 0.05	-18.34 to 15.14
RZF vs bcl-2	-11.45	3.387	P > 0.05	-28.19 to 5.287
pCDNA3 vs CHO	-3.577	1.058	P > 0.05	-20.32 to 13.16
pCDNA3 vs bcl-2	-13.43	3.971	P > 0.05	-30.17 to 3.310
CHO vs bcl-2	-9.853	2.914	P > 0.05	-26.59 to 6.887

IMAGE EVALUATION TEST TARGET (QA-3)

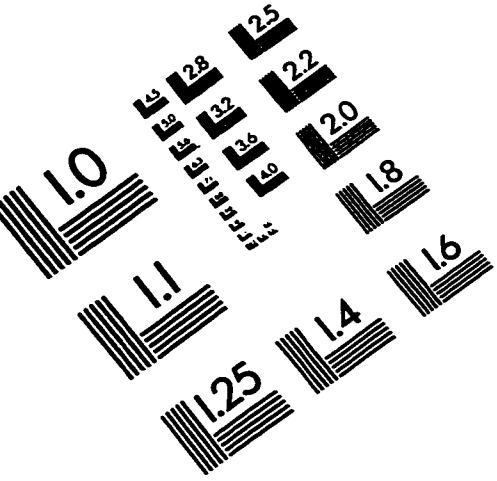

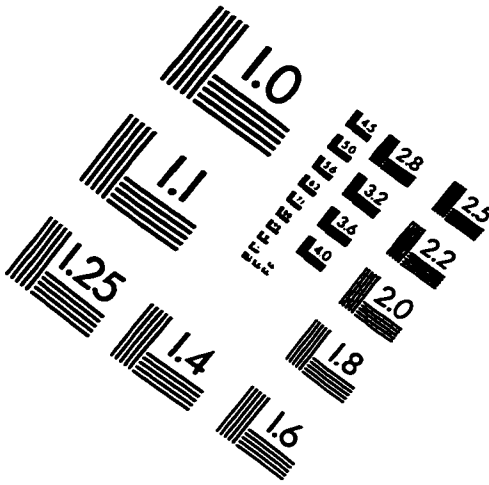

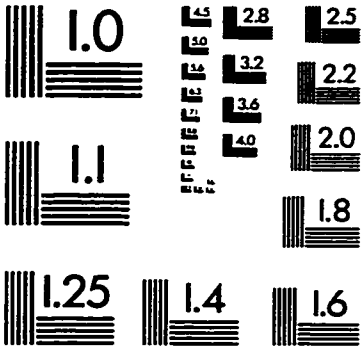

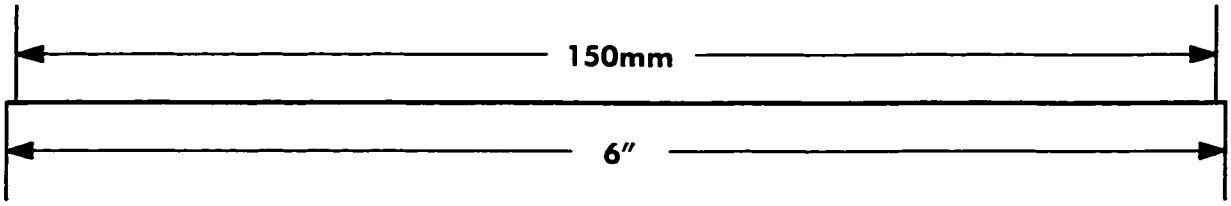

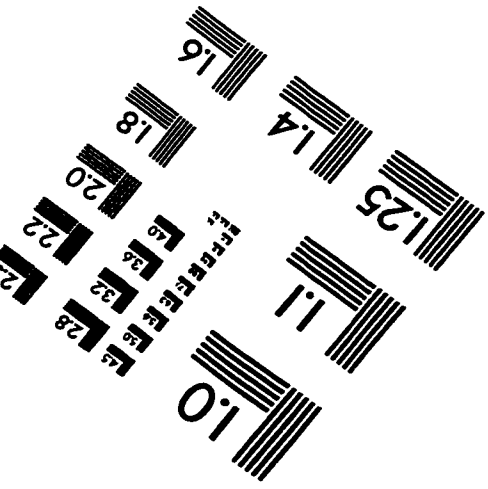

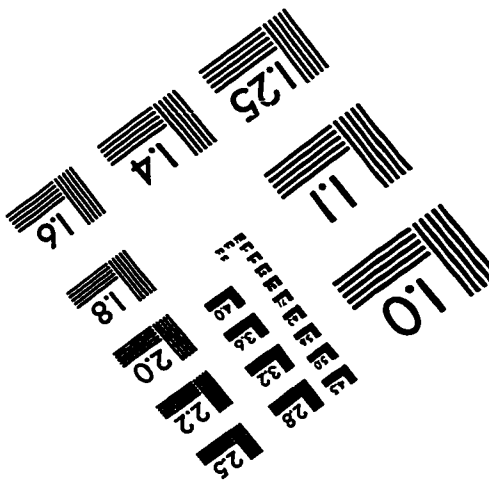

APPLIED IMAGE, Inc
1653 East Main Street
Rochester, NY 14609 USA
Phone: 716/482-0300
Fax: 716/288-5989